Dissertation zur Erlangung des Doktorgrades

der Fakultät für Chemie und Pharmazie

der Ludwig-Maximilians-Universität München

Photoswitchable Molecules for the Optical Control of GPCRs and Ion Channels

Arunas Jonas Damijonaitis

aus Giessen, Deutschland

2015

Erklärung

Diese Dissertation wurde im Sinne von § 7 der Promotionsordnung vom 28. November 2011 von Herrn Prof. Dirk Trauner betreut.

Eidesstattliche Versicherung

Diese Dissertation wurde eigenständig und ohne unerlaubte Hilfe erarbeitet

München, den 29.10.2015

Arunas Damijonaitis

Dissertation eingereicht am: 11.8.2015

1. Gutachter: Prof. Dr. D. Trauner

2. Gutachter: Prof. Dr. T. Gudermann

Mündliche Prüfung am: 13.10.2015

Meiner Familie

Silvija, Romana, Vingaudas, Darius, Theo, Julija, Artūras, Adomas, Anelė, Juozas, Tomas
… und meinem Kind!

"*Happiness in science is what you should strive for.*

And that comes from doing beautiful experiments with interesting colleagues."

Erik Kandel, 03 - 30 - 2015 Boston, MA

Parts of this dissertation have been published or are considered for publication in peer reviewed journals:

Schoenberger, M., Damijonaitis, A., Zhang, Z., Nagel, D., & Trauner, D., Development of a New Photochromic Ion Channel Blocker via Azologization of Fomocaine. ACS Chem. Neurosci. 5 (7), 514-518 (2014)

Damijonaitis, A. et al., AzoCholine Enables Optical Control of Alpha 7 Nicotinic Acetylcholine Receptors in Neural Networks. ACS Chem. Neurosci. 6 (5), 701-707 (2015).

Damijonaitis, A., Barber, D., Trauner, D., Photopharmacology of nicotinic acetylcholine receptors. Current Signal Transduction Therapy. (2015) accepted

Broichhagen, J.*, Damijonaitis, A.*, Levitz, J.*, Sokol K.R., Leippe, P., Konrad, D., Isacoff, E.Z., & Trauner, D., Orthogonal optical control of a G protein-coupled receptor with a SNAP-tethered photochromic ligand. ACS Central Science (2015)
DOI: 10.1021/acscentsci.5b00260
* = *equal contribution, alphabetical order*

Note: The formatting of figures, tables, schemes and citations of the manuscripts have been adjusted to fit the format of this thesis.

Photoswitchable Molecules for the Optical Control of GPCRs and Ion Channels

Content

Forschungszusammenfassung

Dissertation zur Erlangung des Doktorgrades der Fakultät für Chemie und Pharmazie

der Ludwig-Maximilians-Universität München; von Arunas Damijonaitis aus Giessen

Photoschaltbare Moleküle für die optische Kontrolle von GPCRs und Ionenkanälen

(Photoswitchable Molecules for the Optical Control of GPCRs and Ion Channels)

Photopharmakologie

Photopharmakologie beschreibt die raumzeitliche Kontrolle biologischer Prozesse mit Licht. Ähnlich den sogenannten „Prodrugs", welche durch Verstoffwechselung bestimmter „Schutzgruppen" erst im Zielgewebe ihre Wirkung entfalten, läßt sich bei der Photopharmakologie der Wirkstoff lokal und zeitlich kontrolliert durch Licht einer bestimmten Lichtfarbe (Wellenlänge) aktivieren. Ein weiterer Vorteil dieser Anwendung gegenüber den „Photodrugs" ist die Reversibilität, d.h. der Wirkstoff kann durch Licht einer zweiten Wellenlänge wieder ausgeschaltet werden. Hierfür werden in bestehende oder neu entwickelte Wirkstoffe chemische Gruppen eingebaut (z.B. ein Azobenzol), welche bei Bestrahlung mit bestimmten Wellenlängen ihre dreidimensionale Struktur aufgrund von Photoisomerisierung (Abbildung 1) ändern. Diese Isomerisierung führt zur Veränderung der pharmakologischen Eigenschaften des Moleküls, d.h. die aktive Forms des Wirkstoffs wird je nach Wellenlänge angereichert oder verringert.

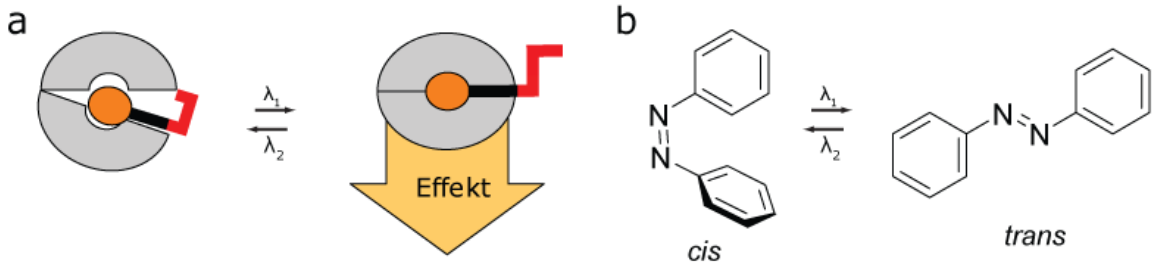

Abbildung 1. Das Prinzip der Photopharmakologie. a) Ein Rezeptor (grau) bindet den PCL, bestehend aus dem Liganden (orange), dem Linker (schwarz) und dem Azobenzol (rot), nur in einer Konformation. b) Die *cis*- und *trans*- Konformationen des Azobenzols lassen sich durch Bestrahlung mit bestimmten Wellenlängen (λ_1 oder λ_2) reversibel ineinander umwandeln.

In dieser Arbeit wird die Entwicklung von mehreren frei diffundierenden photoschaltbaren Liganden (photochromic ligands, PCLs) und einem gebundenen photoschaltbaren Liganden (Photoswitchable Orthogonal Remotely Tethered Ligand, PORTL) beschrieben. Dabei werden neuartige Konzepte zur Photokontrolle von biologischen Prozessen untersucht und vorgestellt.

1) Photoschaltbare Agonisten für nikotinische Acetylcholinrezeptoren

Nikotinische Acetylcholinrezeptoren (nAChR) sind in der Tierwelt weit verbreitet. Sowohl in kleinen Würmern, als auch in großen Säugetieren erfüllen sie viele unterschiedliche Funktionen. Im Menschen gibt es 17 Gene, die für unterschiedliche Rezeptoruntereinheiten kodieren. Fehlfunktionen von homopentameren α7 nAChR werden mit diversen Krankheiten, wie Alzheimer oder Parkinson, in Verbindung gebracht. Um die Aktivität dieser Rezeptoren präzise steuern zu können, wurde eine photoschaltbare Variante des Agonisten Acetylcholin entwickelt – AzoCholin (Abbildung 2a). Dieses Molekül ist in der Lage, den α7 nAChR reversibel mit Hilfe von Licht zu steuern. Es wurde gezeigt, dass AzoCholin an den in HEK293T Zellen heterolog exprimierten α7/GlyR nAChR lichtabhängig binden und effizient aktivieren kann. Des Weiteren wurde die Funktionalität von AzoCholin in Gewebeproben von Spinalganglionneuronen und im Hippocampus gezeigt. Zusätzlich konnte durch *in vivo* versuche bestätigt werden, dass über intrinsische nAChR und AzoCholin das Schwimmverhalten des Nematoden *Caenorhabditis elegans* (*C. elegans*) mit Licht gesteuert werden kann.

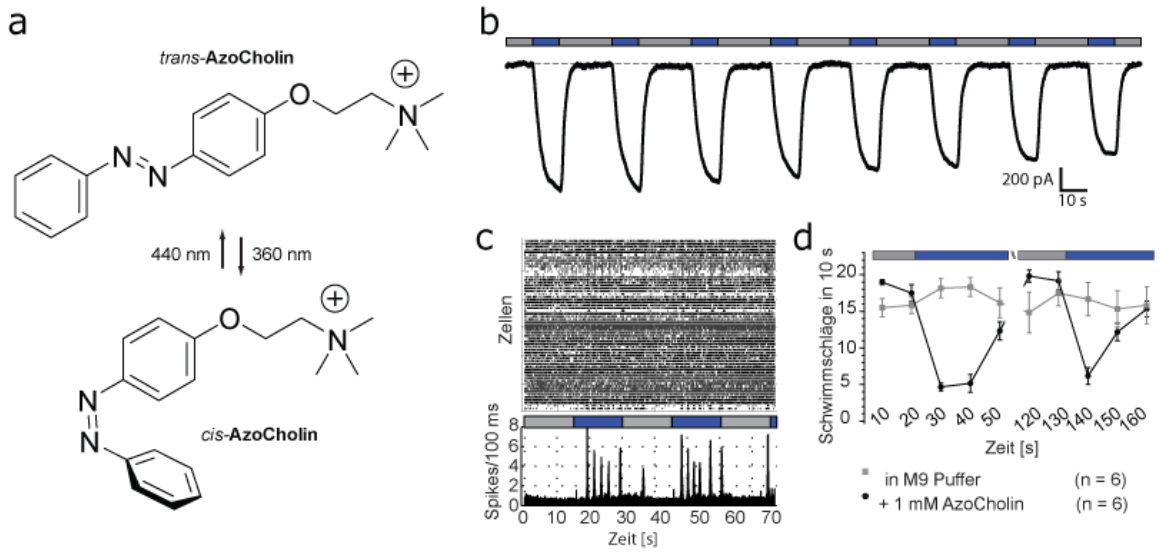

Abbildung 2. Photokontrolle von neuronalen Netzwerken mit AzoCholin. a) Chemische Struktur und Photoisomerisierung von AzoCholin. b) AzoCholin aktiviert den α7/GlyR nAChR reversibel und lichtabhängig. Elektrophysiologische Ableitung von HEK293T Zellen die den α7/GlyR exprimieren. c) Multielektrodenaufnahme der Aktivierung cholinerger Neurone im Hippocampus der Maus. Der Raster Plot zeigt die Aktivität der einzelnen Zellen. Das Histogramm darunter zeigt die lichabhängige Aktivität als Summe aller Zellen. d) Quantifizierung der Schwimmschläge von Nematoden (*C. elegans* Stamm *Lite1)*. Schwimmen die Tiere im physiologischen Puffer M9 (grau), hat Lichtmodulation keinen Effekt auf das Schwimmverhalten. Im Puffer mit 1 mM AzoCholin (schwarz) wird das schwimmen bei Beleuchtung mit 350 nm Licht abrupt unterbrochen.

2) Ein photoschaltbarer Blocker für spannungsabhängige Ionenkanäle

Wie alle Wahrnehmungsarten wird die Information über einen empfundenen Schmerz von Neuronen in das Gehirn weitergeleitet und dort weiter verarbeitet. Aktionspotentiale (APs), d.h. schnelle elektrische Signale in den Neuronen, welche durch das konzertierte Öffnen und Schließen von spannungsgesteuerten Ionenkanälen geformt werden, dienen hierbei den Neuronen als primärer Informationsträger. Werden diese Informationswege blockiert, so wird ebenfalls die Schmerzinformation gehemmt. Lokalanästhetika wie Fomocain, welche als Kanalblocker fungieren, können diese Reizweiterleitung stoppen.

Durch die „Azologisierung" von Fomocain zu Fotocain, d.h. die Einbettung eines Azobenzols in die chemische Struktur wurde das Lokalanästhetikum mit einer weiteren Eigenschaft ausgestattet – Lichtsensibilität (Abbildung 3). Somit lässt sich die Aktivität des Wirkstoffs präzise steuern. Dies wurde an dissoziierten Neuronen, sowie akuten Hirnschnitten von Mäusen demonstriert. Mittels Elektrophysiologie ließ sich verfolgen, wie neuronale Aktivität durch das Zusammenspiel von Fotocain und Licht kontrolliert werden konnte. Wie Fomocain, wirkte Fotocain im Dunkeln, da es vorwiegend in der blockierenden *trans*-Form vorlag. Durch Bestrahlung mit Licht der Wellenlänge 350 nm (violett) wurde das *cis*-isomer angereichert und die Blockade gelöst. Bei Bestrahlung mit 450 nm Licht (hell blau) wurde das Molekül wieder zur *trans*-Form photoisomerisiert.

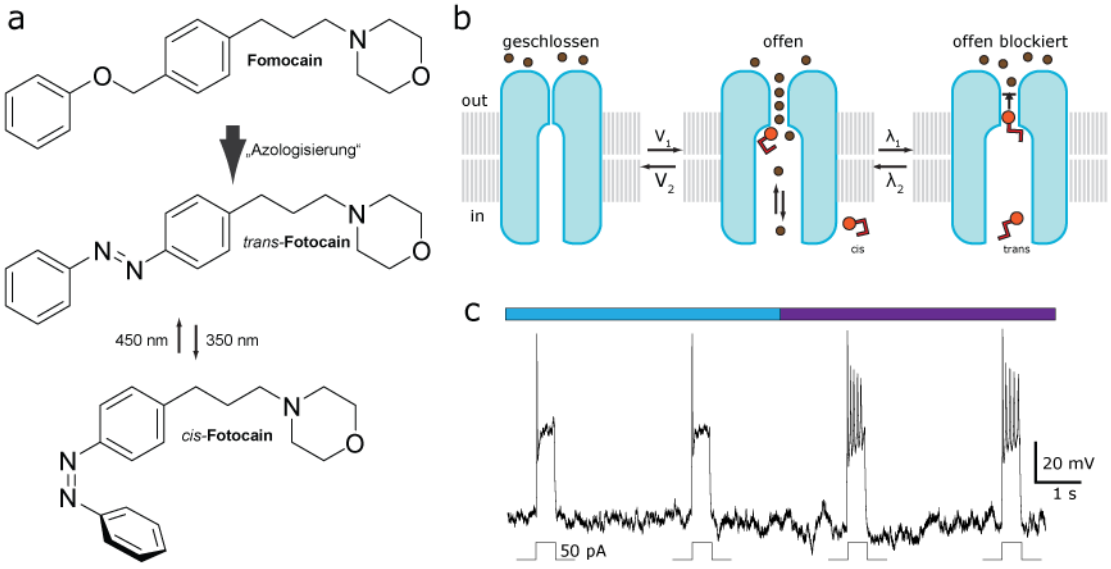

Abbildung 3. Photokontrolle spannungsabhängiger Ionenkanäle mit Fotocain. a) Azologisierung von Fomocain zu Fotocain und dessen Photoisomerisierung. b) Graphische Darstellung der vermuteten Funktionsweise von Fotocain. c) Elektrophysiologische Ableitung von neuronaler Aktivität. Durch Fotocain ist das Feuern von Aktionspotentialen nur bei Beleuchtung mit 350 nm (violett) möglich.

3) Ethylen-überbrückte Azobenzole sind in der *cis*-Konfiguration thermisch stabil.

Photochrome Liganden (PCLs), die herkömmliche Azobenzole enthalten, sind typischerweise in ihrer *trans*-Konfiguration thermisch stabil. Dies kann zu Komplikationen führen, wenn die Aktivität des Moleküls ebenfalls aus der *trans*-Konfiguration rührt, d.h. die PCLs sind auch im Dunkeln aktiv. In diesem Fall muss im Experiment über längere Zeit mit der inaktivierenden Wellenlänge (oft UV-Licht) beleuchtet werden, um das Zielprotein nicht durchgehend zu aktivieren. Dies ist aufgrund phototoxischer Effekte nicht wünschenswert. Hier wird die Verwendung von Ethylen überbrückten Azobenzolen beschrieben, die in ihrer *cis*-Konfiguration thermisch stabil sind. Dieses Konzept wurde auf den PCL QAQ angewendet, um das überbrückte Azobenzol BAQ (bridged azobenzene QAQ) zu erhalten (Abbildung 4).

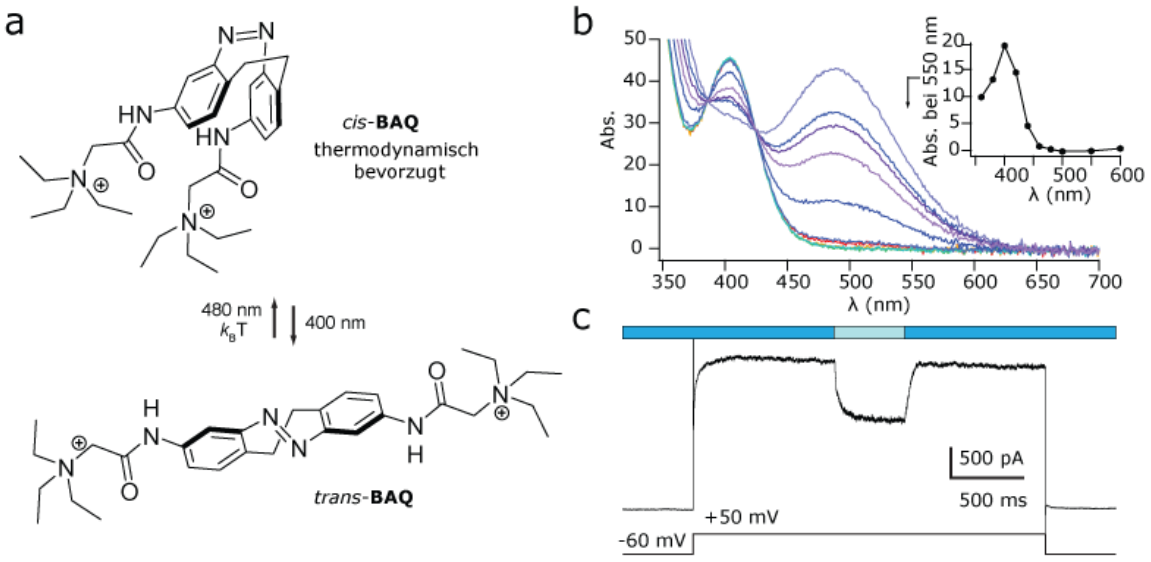

Abbildung 4. Photokontrolle spannungsabhängiger Ionenkanäle mit BAQ. a) Chemische Struktur und Photoisomerisierung von BAQ. b) Spektroskopische Analyse von BAQ in DMSO. Beste Wellenlängen zur Isomerisierung sind 400 nm und 480 nm. c) Elektrophysiologische Ableitung hippocampaler Neuronen der Maus. Ein depolarisierender Puls von −60 mV auf +50 mV erzeugt einen Kaliumstrom der lichtabhängig von BAQ blockiert wird.

4) Die Entwicklung eines photoschaltbaren Antagonists für den glutamat-gesteuerten Chloridkanal

Es gibt mehrere Möglichkeiten, einen PCL zu entwerfen. Der Ansatz der „Azologisierung" beinhaltet den Einbau eines Azobenzols in die Struktur eines bekannten Liganden (siehe Fotocain). Bei Beleuchtung mit unterschiedlichen Wellenlängen kann der PCL dann reversibel zwischen seiner aktiven und inaktiven Form geschaltet werden. Wenn jedoch keine „azologisierbaren" Liganden bekannt sind, müssen alternative Wege gesucht werden. Hier stellen wir das rationale Design eines photoschaltbaren Antagonisten für den glutamatgesteuerten Chloridkanal (GluCL), vor – AzoAPG (Abbildung 5). Ausgehend von Glutamat wurden unterschiedliche Substitutionsmotive mit variierender Länge am α-Kohlenstoff generiert. Zuletzt wurde durch die Addition eines Azobenzols der Photoschalter AzoAPG hergestellt. Dieser wirkt jedoch nicht als Agonist, sondern als partieller Antagonist.

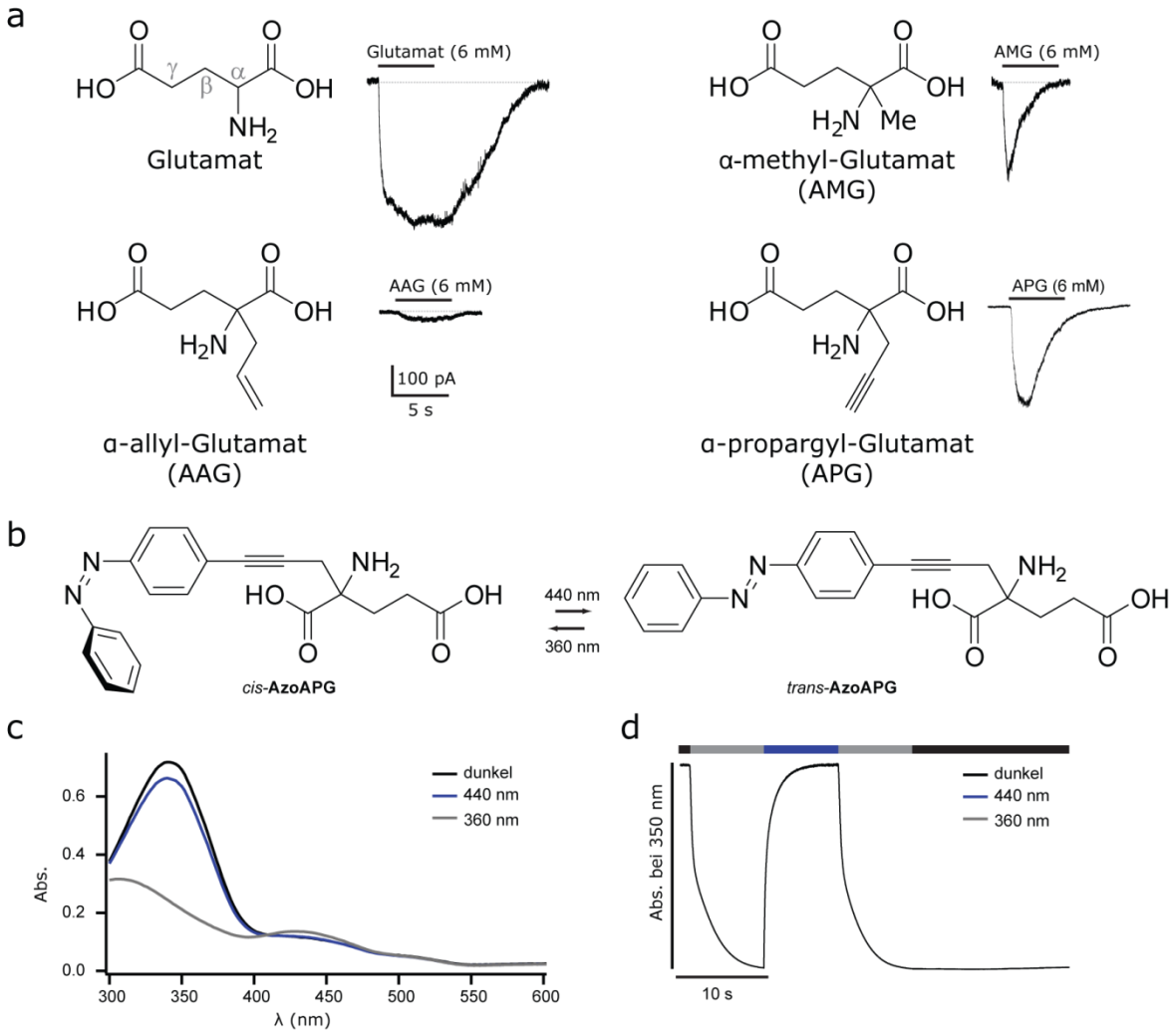

Abbildung 5. Entwicklung von AzoAPG. a) Alterniernde Synthese- und Evaluierungsschritte führen von Glutamat über α-methyl- und α-allyl- zu α-propargyl-Glutamat. b) Chemische Struktur und Photoisomerisierung von AzoAPG. b) Spektroskopische Analyse von AzoAPG in physiologischem Puffer. c) Analyse des Schaltverhaltens über die Zeit im UV-Vis.

5) Der photoschaltbare und orthogonale entfernt gebundene Ligand – PORTL

Die kovalente Bindung von synthetischen Photoschaltern ist ein allgemeiner Ansatz Rezeptoren mit Lichtempfindlichkeit auszustatten. Bei dem photoschaltbaren und orthogonalen entfernt gebundenen Liganden (Photoswitchable Orthogonal Remotely Tethered Ligand, PORTL) handelt es sich um einen lichtschaltbaren Wirkstoff an einer langen Leine (Abbildung 6). Die Bindung erfolgt spezifisch über den genetisch kodierten SNAP-Tag, welcher extrazellulär an den Zielrezeptor kloniert wurde. Dieser reagiert mit dem Benzylguanin, welches über einen langen flexiblen Linker mit dem photochromen Liganden verbunden ist. PORTL ist in physiologischer Lösung stabil und Biokonjugation tritt bei sehr geringen Konzentrationen mit hoher Selektivität und extrem schneller Kinetik ein.

Wir entwickeln diese neuartige Methode, um den G-Protein-gekoppelten Rezeptor mGluR2, einen metabotropen Glutamatrezeptor, in einen Photorezeptor (SNAG-mGluR2) zu verwandeln. Das ermöglicht uns die schnelle und reversible optische Kontrolle über zwei der wichtigsten Signalwege, die von mGluR2 vermittelt werden: (1) Hemmung der Transmitterfreisetzung über das präsynaptische Nervenende und (2) Kontrolle der Erregbarkeit von Neuronen über die Aktivierung von Kaliumkanälen im somato-dendritischen Raum.

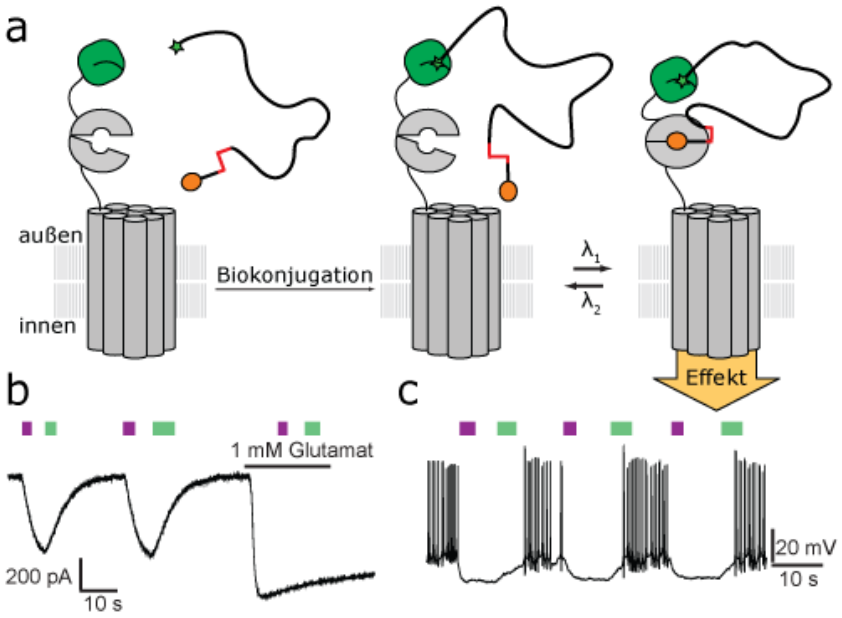

Abbildung 6. Der photoschaltbare und orthogonale entfernt gebundene Ligand (Photoswitchable Orthogonal Remotely Tethered Ligand, PORTL). a) Am metabotropen Glutamatrezeptor (mGluR2, grau) befindet sich der SNAP-Tag (grün). Dieser kann durch Biokonjugation eine kovalente Bindung mit dem Benzylguanin (grüner Stern) eingehen (SNAG-mGluR2). Am Ende des langen Linkers befindet sich der gebundene PCL. b) Bei Beleuchtung mit einer bestimmten Wellenlänge (λ = 380 nm, violett und λ = 500 nm, grün), wird die Konfiguration des PCLs geändert und der SNAG-mGluR2 (exprimiert in HEK293T Zellen) kann aktiviert werden. c) Neuronale Aktivität wird duch SNAG-mGluR2 lichtabhängig moduliert.

6) Pharmakologische Studie an Lolinalkaloiden

Lolinalkaloide, oder auch kurz Loline genannt, sind bioaktive Naturstoffe und gehören zu den Alkaloiden. Sie werden von endophytischen Pilzen (*Clavicipitaceae*) gebildet, welche vor allem auf Süßgräsern (*Poaceae*) wachsen. Die produzierten Alkaloide dienen den Wirtspflanzen und den Pilzen als Fraßschutz vor Insekten. In dieser Arbeit werden die Optimierung der Gewinnung von Lolinalkaloiden und Schritte zu Entschlüsselung deren biologischer Aktivität beschrieben (Abbildung 7). Hierzu wurden Chloroform-Extraktionen von Samen des Wiesenschweidels (*Festulolium loliaceum*) vorgenommen, die zuvor mit dem endophytischen Pilz *Neotyphodium uncinatum* infiziert wurden. Neben dem Hauptprodukt Lolin wurden auch weitere Alkaloide wie *N*-acetyl Lolin oder *N*-formyl Lolin isoliert. Temulin, *N*-acetyl Temulin, *N*-formyl Temulin wurden synthetisch hergestellt. Zur Untersuchung der biologischen Aktivität der Alkaloide wurden unter anderem Versuche an dem Nematoden *C. elegans* durchgeführt. *N*-acetyl Temulin und Lolin verursachten im Schwimmversuch eine gesteigerte Schwimmschlagfrequenz.

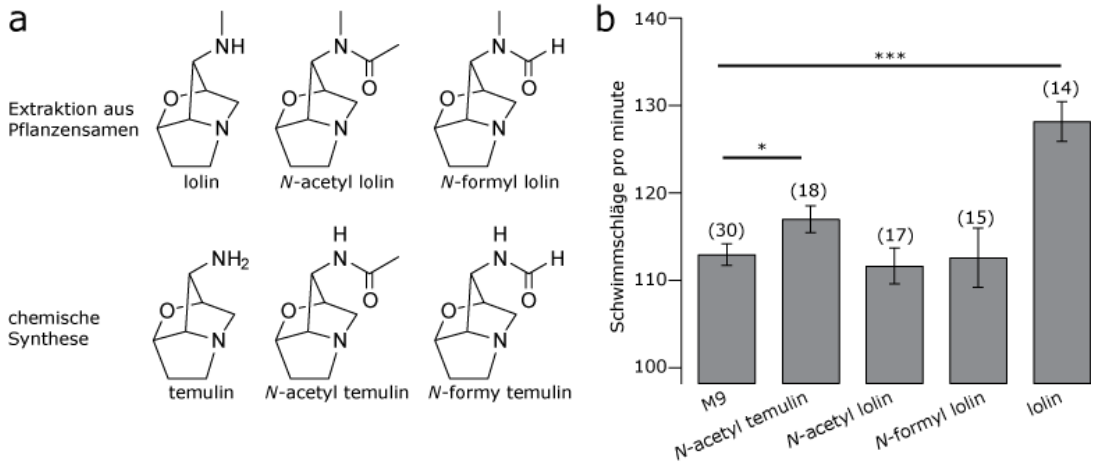

Abbildung 7. Lolinalkaloide ändern das Schwimmverhalten von Nematoden. a) Die Alkaloide Lolin, *N*-acetyl Lolin, *N*-formyl Lolin können aus Pflanzensamen extrahiert werden. Temulin, *N*-acetyl Temulin, *N*-formyl Temulin werden synthetisch hergestellt. b) Im Schwimmversuch reagieren Nematoden (*C. elegans*) mit höherer Schwimmfrequenz auf *N*-acetyl Temulin und Lolin.

I: Photopharmacology of Nicotinic Acetylcholine Receptors

The Photopharmacology of Nicotinic Acetylcholine Receptors

Arunas Damijonaitis, David M. Barber and Dirk Trauner

Department of Chemistry and Pharmacy, Ludwig-Maximilians Universität München and Center for Integrated Protein Science Munich, 81377 München, Germany

This work will be published in Current Signal Transduction Therapy (2015)

Editor of the thematic issue: Hugo R. Arias

Publisher: Bentham Science Publishers

Abstract

Nicotinic acetylcholine receptors (nAChRs) are one of the most abundant classes of receptors present in the mammalian nervous system and play a significant role in synaptic transmission. The development of new tools that can precisely control the function of nAChRs is important for the study of their complex biological processes. It could also lead to new therapeutic treatments for neurological diseases associated with nAChRs. Herein, we present a review of the photopharmacology of nAChRs, where small photochromic ligands are used to control function using the high spatial and temporal precision of light. A survey of the literature shows that, although several diffusible photochromic ligands and photochromic tethered ligands exist, further development of new molecules is required to allow in-depth studies into the role of different nAChR subtypes.

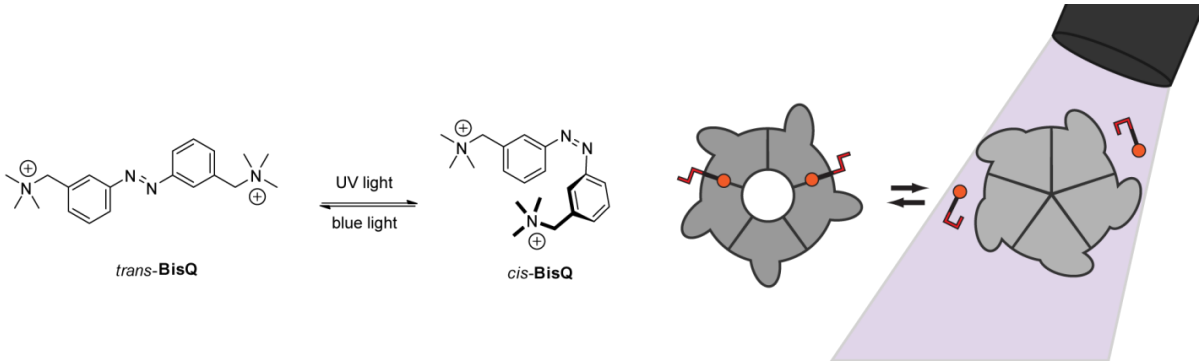

Graphical abstract.

Keywords: nicotinic acetylcholine receptor, photopharmacology, azobenzene, photoswitch, BisQ, optochemical genetics, photochromic tethered ligand

Abbreviations: nAChR, nicotinic acetylcholine receptor; mAChR, muscarinic acetylcholine receptor; AChE, acetylcholinesterase; RT, room temperature; PCL, photochromic ligand; DRG, dorsal root ganglion; UV, ultra violet; MEA, multielectrode array; HEK293T cells, Human Embryonic Kidney cells type 293T

Nicotinic Acetylcholine Receptors in the Neural System

Nicotinic acetylcholine receptors (nAChRs) are ligand-gated ion channels that are highly abundant in the mammalian nervous system, playing a major role in synaptic transmission between neurons and at the neuromuscular junction. These receptors are highly important for movement and cognitive functions, such as memory and reward mechanisms. Beside the crucial involvement in nicotine addiction, malfunctions in cholinergic communication often lead to severe diseases like epilepsy, Parkinson's or Alzheimer's disease [1,2]. In general, neuronal nAChRs consist of five subunits, which can be either heteropentamers (combinations of α2 - α10 and β2 - β4) or homopentamers (α7 - α9). Because of the complexity and diversity of cholinergic function, a variety of these nAChR subtype compositions can be found in the brain. These subtypes not only differ in their affinities towards their endogenous ligand acetylcholine (ACh), but also in their kinetic profiles of channel activation and deactivation [3]. For example, homopentameric α7 nAChRs show lower affinity and faster desensitization compared to heteropentameric α4β2 nAChRs, resulting in a different cellular response to the same stimulus. This response is shaped by the different kinetics and ion permeability of individual receptors.

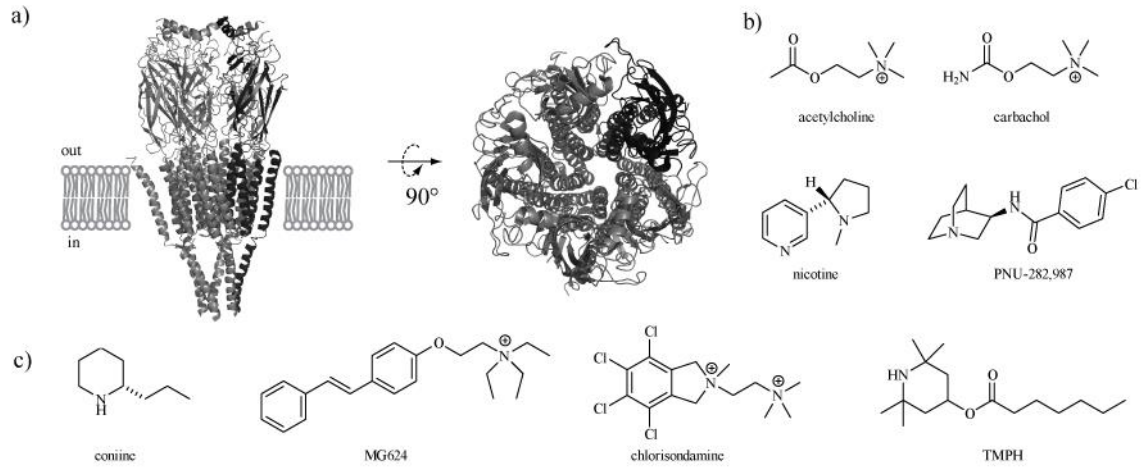

Fig. (1). Structure of the muscle-type nAChR with a selection of agonists and competitive antagonists. a) Structural model derived from cryo-electron microscopy data of Torpedo nAChRs as viewed from the side and the top (pdb:2bg9) [5]. b) Selection of agonists for nAChRs, including the endogenous ligand acetylcholine and the natural product nicotine. c) Selection of synthetic and natural antagonists for nAChRs.

In order to study cholinergic systems, a broad pharmacological toolset has been developed over recent decades [4]. It is now possible to target many receptor subtypes with highly specific agonists and antagonists (Fig. **1**). However, nAChRs are usually investigated with electrophysiology experiments that use bath application of an agonist or antagonist. These conditions are slow, imprecise and often do not correspond to physiological conditions, since the compound is used at high concentrations and cannot be quickly cleared. These properties stand in contrast to the fast dynamic characteristics of activation of cholinergic signals. Lately several methods have been introduced to overcome these limitations, unfortunately bringing other disadvantages with them. For instance, local pressure pulse application of cholinergic ligands is spatially precise and quick, but nevertheless is only applicable for single cell investigations. When investigating neural circuits, this method meets its limitations. Thus, there is a need for a pharmacological solution that can overcome these restrictions. This is where photopharmacology comes into its own.

Photopharmacology and Azobenzene Photoswitches

Due to the numerous subtypes and the complex pharmacology of nAChRs, there is a great need for new methods that can reversibly control their function [6]. To achieve the desired dynamic control, an external stimulus is required that can be accurately controlled with high spatial and temporal precision, as well as exhibiting low or negligible toxicity in biological systems. The use of light as the external stimulus fulfills all of these requirements, for it can be efficiently manipulated by adjusting its wavelength and intensity, whilst not interfering with other biological processes [7-9].

To enable the optical control of a protein, the structure of an organic molecule that interacts with the desired target has to be modified to incorporate a functionality that undergoes a transformation when exposed to light. In its most simple incarnation, a photolabile component is introduced resulting in an inactive caged molecule [10]. Upon exposure to light, the cage is removed and the active molecule is released enabling it to affect its biological target. Several caged molecules that target nAChRs, have been reported over recent years (Fig. **2**) [11-13]. NPE-Carbachol and CNB-carbachol have the cage covalently attached to the carbachol, while RuBi-nicotine is a metal complex with a non-covalently attached caging moiety. Although they have proved useful for the study of nAChRs, they do suffer from several drawbacks. For example, the light induced removal of the cage can only occur once, therefore reversible control of the desired target cannot be easily achieved. Additionally, the remainder of the cage needs to be compatible with the biological system under investigation [14]. It should be noted that several caged derivatives of choline, the biosynthetic precursor and cleavage product of ACh, have also been reported. However, they were used as tools to investigate the action of acetylcholinesterase (AChE) and not the function of nAChRs [15].

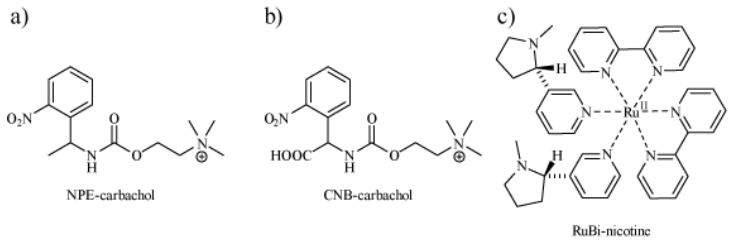

Fig. (2). Examples of caged agonists for nAChRs. a) NPE-carbachol [11]. b) CNB-carbachol [12]. c) RuBi-nicotine [13]. NPE = 1-(2-nitrophenyl)ethyl. CNB = α-carboxy-2-nitrobenzyl. RuBi = tris(bipyridine)ruthenium(II).

Another method that exploits the high spatial and temporal precision of light is provided by optogenetics [16]. Rather than using a synthetic organic compound, optogenetics achieves dynamic control of biological functions via photoresponsive proteins, such as rhodopsins [17], phototropins [18] and phytochromes [19]. These gain their photosensitivity through incorporation of abundant natural chromophores (retinal, flavine mononucleotide, biliverdin). Optogenetics has proven extremely useful for the study of biological processes, especially in neuroscience [20]. Cholinergic systems have been extensively studied using this method [21]. However, the nAChRs themselves have not been rendered photosensitive with mere genetic manipulation and the reliance on natural chromophores alone, which limits insights into the role of individual subtypes [22].

The photopharmacology approach involves the incorporation of *synthetic* photoswitchable ligands into proteins [23, 24]. Upon exposure to a certain wavelength of light, the ligand undergoes a conformational change, which can be reversed using light of another

wavelength or by thermal relaxation. If the pharmacological efficacy of the ligand changes upon switching, the target protein is essentially converted into a photoreceptor. Photopharmacology works particularly well in nonlinear systems, such as nervous systems and can enable ultra-fast and highly accurate control of biological functions.

There are several classes of molecular photoswitches reported in the literature, each with their own unique properties and characteristics [25]. Amongst these, the azobenzenes have arguably attracted the most attention from the scientific community, at least as far as biological applications are concerned (Fig. **3**) [26, 27]. This could be due to the fact that they can be synthesized with relative ease but also results from their advantageous geometrical and photophysical properties.

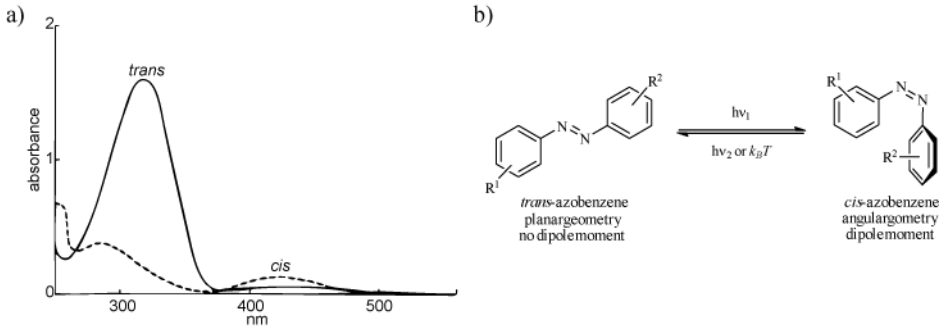

Fig. (3). Photoswitching characteristics of azobenzenes. a) UV-Vis spectrum of BisQ [31]. The difference in the UV-Vis absorption spectra of the *trans* and *cis* isomers is clearly visible. Figure modified from reference [28]. b) The structure of *trans* and *cis* azobenzene showing the putative change in geometry that occurs during the isomerization process. BisQ = [(*E*)-diazene-1,2-diyldibenzene-3,1-diyl]bis(*N*,*N*,*N*-trimethylmethanaminium).

Azobenzenes, which belong to the smallest photoswitches, can exist as *trans* and *cis* isomers, where the *trans* isomer is the thermodynamically more stable [28]. When irradiated with light (typically 360-480 nm), the *trans* isomer undergoes photochemically induced isomerization to form the *cis* isomer. The *cis* isomer can be converted back to its *trans* isomer using a longer wavelength or via thermal relaxation. Both light induced isomerizations generally occur in the range of picoseconds, whereas the thermal relaxation takes place anywhere in the range of milliseconds to days depending on the substitution pattern of the azobenzene [29, 30]. The fastness of photoswitching prevents intersystem crossing to triplet states, which could result in formation of singlet oxygen under biological conditions. The *trans* to *cis* isomerization of the azobenzene comes along with a considerable change in its geometry. A *trans* azobenzene is almost planar and has little or no dipole moment. In contrast, a *cis* azobenzene exhibits an angular geometry and has a considerable dipole moment [30].

Analysis of the UV-Vis absorption spectrum of the azobenzene BisQ [31], photochromic agonist for neuromuscular nAChRs (see below), reveals two distinct absorption bands (Fig. **3a**). The very intense band (280-340 nm) is indicative of the $\pi \rightarrow \pi^*$ transition whereas the weaker band (380-480 nm) is characteristic of the $n \rightarrow \pi^*$ transition. The variation of substituents on the azobenzene core can change the spectral sensitivity and kinetics of the photochemical and thermal isomerization (Fig. **4**) [32-35]. For example, the addition of an electron-donating group in the *para* position on one aromatic ring creates a class of azobenzenes referred to as 'aminoazobenzenes' (Fig. **4b**). The absorption maxima in these compounds is red-shifted towards the visible region of the spectrum and the thermal relaxation of the *cis* isomer is faster. Also, the $\pi \rightarrow \pi^*$ and $n \rightarrow \pi^*$ bands lie closer together. Azobenzenes that contain both a *para* electron-donating group and a *para* electron-withdrawing group are called 'pseudo-stilbenes' (Fig. **4c**).

Their absorption maxima are further red-shifted with thermal relaxation occurring very fast. In this regard, the addition of substituents to azobenzene photoswitches enables them to effectively be tuned to give the desired properties for a certain purpose [36]. Very recently, there has been a surge in new azobenzene motifs that offer interesting and remarkable photoswitching properties, such as bistability (i.e. the molecule stays in its excited conformational state without further illumination) and very red-shifted photoswitching wavelengths (Fig. **4d-g**) [37-40]. Of particular interest to photopharmacology are the red-shifted azobenzenes as they can take advantage of the increased tissue penetration of red light [41].

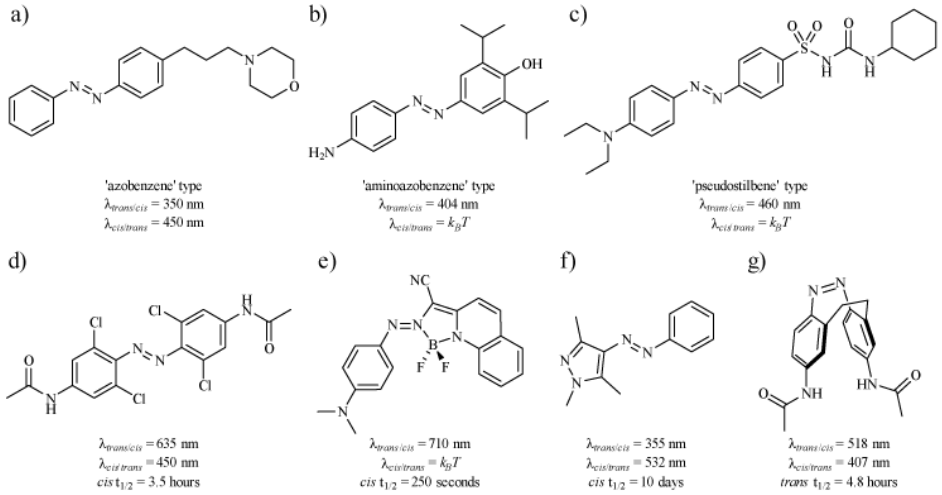

Fig. (4). Examples of azobenzenes that exhibit different photoswitching properties. a) Fotocaine is an 'azobenzene class' photoswitch [33]. b) Azo-propofol is an 'aminoazobenzene class' photoswitch [34]. c) JB253 is a 'pseudo-stilbene class' photoswitch [35]. d) A tetra-*ortho* substituted azobenzene that is photoswitched with red and blue light [37]. e) A photoswitch that is isomerized with near-infrared light [38]. f) A bistable arylazopyrazole photoswitch [39]. g) A bistable cyclic azobenzene derivative that is thermodynamically more stable in its *cis* form [40]. Fotocaine = 4-(3-{4-[(*E*)-phenyldiazenyl]phenyl}propyl)morpholine. Azo-propofol = 4-[(*E*)-(4-aminophenyl) diazenyl]-2,6-di(propan-2-yl)phenol. JB253 = *N*-(cyclohexylcarbamoyl)-4-{(*E*)-[4-(diethylamino)phenyl]diazenyl} benzenesulfonamide.

Although azobenzene photoswitches have dominated photopharmacology thus far, many other photoswitches have been used in biological systems with great success. Some of the photoswitches also exhibit interesting photoswitching properties that could be advantageous for photopharmacology. Among these photoswitches, stilbenes, dithienylethenes (DTEs), spiropyrans and hemithioindigos (HTIs) have received a large amount of attention from the community (Fig. **5**).

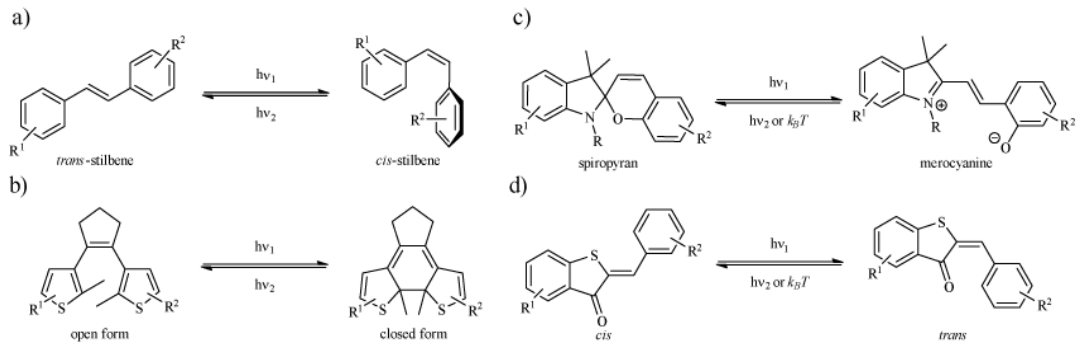

Fig. (5). Molecular structures and isomers of various photoswitches. a) The *cis* and *trans* isomers of a stilbene photoswitch. b) The open and closed forms of a DTE photoswitch. c) The isomeric forms of a spiropyran photoswitch. d) The *cis* and *trans* isomers of a HTI photoswitch.

Stilbenes are isoelectronic to azobenzenes and undergo photoisomerization to switch between their *cis* and *trans* isomers. The main difference between stilbenes and azobenzenes is that the *cis* isomer of stilbene is metastable, meaning that it does not thermally convert back to its *trans* isomer [42]. Although they are similar to azobenzenes, stilbene photoswitches exhibit two major disadvantages for applications in biological systems. Firstly, strong UV irradiation is required for the *trans* to *cis* isomerization and secondly, stilbenes suffer from a tendency to irreversibly cyclize and oxidize while in their *cis* forms preventing reversion back to their *trans* isomer [43]. DTE photoswitches are related to stilbenes by the fact that they are effectively *cis*-stilbenes that are fixed in the *cis* conformation by a bridging cyclohexene ring. The photochromism of diarylethenes arises from their ability to reversibly undergo photochemically induced cyclisation from its open form to its closed form [44]. Typically the open form is converted to the closed form by irradiating with UV light, with the reverse isomerization to the open form occurring with visible light illumination. Both the open and closed forms of the DTE photoswitches are thermally stable [44], this gives them unique opportunities for photopharmacology. Spiropyrans are a class of photoswitches that exhibit photochromism via reversible C-O bond cleavage that is induced by UV light. The cleavage of the C-O bond results in a zwitterionic conjugated system that is referred to as the merocyanine form. The reverse reaction back to the spiropyran can occur either thermally or by illumination with visible light [45]. The addition of substituents to the spiropyran motif can result in different equilibria between the spiropyran and merocyanine states, with some substituents resulting in complete reversal of the photochromism usually observed for spiropyran photoswitches [46]. HTIs are another class of photoswitch that exhibit *cis* to *trans* isomerization upon irradiation with distinct wavelengths of light. Illuminating with 400 nm light drives the *cis* to *trans* isomerization, with 480 nm light facilitating the reverse isomerization [47]. The photoswitching of hemithioindigos is very fast, occurring on the picosecond time scale and the thermal relaxation of the *trans* isomer back to the more stable *cis* isomer is very slow [48].

Optical control of nicotinic acetylcholine receptors.

Within the field of photopharmacology, two main strategies for ligand function and design are usually implemented. The first strategy is referred to as the photochromic ligand (PCL) approach, whereas the second strategy is called the photochromic tethered ligand (PTL) approach (Fig. **6**) [23]. The PCL approach consists of a soluble ligand that is endowed with a photoswitchable moiety, such as an azobenzene. Ideally, the PCL activates the target receptor as one isomer, but not as the other isomer. In the example shown in Fig. **6a**, the *trans* isomer of the PCL is able to bind to the ligand binding domain of the receptor and opens the channel, whereas the *cis* isomer of the PCL cannot bind to the receptor, resulting in closure of the channel. In contrast, the PTL approach involves molecules that incorporate a ligand, an azobenzene tether, and a bio-conjugation motive, allowing the entire construct to be conjugated to a genetically modified protein. In the example shown in Fig. **6c,** the *trans* photoswitch does not reach the binding pocket. When the ligand is photo isomerized, the *cis* conformation of the ligand reaches the binding pocket and activates the receptor. If the ligand is an antagonist (Fig. **6b, d**), the PCL or PTL can compete with the endogenous ligand for the binding pocket, which allows for another type of photocontrol. Ideally, this photoinhibition or activation occurs only in one configuration, enabling normal receptor function in the other configuration.

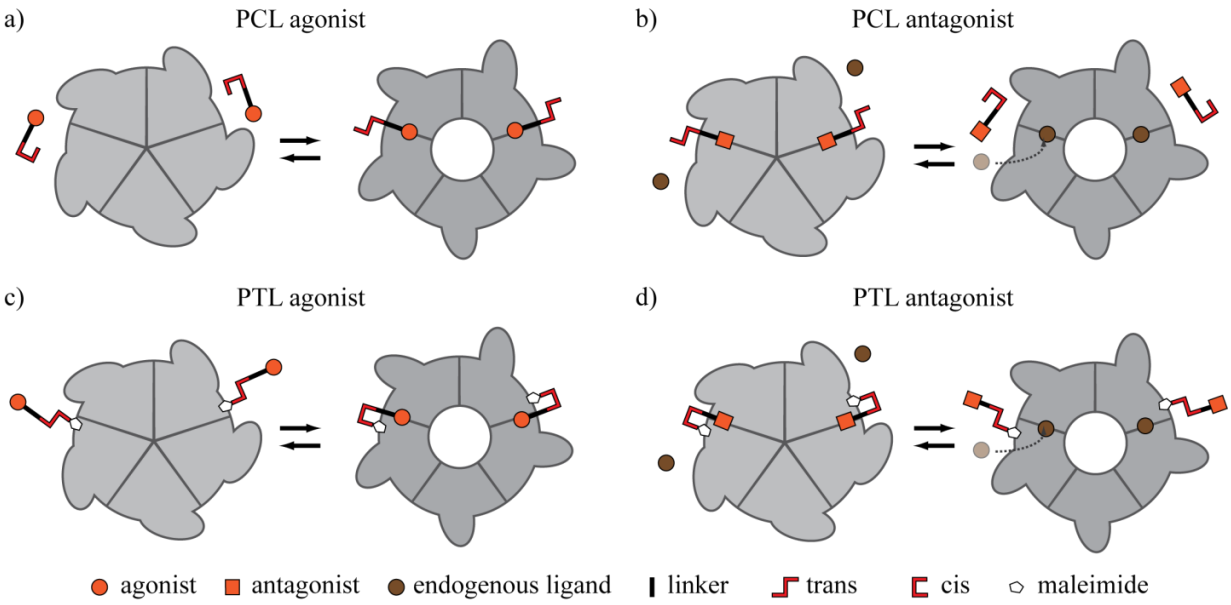

Fig. (6). Concept of the PCL and PTL approaches at pentameric ligand-gated ion channels. a) Agonistic PCL that is inactive as its *cis* isomer whilst the *trans* isomer is 'active'. b) Antagonistic PCL that displaces the endogenous ligand as its *trans* isomer and does not occupy the binding pocket as its *cis* isomer. c) Agonistic PTL that is active as its *cis* isomer and inactive as its *trans* isomer. d) Antagonistic PTL that displaces the endogenous ligand as its *cis* isomer and does not occupy the binding pocket as its *trans* isomer.

Both, the PCL and the PTL strategies, have their respective advantages and disadvantages. For example, one benefit of a PCL approach is that it does not require any genetic manipulation of the target cell or organism, making it applicable to endogenous receptors. The specific interaction of the PCL with the target receptor dictates if the activation occurs through the binding of the *cis* isomer or *trans* isomer. Because of the complexity of this binding it is difficult to predict the active form. When using the PTL approach, the attachment site of the photoswitch can be chosen based on the intended binding mode. Based on a three dimensional structural model of the target protein it is

possible to computationally model the binding of the ligand to the protein and then screen for suitable attachment sites.

In addition, the genetic modification required for PTLs allows the users to specifically target the exact receptor type and subtype that they wish to study. Over recent years, many PTLs have been developed that feature a maleimide as the electrophile for bio-conjugation to genetically engineered cysteines [49]. Maleimide chemistry *in vivo* bears many problems when the electrophile unspecifically reacts with freely accessible cysteines in the extracellular space or cytoplasm. Therefore alternative bio-conjugation motives like electrophiles that react specifically with certain genetically encoded protein domains such as SNAP or CLIP Tags might be more applicable in the future [50]. Nevertheless, both PCL and PTL strategies have been used to great effect with respect to nAChRs.

Turning nAChRs into Photoreceptors.

In the late 1960s, Erlanger and co-workers recognized that incorporating azobenzene photoswitches into known pharmacophores could enable the precise control of biological function using light. They envisaged that the *cis* or *trans* isomers of the azobenzene photodrug could have different bioactivities for the biological target, effectively resulting in the function of the target being turned 'on' or 'off' with different wavelengths of light. In essence, the relative concentration of the 'active' and 'inactive' compounds could be fine-tuned by the applying distinct wavelengths of light. This hypothesis was first successfully applied in 1968, when a PCL was used to optically control the inhibition of the digestive enzyme chymotrypsin [51]. In this study, the authors found that the *cis* isomer of their PCL was five times more efficient at inhibiting the effect of chymotrypsin than the *trans* isomer was. Shortly after this report, Erlanger and Nachmansohn demonstrated that the PCLs *p*-phenylazophenyltrimethylammonium (azo-PTA) and *N*-*p*-phenylazophenyl-*N*-phenylcarbamylcholine (azo-Ph-carbachol) were photoswitchable inhibitors of acetylcholine receptors (AChRs) (Fig. **7**) [52]. When tested on the excitable membrane obtained from the *Electrophorus electricus* electroplax of, both azo-PTA and azo-Ph-carbachol were found to function as antagonists in their *trans* forms. Exposure to 320 nm UV light with the accompanied *trans* to *cis* isomerization, resulted in a large depolarization of the electroplax membrane in the presence of the agonist carbachol. At this time it was not possible to distinguish whether this observation was due to nAChRs or muscarinic acetylcholine receptors (mAChRs).

An interesting feature of this study was that azo-PTA and azo-Ph-carbachol were derived from known agonists of nAChRs, such as phenyltrimethylammonium (PTA) (Fig. **7**) and carbachol (Fig. **1**). However, the presence of the azobenzene functionality in each of these compounds converts them from agonists to antagonists. This is an example of how the introduction of a photoswitch can have a profound effect on the pharmacology of a compound.

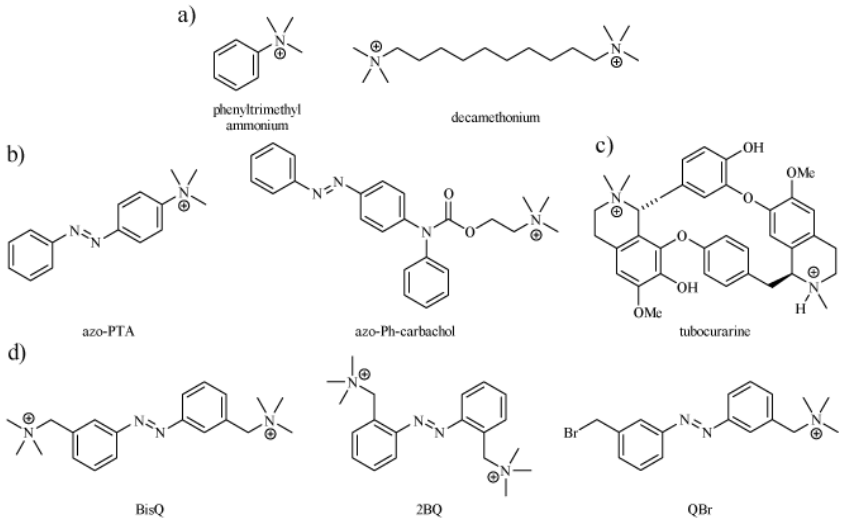

Fig. (7). nAChR agonists, PCLs and the first PTL for nAChRs. a) Agonists of nAChRs. b) Azo-PTA and azo-Ph-carbachol PCL antagonists of nAChRs. c) The nAChR antagonist tubocurarine. d) PCLs BisQ and 2BQ with the PTL QBr. Azo-PTA = *N*,*N*,*N*-trimethyl-4-[(*E*)-phenyldiazenyl]anilinium. Azo-Ph-carbachol = *N*,*N*,*N*-trimethyl-2-[(phenyl{4-[(*E*)-phenyldiazenyl]phenyl}carbamoyl)oxy]ethanaminium. 2BQ = [(*E*)-diazene-1,2-diyldibenzene-2,1-diyl]bis(*N*,*N*,*N*-trimethylmethanaminium). QBr = (3-{(*E*)-[3-(bromomethyl)phenyl] diazenyl}phenyl)-*N*,*N*,*N*-trimethylmethanaminium.

Shortly after the discovery of azo-PTA and azo-Ph-carbachol, Erlanger and Wassermann disclosed the photochromic nAChR agonist BisQ (Fig. **7d**) [53]. BisQ is a PCL that can be considered as the azologue [33] of the known nAChR partial agonist decamethonium, where the 10 membered carbon chain is replaced by an azobenzene moiety. BisQ was evaluated in the electroplax membrane in a similar fashion to their previous studies (Fig. **8**). The *trans* isomer of BisQ was found to be a very potent nAChR agonist, inducing depolarization of the electroplax membrane. Rapid repolarization of the membrane then occurred when irradiating with 360 nm light.

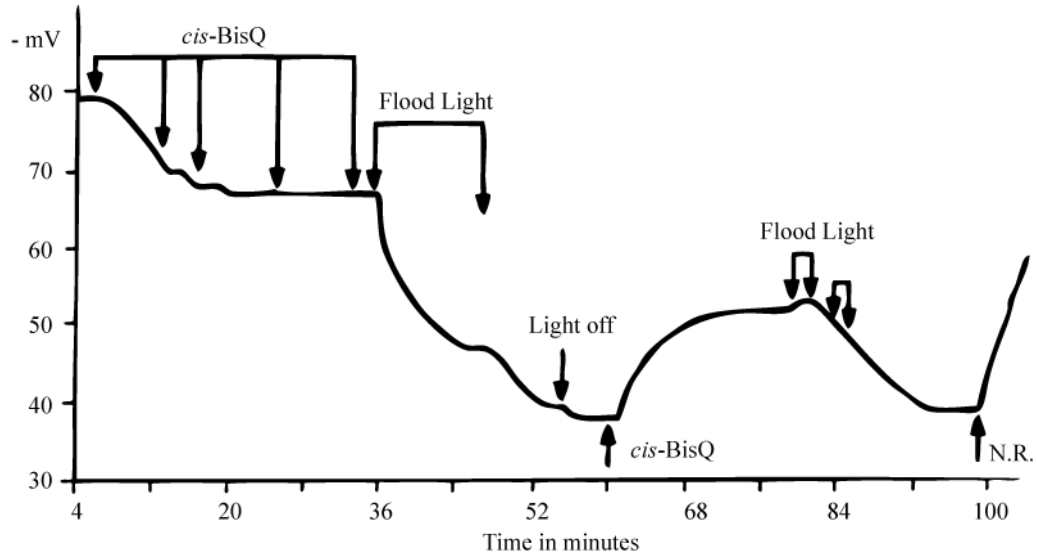

Fig. (8). Photoregulation of the nAChR function by BisQ using electroplax membranes. BisQ was washed in its *cis* form. Irradiation with an intense light source (Flood Light) isomerized BisQ to its *trans* form activating the receptor. N.R. is normal Ringer's solution. Figure modified from reference [53].

Concentration-response studies revealed that *trans*-BisQ (EC_{50} = 60-80 nM) is 500 times more potent than the AChR agonist carbachol. However, the maximal response to *trans*-BisQ is lower (i.e., partial agonist) than that of carbachol at high concentrations. In contrast to *trans*-BisQ, *cis*-BisQ showed very low activity, with the authors postulating that a pure sample of *cis*-BisQ may not exhibit any activity towards nAChRs at all. Studies on the activity of *trans*-BisQ in the presence of the nAChR antagonist tubocurarine showed that at low concentrations of *trans*-BisQ, the depolarization was blocked. When the concentration of *trans*-BisQ was increased, repolarization of the membrane ensued. This occurred both in the presence and in the absence of d-tubocurarine, therefore the authors speculated, that there are two binding sites for *trans*-BisQ with only one competing with tubocurarine.

Later, the successful photochromic agonist BisQ was turned into an antagonist by changing the positions of the quarternized amines from the 3,3' to the 2,2' positions [54]. This resulted in the PCL 2BQ (Fig. **7d**), which enabled investigations to further understand antagonist-receptor binding. Studies in *Electrophorus* electroplaques revealed that the receptor activation by carbachol could be allowed by the *cis* to *trans* isomerization of 2BQ, while flash-induced *trans* to *cis* concentration jumps decreased agonist induced currents within milliseconds [55].

In 1969, Siliman and Karlin introduced the idea of covalently attaching an agonist to a nAChR [56]. For this, a disulfide bond near the active site of the receptor was reduced with dithiothreitol and the agonist was tethered to the protein. With Erlanger's knowledge of photocromic agonists, this technique was combined with BisQ yielding QBr (Fig. **7**). QBr has a very similar structure to BisQ except that a bromine atom replaces one of the trimethylammonium groups. This converts the PCL into a PTL as the reduced disulfides can now react with the benzylic bromide, tethering it to the receptor. The attached agonist could now be presented to the active site and removed from it by changing the illumination wavelength. This overcame the major drawback of Karlin's approach, namely desensitization of the receptor [56]. Interestingly, both the freely diffusible BisQ and the tethered QBr activate the receptor in their *trans* configurations and not in their *cis*

configurations [57]. When attached to the receptor, QBr induced currents were not blocked by the competitive antagonist d-tubocurarine. Nevertheless, the receptor remained sensitive to open-channel blockers. When compared with each other, BisQ and QBr induce similar kinetics for channel opening and closing. Thus, the authors speculated that the rate-limiting step was not the diffusion of the molecules, but rather the conformational change of the agonist-receptor-channel complex [57].

Since the introduction of QBr, molecular cloning, heterologous expression, X-ray crystal structures and molecular modeling have revolutionized our ability to understand and control biological systems. Nowadays, with knowledge of the genetic code and the availability of three dimensional receptor structures, it is possible to change the DNA via site directed mutagenesis to exchange a single amino acid in the protein at a desired position. Furthermore, when investigating neural circuits, cell and receptor subtype specificity can be achieved within a tissue by using specific promoters or a Cre-Lox expression system. Additional spatiotemporal control can be provided by attaching a photoswitch to the engineered protein that ultimately can be controlled with light. In 2012, Trauner and Kramer introduced the genetically engineered light-controlled nAChR (LinAChR) [58]. Through structure-based design, an azobenzene photoswitch and a maleimide functionality were added to the nAChR photoaffinity label AC-5, affording the photoswitchable nAChR agonist MAACh (Fig. **9**). The known nAChR agonist homocholine phenyl ether (HoChPE) was converted to the photoswitchable nAChR antagonist MAHoCh.

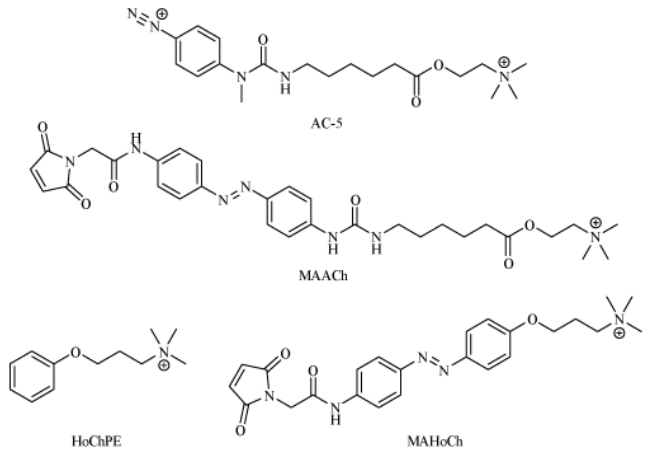

Fig. (9). The nAChR PTLs MAACh and MAHoCh along with their parent ligands AC-5 and HoChPE. AC-5 = 2-{4-[(*E*)-(4-diazoniophenyl)diazenyl]phenyl}-14,14-dimethyl-3,10-dioxo-11-oxa-2,4-diaza-14-azoniapentadecane. MAACh = 2-({6-[({4-[(*E*)-(4-{[(2,5-dioxo-2,5-dihydro-1H-pyrrol-1-yl)acetyl]amino}phenyl)diazenyl]phenyl} carbamoyl)amino]hexanoyl}oxy)-*N*,*N*,*N*-trimethylethanaminium. MAHoCh = 3-{4-[(*E*)-(4-{[(2,5-dioxo-2,5-dihydro -1*H*-pyrrol-1-yl)acetyl]amino}phenyl)diazenyl]phenoxy}-*N*,*N*,*N*-trimethylpropan-1-aminium. HoChPE = *N*,*N*,*N*-trimethyl-3-phenoxypropan-1-aminium.

By modeling the molecules into the binding domain of the X-ray crystal structure of the acetylcholine binding protein (AChBP) and the *Torpedo* nAChR, several candidate amino acid positions were identified to carry the cysteine mutation for bio-conjugation with the maleimide. Ideally the photoswitch does not interfere with the receptors natural function when attached to the protein. Only when light is applied the molecule should evoke an effect. Therefore the conjugation site was chosen at a position where the *cis*, but not the *trans* isomer of the photoswitch reaches the binding pocket. The engineered $\alpha3\beta4$ and the $\alpha4\beta2$ nAChRs, expressed in *Xenopus* oocytes, were both turned into photoreceptors when the agonist MAACh was used (Fig. **10a**). By shining 380 nm light onto the oocyte, LinAChR was activated evoking an inward current, which was recorded via two electrode voltage clamp (TEVC). Changing the wavelength to 500 nm allowed closing of the

receptor. Furthermore, light induced inhibition of nAChR current was achieved by attaching the antagonistic photoswitch MAHoCh to the same cysteine residue in α3β4 and α4β2 nAChRs (Fig. **10b**). The effect of ACh (300 µM) application could be blocked to a certain degree by irradiation of 380 nm light, while the same stimulus resulted in a strong inward current when illuminated with 500 nm light. Notably, both variants behaved like normal nAChRs in the dark. The authors speculated that inhibition of the receptor might be also achieved by attaching the agonistic molecule to another position, where it occupies the binding pocket, but does not induce a current [59].

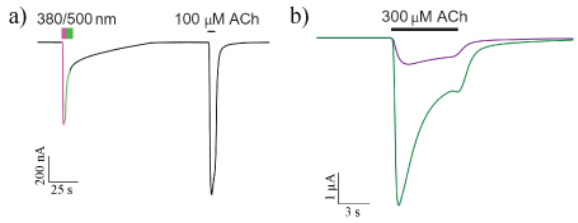

Fig. (10). Photocontrol of α4β2 LinAChRs in *Xenopus* oocytes. a) Photoactivation of the α4β2E61C mutant receptor by MAACh followed by activation with ACh. b) Photodependent antagonism of the α4β2E61C mutant receptor by MAHoCh under 500 nm light (green lines) and 380 nm light (violet lines). Figure modified from reference [58].

The latest addition to the cholinergic photopharmacology toolbox is the PCL AzoCholine (Fig. **11**), which consists of a choline moiety that is attached to an azobenzene [60]. Structurally it closely resembles the α7 nAChR antagonist MG624 (Fig. **1**) with one crucial difference. The quaternary amine of AzoCholine bears three methyl groups instead of three ethyl groups. UV/Vis studies revealed that the *cis* isomer can be enriched by illuminating the sample with 360 nm light. To convert the molecule to its *trans* isomer 460 nm was the most efficient wavelength. Experiments in Human Embryonic Kidney (HEK) cells heterologously expressing either the neuronal α7 nAChR or the neuromuscular nAChR, showed that photoactivation of AzoCholine could induce a rapid and strong inward current at the neuronal nAChR, while having no photoswitchable effect at the neuromuscular nAChR. In dissociated rat dorsal root ganglion (DRG) cells activation could be triggered by photoactivation of AzoCholine, which could be recorded via calcium imaging. Here, the specificity of AzoCholine for the endogenous α7 nAChRs was demonstrated by blocking the effect with the α7 specific antagonist MG624. Furthermore, network activity could be modulated as demonstrated by multielectrode array (MEA) recordings from acute mouse hippocampal brain slices. When illuminating the preparation containing AzoCholine with 460 nm light, bursting activity in the hippocampal region increased, while 360 nm light decreased neural activity. Finally, the in vivo applicability of AzoCholine was demonstrated when swimming behavior of *C. elegans* could be controlled with AzoCholine and light irradiation.

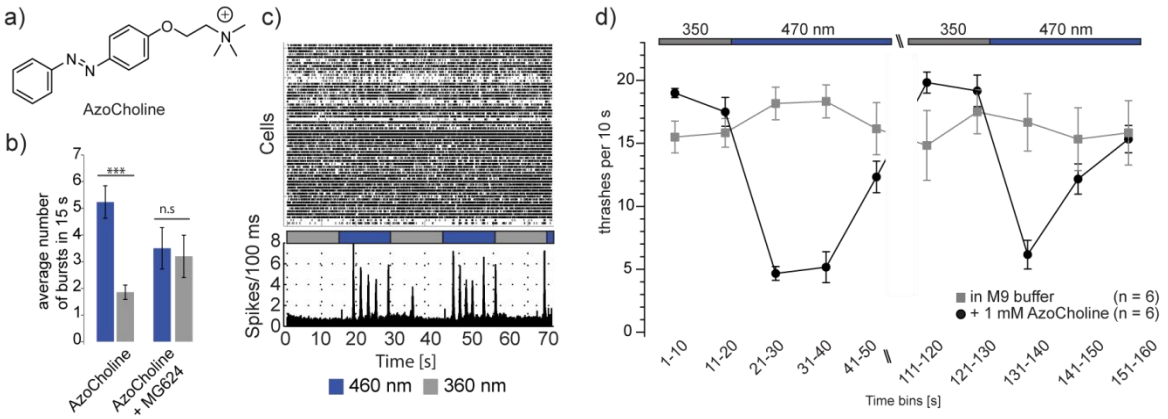

Fig. (11). Photocontrol of neural networks with AzoCholine. a) Molecular structure of AzoCholine. b) Bursting activity in mouse hippocampal brain slices. Summary of 6 MEA experiments showing the photo-modulative effect of AzoCholine and the effect of MG624. c) Raster plot of single cell spiking activity in the presence of AzoCholine (50 μM) with the correlating histograms over all cells. Switching light from 360 nm (gray bar) to 460 nm light (blue bar) leads to an increase in bursting activity and *vice versa*. d) Quantification of *C. elegans* swimming cycles showing photo-dependent perturbation when 470 nm light is applied. Figure modified from reference [60].

AzoCholine effectively turns endogenous α7 nAChRs into photoreceptors. By varying the irradiation wavelengths, the concentration of the active form of AzoCholine can be adjusted in a graded fashion, an effect which is termed photodosing. Thus, it is now feasible to control endogenous nAChRs with high spatiotemporal precision. This will be instrumental for elucidating their roles in the nervous system and may prove to be therapeutically useful as well.

Other Cholinergic Targets for Photopharmacology

Apart from nAChRs, the mAChRs [61] are also attractive targets for photopharmacology. In 1982, Lester and co-workers reported several photoswitchable ligands that behaved as antagonists of mAChRs in frog myocardium [62]. These compounds included known PCLs for nAChRs, such as BisQ, 2BQ and azo-Ph-carbachol (Fig. **7**), as well as the new PCLs 4BQ, azo-carbachol and azo-Me-carbachol (Fig. **12a**). They were all found to block the outward currents that were produced by mAChR agonists in frog atrial trabeculae. It was demonstrated that the compounds were more potent antagonists as their *trans* isomers. The *cis* isomers still exhibiting blocking activity, albeit in a much weaker fashion than their *trans* isomers. The action of BisQ on mAChRs was studied in further detail due to its greater availability. Despite this promising first report, further research into PCLs for mAChRs has not yet been disclosed. Recent work has focused on the development of photoaffinity labels [63] that can either activate or inhibit the function of mAChRs [64-66].

Another related target for photopharmacology is that of the enzyme AChE [67]. Although this is not a receptor, AChE plays a crucial role in the cholinergic nervous system by removing ACh from the synaptic cleft. Long-term inhibition of AChE can have catastrophic effects on organisms, as demonstrated by nerve gas agents such as sarin. However, short-term inhibiting the AChE can instead have beneficial effects, for instance in decreasing the symptoms of Alzheimer's disease. Therefore, photoswitches that can control the function of AChE would be important biological tools. The first report on the optical control of AChE function was disclosed in 1969 using azo-PTA (Fig. **7b**) [68]. This

compound was found to be most active as its *trans* isomer, whilst exposure to UV light reduced the amount of inhibition observed as conversion to the *cis* isomer occurred. Azo-PTA could also be used to reversibly control AChE activity, with the compound being shown to exhibit no significant loss of activity over several switching cycles. However, the overall change in AChE inhibition upon isomerization between the trans and cis isomers of azo-PTA was only modest. Shortly after this initial report, Erlanger and co-workers demonstrated that they were able to control the inhibition of AChE using the PCL azo-carbachol [69]. Azo-carbachol was able to induce moderate changes in AChE activity when using filtered UV light (366 nm) and darkness for the isomerization of the azobenzene photoswitch. Relaxation of the *cis* isomer back to the more thermodynamically stable *trans* isomer occurred within 600 seconds in the dark, with a half-life of around 120 seconds. The *trans* isomer of azo-carbachol was found to be the most active, resulting in the largest amount of AChE inhibition. Interestingly, in this publication the authors demonstrated that sunlight could also be used for the *trans* to *cis* isomerization of azo-carbachol. This process was show to be reversible over many switching cycles without substantial loss of activity for either the *trans* or *cis* isomers.

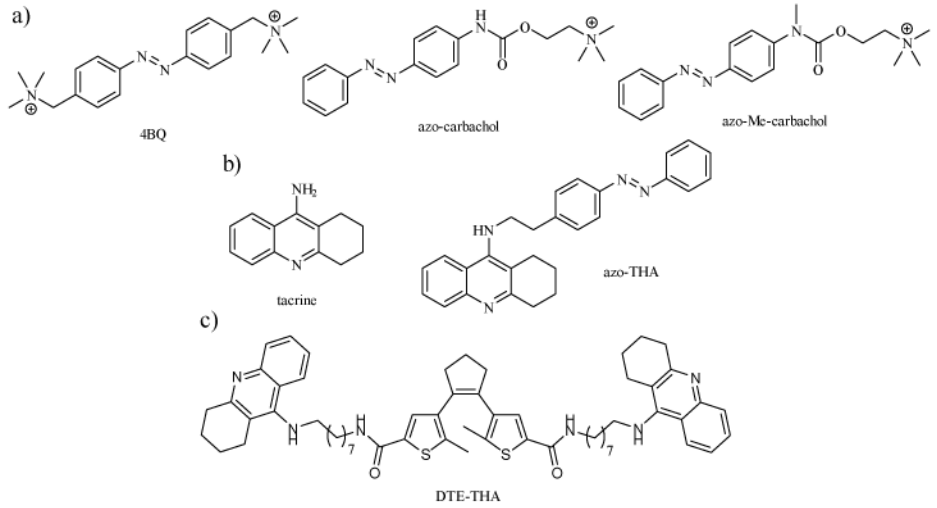

Fig. (12). Examples of PCLs for the control of mAChRs and AChE. a) The PCLs 4BQ, azo-carbachol and azo-Me-carbachol. b) Structure of tacrine, an AChE inhibitor used in the treatment of Alzheimer's disease and azo-THA. c) Molecular structure of DTE-THA. 4BQ = ([(*E*)-diazene-1,2-diyldibenzene-4,1-diyl]bis(*N*,*N*,*N*-trimethyl methanaminium). Azo-carbachol = (*N*,*N*,*N*-trimethyl-2-[({4-[(*E*)-phenyldiazenyl]phenyl}carbamoyl)oxy] ethanaminium. Azo-Me-carbachol = (*N*,*N*,*N*-trimethyl-2-[(methyl{4-[(*E*)-phenyldiazenyl]phenyl}carbamoyl)oxy] ethanaminium. Azo-THA = (*N*-(2-{4-[(*E*)-phenyldiazenyl]phenyl}ethyl)-1,2,3,4-tetrahydroacridin-9-amine). DTE-THA = 5-methyl-4-[2-(2-methyl-5-{[7-(1,2,3,4-tetrahydroacridin-9-ylamino)heptyl]carbamoyl}thiophen-3-yl)cyclo pent-1-en-1-yl]-*N*-[8-(1,2,3,4-tetrahydroacridin-9-ylamino)octyl]thiophene-2-carboxamide.

The seminal work of Erlanger and co-workers was not further expanded until very recently, when Trauner [70] and Decker [71] reported photoswitchable inhibitors for the optical control of AChE function. Although the reports were published independently, both groups used the AChE inhibitor tacrine as the pharmacophore. The difference between the two approaches came in the form of the photoswitch used. Trauner and co-workers prepared a photoswitchable tacrine derivative (azo-THA) that was linked to an azobenzene photoswitch via the tacrine amine functionality (Fig. **12b**). Azo-THA was evaluated for its AChE inhibition activity using a colorimetric assay in conjunction with acetylthiocholine (ATCh) and Ellman's reagent. Under illumination with 440 nm light, *trans* azo-THA enabled the ATCh is to hydrolyzed, indicating that *trans* azo-THA does not act as an AChE inihibitor. Changing the illumination to UV light at 350 nm completely

stopped the hydrolysis of ATCh, showing that the AChE was inhibited. The photoswitching process could be dynamically controlled over many switching cycles. The effect that azo-THA had on mouse trachea preparations was also studied. The smooth muscle of the trachea constricts in response to ACh, this can be recorded by tracheal tensometry. It was observed that different relaxation kinetics were observed in the trachea preparations depending on the light illumination. In the presence of *cis* azo-THA (UV light), AChE is inhibited to a greater extent resulting in slower relaxation kinetics (15.25 seconds). In contrast, with *trans* azo-THA there is less inhibition and therefore the relaxation of the trachea occurs at a faster rate (11.29 seconds).

Decker and co-workers designed their photoswitchable AChE inhibitor with two molecules of tacrine that were linked by a DTE photoswitch (Fig. **12c**). The photochromic molecule DTE-THA was converted to its closed form within 30 seconds when irradiated with UV light (312 nm). The reverse isomerization to the open form occurred when illuminating the photoswitch with >420 nm light. However, this isomerization was considerably slower with illumination times of 5 minutes being required. It is worth noting that some fatigue of the photoswitch ensued after 8 switching cycles. This could be a major drawback for prolonged use of DTE-THA as a reversible AChE inhibitor. The IC_{50} values of the open and closed forms of DTE-THA were determined using a human AChE (hAChE) assay. The closed form was found to be the most potent inhibitor of hAChE (IC_{50} closed = 19.1 nM). However, the open form also exhibited inhibitory activity within the nanomolar range (IC_{50} open = 49.6 nM). Although the open and closed forms of DTE-THA varied in their amounts of hAChE inhibition, dynamic control of hAChE inhibition was not demonstrated in this report.

Summary

Over the last five decades, an impressive toolset for the optical control of nAChRs has been developed. This includes compounds that function as soluble and tethered agonists and competitive antagonists. Some of these compounds have also been applied to mAChRs and AChEs. However, because of the diversity of nAChRs there is still a need for the development of selective PCLs that can optically control nAChR function. In addition, the potential of PTLs with regard to controlling specific receptor subtypes has yet to be fully realized. This will make it possible to investigate the differences between individual receptor subtypes in the same cell, also differentiating between different binding sites. We envisage that major advances in the field will be made shortly, allowing scientists to further their understanding of nAChRs and the many roles they play in the nervous system. We also postulate that new light controlled drugs (photopharmaceuticals) will emerge from this photopharmacological toolset, opening new therapeutic avenues for the treatment of debilitating cholinergic diseases.

Acknowledgements: We gratefully acknowledge the generous financial support of the International Max Planck Research School for Molecular and Cellular Life Sciences (Fellowship to A.D.), the European Commission (Marie Skłodowska-Curie Intra-European Fellowship to D.M.B [PHOTOLEG, 627990]), the Center for Integrated Proteins Science Munich (D.T.) and the European Research Council (Advanced Grant to D.T. [268795]).

References:

[1] Kalamida D, Poulas K, Avramopoulou V, *et al.* Muscle and neuronal nicotinic acetylcholine receptors. Structure, function and pathogenicity. FEBS J 2007; 274: 3799-845.
[2] Lemoine D, Jiang R, Taly A, Chataigneau T, Specht A, Grutter T. Ligand-gated ion channels: new insights into neurological disorders and ligand recognition. Chem Rev 2012; 112: 6285-318.
[3] Dani JA, Bertrand D. Nicotinic acetylcholine receptors and nicotinic cholinergic mechanisms of the central nervous system. Annu Rev Pharmacol Toxicol 2007; 47: 699-729.
[4] Wonnacott S, Barik J. Nicotinic ACh receptors. Tocris Reviews 2007; 28: 1-20.
[5] Unwin N. Refined structure of the nicotinic acetylcholine receptor at 4A resolution. J Mol Biol 2005; 346: 967-89.
[6] Muñoz W, Rudy B. Spatiotemporal specificity in cholinergic control of neocortical function. Curr Opin Neurobiol 2014; 26:149-60.
[7] Gardner L, Deiters A. Light-controlled synthetic gene circuits. Curr Opin Chem Biol 2012; 16: 292-9.
[8] Mayer G, Heckel A. Biologically active molecules with a "light switch". Angew Chem Int Ed 2006; 45: 4900-21.
[9] Brieke C, Rohrbach F, Gottschalk A, Mayer G, Heckel A. Light-controlled tools. Angew Chem Int Ed 2012; 51: 8446-76.
[10] Klán P, Šolomek T, Bochet CG, *et al*. Photoremovable protecting groups in chemistry and biology: Reaction mechanisms and efficacy. Chem. Rev 2013; 113: 119-91.
[11] Walker JW, McCray JA, Hess GP. Photolabile protecting groups for an acetylcholine receptor ligand. Synthesis and photochemistry of a new class of *o*-nitrobenzyl derivatives and their effects on receptor function. Biochemistry 1986; 25: 1799-805.
[12] Milburn T, Matsubara N, Billington AP, *et al*. Synthesis, photochemistry, and biological activity of a caged photolabile acetylcholine receptor ligand. Biochemistry 1989; 28: 49-55.
[13] Filevich O, Salierno M, Etchenique R. A caged nicotine with nanosecond range kinetics and visible light sensitivity. J Inorg Biochem 2010; 104: 1248-51.
[14] Givens RS, Weber JFW, Jung AH, Park CH. In: Marriott G, Ed. Methods in Enzymology. New York, Academic Press 1998; Vol. 291: pp 1-29.
[15] Peng L, Goeldner M. Synthesis and characterization of photolabile choline precursors as reversible inhibitors of cholinesterases: Release of choline in the microsecond time range. J Org Chem 1996; 61: 185- 91.
[16] Fenno L, Yizhar O, Deisseroth K. The development and application of optogenetics. Annu Rev Neurosci 2011; 34: 389-412.
[17] Zhang F, Vierock J, Yizhar O, et al. The microbial opsin family of optogenetic tools. Cell 2011; 147: 1446-57.
[18] Christie JM. Phototropin blue-light receptors. Annu Rev Plant Biol 2007; 58: 21-45.
[19] Bae G, Choi G. Decoding of light signals by plant phytochromes and their interacting proteins. Annu Rev Plant Biol 2008; 59: 281-311.
[20] Deisseroth K, Feng G, Majewska AK, Miesenböck G, Ting A, Schnitzer MJ. Next-generation optical technologies for illuminating genetically targeted brain circuits. J Neurosci 2006; 26: 10380-86.
[21] Zhang F, Wang LP, Brauner M, *et al*. Multimodal fast optical interrogation of neural circuitry. Nature 2007; 446: 633-9.
[22] Jiang L, López-Hernández GY, Lederman J, Talmage DA, Role LW. Optogenetic studies of nicotinic contributions to cholinergic signaling in the central nervous system. Rev Neurosci 2014; 25: 755-71.
[23] Fehrentz T, Schönberger M, Trauner D. Optochemical genetics. Angew Chem Int Ed 2011; 50: 12156-82.
[24] Velema WA, Szymanski W, Feringa BL. Photopharmacology: Beyond proof of principle. J Am Chem Soc 2014; 136: 2178-91.
[25] Feringa BL, Browne WR. Molecular switches. Wiley-VCH: Weinheim 2011.
[26] Szymański W, Beierle JM, Kistemaker HA, Velema WA, Feringa BL. Reversible photocontrol of biological systems by the incorporation of molecular photoswitches. Chem Rev 2013; 113: 6114-78.

[27] Beharry AA, Woolley GA. Azobenzene photoswitches for biomolecules. Chem Soc Rev 2011; 40: 4422-37.
[28] Brown EV, Granneman GR. *Cis-trans* isomerism in the pyridyl analogs of azobenzene. A kinetic and molecular orbital analysis. J Am Chem Soc 1975; 97: 621-7.
[29] Rau H. In: Rabek JF, Ed. Photoisomerization of azobenzenes. In photochemistry and photophysics. Boca Raton, FL, USA, CRC Press 1990; Vol. 2: pp 119-42.
[30] Merino E, Ribagorda M. Control over molecular motion using the *cis-trans* photoisomerization of the azo group. Beilstein J Org Chem 2012; 8: 1071-90.
[31] Nass MM, Lester HA, Krouse ME. Response of acetylcholine receptors to photoisomerizations of bound agonist molecules. Biophys J 1978; 24:135-60.
[32] Bandara HMD, Burdette SC. Photoisomerization in different classes of azobenzene. Chem Soc Rev 2012; 41: 1809-25.
[33] Schoenberger M, Damijonaitis A, Zhang Z, Nagel D, Trauner D. Development of a new photochromic ion channel blocker via azologization of fomocaine. ACS Chem Neurosci 2014: 5: 514-8.
[34] Stein M, Middendorp SJ, Carta V, *et al*. Azo-propofols: Photochromic potentiators of $GABA_A$ receptors. Angew Chem Int Ed 2012: 51: 10500-4.
[35] Broichhagen J, Schönberger M, Cork SC, *et al*. Optical control of insulin release using a photoswitchable sulfonylurea. Nat Commun 2014; 5: 5116.
[36] Mourot A, Kienzler MA, Banghart MR, *et al*. Tuning photochromic ion channel blockers. ACS Chem Neurosci 2011; 2: 536-43.
[37] Samanta S, Beharry AA, Sadovski O, *et al*. Photoswitching azo compounds in vivo with red light. J Am Chem Soc 2013; 135: 9777-84.
[38] Yang Y, Hughes RP, Aprahamian I. Near-infrared light activated azo-BF_2 switches. J Am Chem Soc 2014; 136: 13190-3.
[39] Weston CE, Richardson RD, Haycock PR, White AJ, Fuchter MJ. Arylazopyrazoles: Azoheteroarene photoswitches offering quantitative isomerization and long thermal half-lives. J Am Chem Soc 2014; 136: 11878-81.
[40] Samanta S, Qin C, Lough AJ, Woolley GA. Bidirectional photocontrol of peptide conformation with a bridged azobenzene derivative. Angew Chem Int Ed 2012; 51: 6452-55.
[41] Kalka K, Merk H, Mukhtar H. Photodynamic therapy in dermatology. J Am Acad Dermatol 2000; 42: 389-413.
[42] Waldeck DH. Photoisomerization dynamics of stilbenes. Chem Rev 1991; 91: 415-436.
[43] Cammenga HK, Emel'yanenko VN, Verevkin SP. Re-investigation and data assessment of the isomerization and 2,2'-cyclization of stilbenes and azobenzenes. Ind Eng Chem Res 2009; 48: 10120-10128.
[44] Irie M. Diarylethenes for memories and switches. Chem Rev 2000; 100: 1685-1716.
[45] Berkovic G, Krongauz V, Weiss V. Spiropyrans and spirooxazines for memories and switches. Chem Rev 2000; 100: 1741-1754.
[46] Namba K, Suzuki S. Photo-control of enzyme activity with a photochromic spiropyran compound. Chem Lett 1975; 4: 947-950.
[47] Lougheed T, Borisenko V, Hennig T, Rück-Braun K, Woolley GA. Photomodulation of ionic current through hemithioindigo- modified gramicidin channels. Org Biomol Chem 2004; 2: 2798-2801.
[48] Maerz B, Wiedbrauk S, Oesterling S, *et al.* Making fast photoswitches faster – Using Hammett analysis to understand the limit of donor-acceptor approaches for faster hemithioindigo photoswitches. Chem Eur J 2014; 20: 13984-13992.
[49] Broichhagen J, Trauner D. The in vivo chemistry of photoswitched tethered ligands. Curr Opin Chem Biol 2014; 21: 121-7.
[50] Gautier A, Juillerat A, Heinis C, *et al.* An engineered protein tag for multiprotein labeling in living cells. Chem Biol 2008; 15:128-36.
[51] Kaufman H, Vratsanos SM, Erlanger BF. Photoregulation of an enzymic process by means of a light-sensitive ligand. Science 1968; 162: 1487-9.
[52] Deal WJ, Erlanger BF, Nachmansohn D. Photoregulation of biological activity by photochromic reagents, III. Photoregulation of bioelectricity by acetylcholine receptor inhibitors. Proc Natl Acad Sci USA 1969; 64: 1230-4.

[53] Bartels E, Wassermann NH, Erlanger BF. Photochromic activators of the acetylcholine receptor. Proc Natl Acad Sci USA 1971; 68: 1820-3.
[54] Wassermann NH, Bartels E, Erlanger BF. Conformational properties of the acetylcholine receptor as revealed by studies with constrained depolarizing ligands. Proc Natl Acad Sci USA 1979; 76: 256-9.
[55] Krouse ME, Lester HA, Wassermann NH, Erlanger BF. Rates and equilibria for a photoisomerizable antagonist at the acetylcholine receptor of *Electrophorus* electroplaques. J Gen Physiol 1985; 85: 235-6.
[56] Siliman I, Karlin A. Acetylcholine receptor: Covalent attachment of dopolarizing groups at the active site. Science 1969; 164: 1420-1.
[57] Lester HA, Krouse ME, Nass MM, Wassermann NH, Erlanger BF. A covalently bound photoisomerizable agonist: comparison with reversibly bound agonists at Electrophorus electroplaques. J Gen Physiol 1980; 75: 207-32.
[58] Tochitsky I, Banghart MR, Mourot A, *et al*. Optochemical control of genetically engineered neuronal nicotinic acetylcholine receptors. Nat Chem 2012; 4: 105-11.
[59] Sullivan DA, Cohen JB. Mapping the agonist binding site of the nicotinic acetylcholine receptor. Orientation requirements for activation by covalent agonist. J Biol Chem 2000; 275: 12651-60.
[60] Damijonaitis A, Broichhagen J, Urushima T, *et al.* AzoCholine enables optical control of alpha 7 nicotinic acetylcholine receptors in neural networks. ACS Chem Neurosci 2015.
[61] Kruse AC, Kobilka BK, Gautam D, Sexton PM, Christopoulos A, Wess J. Muscarinic acetylcholine receptors: Novel opportunities for drug development. Nat Rev Drug Discovery 2014; 13: 549-60.
[62] Nargeot J, Lester HA, Birdsall NJM, Stockton J, Wassermann NH, Erlanger BF. Photoisomerizable muscarinic antagonist studies of binding and of conductance relaxations in frog heart. J Gen Physiol 1982; 79: 657-78.
[63] Vodovozova EL. Photoaffinity labeling and its application in structural biology. Biochemistry 2007; 72: 1-20.
[64] Moreno-Yanes JA, Mahler HR. Photoaffinity labeling of specific muscarinic antagonist binding sites of brain: I. Preliminary studies using two *p*-azidophenylacetate esters of tropine. Biochem Biophys Res Commun 1980; 92: 610-7.
[65] Amitai G, Avissar S, Balderman D, Sokolovsky M. Affinity labeling of muscarinic receptors in rat cerebral cortex with a photolabile antagonist. Proc Natl Acad Sci USA 1982; 79: 243-7.
[66] Davie BJ, Sexton PM, Capuano B, Christopoulos A, Scammells PJ. Development of a photoactivatable allosteric ligand for the m1 muscarinic acetylcholine receptor. ACS Chem Neurosci 2014; 5: 902-7.
[67] Soreq H, Seidman S. Acetylcholinesterase - new roles for an old actor. Nat Rev Neurosci 2001; 2: 294-302.
[68] Bieth J, Vratsanos SM, Wassermann N, Erlanger BF. Photoregulation of biological activity by photochromic reagents, II. Inhibitors of acetylcholinesterase. Proc Natl Acad Sci USA 1969; 65: 1103-6.
[69] Bieth J, Wassermann N, Vratsanos SM, Erlanger BF. Photoregulation of biological activity by photochromic reagents, IV. A model for diurnal variation of enzymic activity. Proc Natl Acad Sci USA 1970; 66: 850-4.
[70] Broichhagen J, Jurastow I, Iwan K, Kummer W, Trauner D. Optical control of acetylcholinesterase with a tacrine switch. Angew Chem Int Ed 2014; 53: 7657-60.
[71] Chen X, Wehle S, Kuzmanovic N, *et al*. Acetylcholinesterase inhibitors with photoswitchable inhibition of β-amyloid aggregation. ACS Chem Neurosci 2014; 5: 377-89.

II: AzoCholine – a PCL for alpha 7 nAChRs

AzoCholine Enables Optical Control of Alpha 7 Nicotinic Acetylcholine Receptors in Neural Networks

Arunas Damijonaitis[1], Johannes Broichhagen[1], Tatsuya Urushima[1], Katharina Hüll[1], Jatin Nagpal[2], Laura Laprell[1], Matthias Schönberger[1], David H. Woodmansee[1], Amir Rafiq[3], Martin P. Sumser[1], Wolfgang Kummer[3], Alexander Gottschalk[3], and Dirk Trauner[1]*

[1]Department of Chemistry and Pharmacology, Ludwig-Maximilians-Universität München, Center of Integrated Protein Science Munich, Munich D-81377, Germany; [2]Buchmann Institute for Molecular Life Sciences, Institute of Biochemistry, Johann Wolfgang Goethe-Universität, Frankfurt D-60438, Germany; [3]Institute for Anatomy and Cell Biology, Justus-Liebig-Universität, German Center for Lung Research, Giessen D-35385, Germany

Abstract: Nicotinic acetylcholine receptors (nAChRs) are essential for cellular communication in higher organisms. Even though a vast pharmacological toolset to study cholinergic systems has been developed, control of endogenous neuronal nAChRs with high spatiotemporal precision has been lacking. To address this issue, we have generated photoswitchable nAChR agonists and re-evaluated the known photochromic ligand BisQ. Using electrophysiology, we found that one of our new compounds, AzoCholine, is an excellent photoswitchable agonist for neuronal α7 nAChRs, while BisQ was confirmed as an agonist for the muscle type nAChR. AzoCholine could be used to modulate cholinergic activity in a brain slice and in dorsal root ganglion neurons. In addition, we demonstrate light-dependent perturbation of behavior in the nematode *Caenorhabditis elegans.*

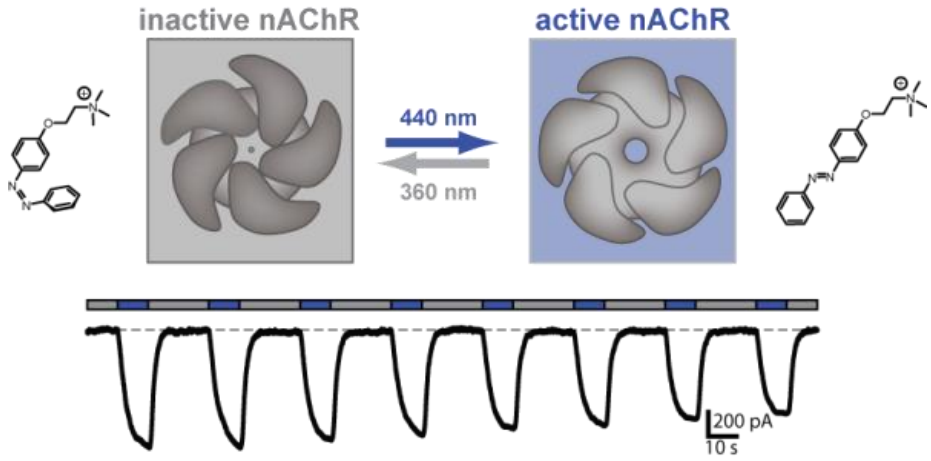

Graphical abstract.

KEYWORDS. Photopharmacology, photochromic ligand, AzoCholine, BisQ, nicotinic acetylcholine receptor, cholinergic system

Introduction

Acetylcholine (ACh) is a classic neurotransmitter that is critically involved in a variety of neural functions, such as movement, cognition and memory[1, 2]. After presynaptic release, it acts on muscarinic and nicotinic acetylcholine receptors (mAChRs and nAChRs respectively). nAChRs are found at the neuromuscular endplate in the periphery and on a variety of cholinergic synapses in the central and the peripheral nervous system. To date, twelve neural and five neuromuscular nAChR subunits have been described in mammals, which assemble as homo- or heteropentamers. While the fetal neuromuscular nAChRs consist of α1-, β1-, δ- and γ-subunits, the γ-subunit is exchanged for the ε-subunit in adults (Fig. 1a). Neural nAChRs can consist of α, β – combinations (made up from α2-α10 and β2-β4) or as α7-α9 homopentamers[1, 2].

The combinatorial diversity and wide spread occurrence of nAChRs requires highly selective and precise tools for investigating cholinergic signaling. Sensitizing these receptors towards light could therefore be advantageous (Fig. 1c). In pioneering studies of Erlanger's group in the late 1960's, a photosensitive azobenzene derived nAChR agonist, called BisQ (Fig. 1d), was used to modulate the membrane potential of the electroplax organ of *Electrophorus electricus* in a light-dependent manner[3-5]. Following up on this, Lester characterized BisQ and other photochromic compounds as photoisomerizable nicotinic agonists and muscarinic antagonists[6-8]. With the advent of modern photopharmacology[9, 10], which relies on molecular cloning and heterologous expression of transmembrane receptors as well as modern light delivery techniques (*e.g.* LEDs), it is possible to investigate individual receptors in more detail. This has been done, for instance, using the photoswitchable tethered ligand approach, which yielded the light-controlled nAChR (LinAChR). LinAChR consists of a nAChR agonist, an azobenzene photoswitch and a maleimide that is covalently attached to engineered cysteines of α3β4 or α4β2 nAChR[11].

Freely diffusible photochromic ligands (PCLs) combine the advantages of conventional pharmacology with the spatiotemporal precision of light. They have been used to optically control ion channels[12-17], metabotropic receptors[18, 19] and enzymes[20]. Here, we revisit the classic PCL BisQ and describe the development of PCLs for neuronal nAChRs. One of these compounds, AzoCholine, could be used to control the activity of dorsal root ganglion (DRG) and hippocampal neurons, as well as the behavior of the nematode *C. elegans,* with light.

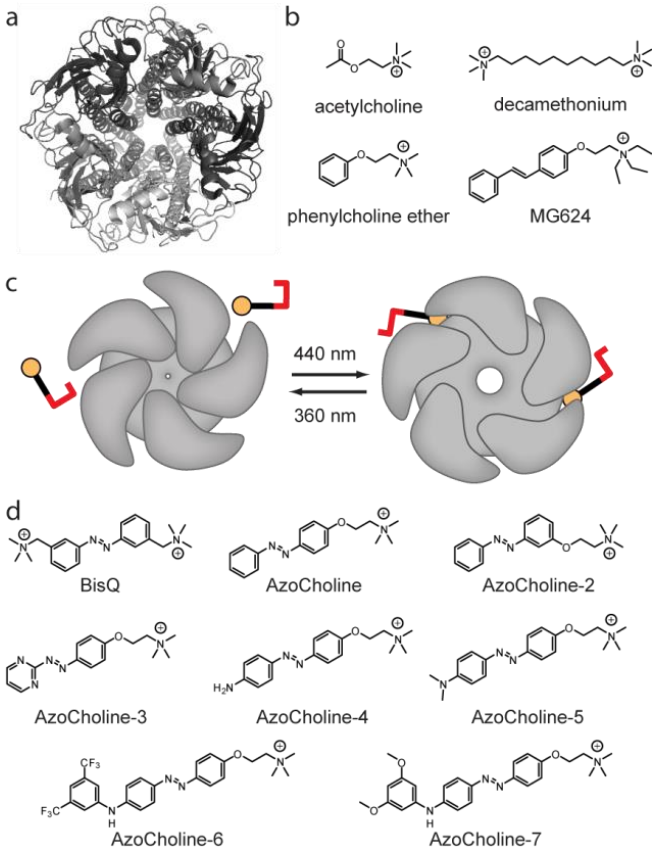

Fig. 1. Structural model of a nAChR, chemical structures of nAChR ligands and schematic function of PCLs. (a) Structural model derived from cryo-electron microscopy data of a neuromuscular nAChR as a top-view (pdb: 2bg9)[21]. (b) Chemical structures of AChR ligands. (c) Schematic representation of the light-dependent activation of a nAChR with a PCL. (d) Chemical structures of azobenzene-containing PCLs designed to act on nAChRs.

Results and Discussion

Design and synthesis of PCLs. To develop a photoswitchable version of ACh that acts on neuronal nAChRs, we prepared a series of photoswitchable derivatives of the known agonist phenylcholine ether (Fig. 1b). These compounds, AzoCholine and its congeners AzoCholine 2-7 (Fig. 1d), also bear resemblance to the α7 nAChR antagonist MG624 (Fig. 1b). The synthesis of AzoCholine is shown in Fig. 2. Exposure of 4-hydroxy azobenzene (**1**) to 2-chloro-*N*,*N*-dimethylethylamine hydrochloride gave tertiary amine **2**. Quarternarization of the amine with methyl iodide then yielded AzoCholine (Fig. 2a). Its structure in the solid state is shown in the Supporting Information (Fig. S1a). AzoCholine could be switched between its *cis*- and *trans*-state by irradiation with 360 nm and 440 nm light, respectively (Fig. 2b). The VU/Vis spectra of AzoCholine irradiated with these wavelengths are shown in Fig. 2c. The synthesis of AzoCholines 2-7 is discussed in the Supporting Information (pages 6-15). While some of these compounds showed red-shifted absorption spectra and reversible switching (Fig. S2), the simplest member of the series, AzoCholine, emerged as the most effective PCL. Therefore our physiological studies focused on this compound and BisQ.

BisQ, is derived from decamethonium (Fig. 1b) as described by Erlanger[3-5]. We improved on the original synthesis and devised a four-step procedure, which relied on a Mills reaction to create the azobenzene moiety (see Supporting Information, pages 3-5).

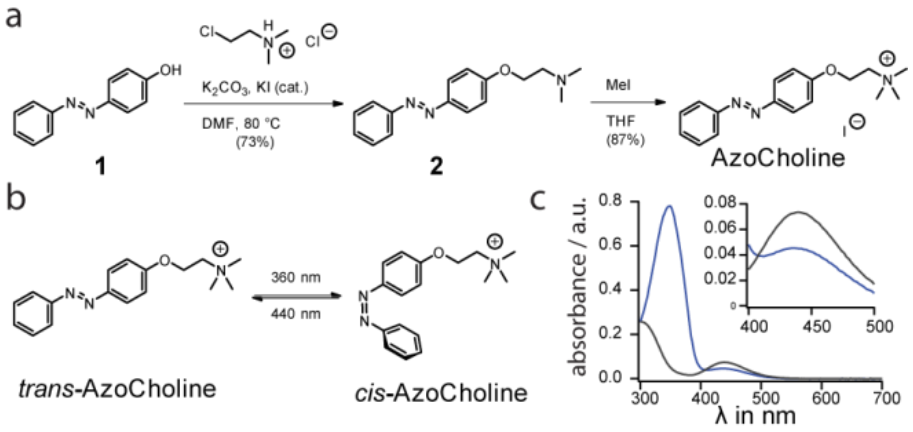

Fig. 2. Synthesis and switching of AzoCholine. (a) Two-step synthesis. (b) *cis*-/*trans* Isomerization. (c) UV/Vis spectra of AzoCholine (50 µM in DMSO at room temperature) irradiated with 360 nm (gray line) and 440 nm (blue line) light. The insert shows a magnification of the n-π*-band.

AzoCholine is a photoswitchable agonist for the α7 nAChR. To characterize the action of our PCLs on a neuronal receptor, we heterologously expressed an α7 nAChR/glycine receptor chimera in HEK293T cells[22]. This chimeric channel is a pharmacological model for the neuronal α7 nAChR[23] with the advantage of high expression levels in HEK293T cells. Action spectra were recorded using patch-clamp electrophysiology to determine the optimal wavelengths for activation and inactivation of the receptors (Fig. S3).

Interestingly, BisQ showed no notable activation of the chimeric α7 nAChR at 50 µM concentration (induced current: 5.93 ± 2.81 pA, *i.e.* 1.15 ± 0.64 % normalized to ACh) (Fig. 3a, Fig. S4). By contrast, AzoCholine (50 µM) proved to be a potent agonist in its *trans*-state, inducing a current of 691.81 ± 278.65 pA (Fig. 3b). Normalized with respect to the natural ligand ACh (50 µM) (Fig. 3c), illumination of AzoCholine with blue light evoked currents almost twice as large (223.66 ± 30.06 %) (Fig. 3d). This process was reversible by alternating the switching wavelengths (360 and 440 nm) over many cycles (Fig. 3e). In addition, the on and off kinetics of receptor activation and inactivation with AzoCholine were faster compared to ACh ($\tau_{on\ AzoCholine}$, = 3.207 ± 0.421 s and $\tau_{off\ AzoCholine}$ = 1.352 ± 0.202 s; $\tau_{on\ ACh}$ = 4.179 ± 0.990 s and $\tau_{off\ ACh}$ = 2.089 ± 0.509 s; n = 4). Using current-clamp measurements, we observed a quick and pronounced change of the membrane potential when alternating the illumination between 360 and 440 nm (Fig. S5a). As with all PCLs, the effective agonist concentration can be adjusted using different wavelengths of light, allowing for discrete levels of activation of the receptor (Fig. S5b, c).

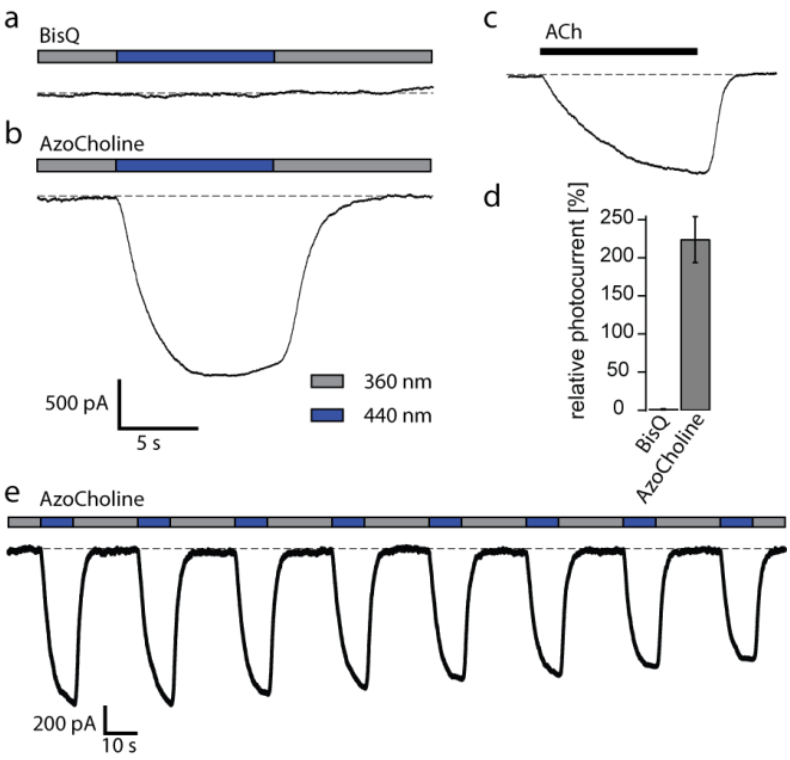

Fig. 3. Light-dependent effect of BisQ or AzoCholine on α7/GlyR chimera expressed in HEK293T cells. Light was switched between 360 nm and 440 nm. (a) BisQ (50 µM) did not induce a photocurrent, whereas (b) AzoCholine (50 µM) triggered large light-dependent inward currents. (c) Puff application of ACh (50 µM) evoked an inward current. (d) Photocurrents normalized to ACh puff application, represented as relative currents (n = 5). (e) Reversibility of AzoCholine switching on α7/GlyR chimera. Traces a-c were recorded from the same cell; bars represent mean; error bars represent SEM.

BisQ, but not AzoCholine, is a photoswitchable agonist for the muscle nAChR. To investigate muscle-type receptors, the human α1, β1, δ, ε nAChR subunits were expressed in HEK293T cells. In accordance with Erlanger's results, BisQ proved to be a photoswitchable agonist at the muscle receptor (Fig. 4a, e). Action spectra were recorded to determine the best switching wavelengths (Fig. S6). While the absorption in the UV/Vis measurements would suggest best *trans* to *cis* conversion at 340 nm, due to the optics of the microscope, with reduced transmissibility in the UV-range (<350 nm), best switching was achieved with 360 nm and 440 nm light. Washing in a solution of BisQ (50 µM) irradiated with 360 nm activated the receptor with a transient peak current, which desensitized to a plateau-current (Fig. S7). This might be due to residual *trans*-BisQ in the solution. When switched to *trans* with 440 nm, BisQ triggered light-dependent currents (156.38 ± 49.13 pA). Reversibility of currents was achieved over multiple cycles (Fig. 4e). When compared to puff-applied ACh at equal concentration, BisQ showed 21.47 ± 7.97 % activation (Fig. 4c,d). However, the kinetics of switching proved to be 2-3 times slower than those observed after ACh puff-application ($\tau_{on\ ACh}$ = 0.106 ± 0.059 s and $\tau_{off\ ACh}$ = 1.515 ± 0.648 s; $\tau_{on\ BisQ}$ = 0.201 ± 0.025 s and $\tau_{off\ BisQ}$ = 4.364 ± 0.369 s, n = 5).

Washing in a solution of AzoCholine (50 µM) irradiated with 360 nm activated the receptor with a transient peak current, followed by deactivation. Subsequent irradiation with 440 nm, however, did not change the current amplitude (3.64 ± 13.16 pA, 0.77 ± 1.82 % normalized to ACh; Fig. 4b,d). Therefore, AzoCholine does not function as a photoswitchable agonist for neuromuscular nAChRs.

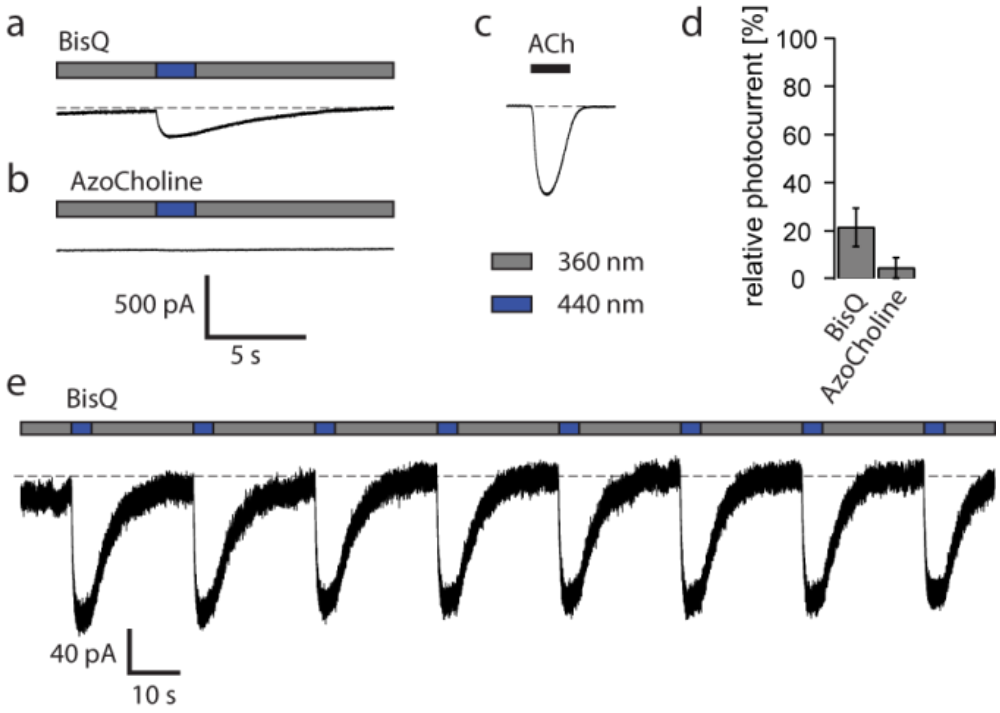

Fig. 4. Light-dependent effect of BisQ or AzoCholine on neuromuscular nAChR expressed in HEK293T cells. (a) BisQ (50 µM) evoked light-dependent currents when light was switched between 360 nm and 440 nm. (b) AzoCholine (50 µM) did not trigger light-dependent currents. (c) Puff application of ACh (50 µM) evoked an inward current. (d) Photocurrents normalized to ACh puff application, represented as relative currents (n = 5). (e) Reversibility of BisQ switching on neuromuscular nAChR. Traces a-c were recorded from the same cell; bars represent mean; error bars represent SEM.

AzoCholine activates α7 nAChRs in rat primary afferent DRG neurons. Cell bodies of primary afferent neurons conveying sensory information from the periphery towards the spinal cord reside in distinct aggregations termed DRG. With respect to their responsiveness to mechanical and chemical stimuli, including cholinergic agonists, they represent a heterogeneous population. In rat DRG, the proportion of α7 nAChR expressing neurons is higher than in mice, and the vast majority of them have nociceptor properties in that it responds to potential noxious stimuli[24-26]. Activation of α7 nAChR results in an increase of intracellular calcium concentration ($[Ca^{2+}]_i$) in these neurons[24, 25, 27]. Illumination of isolated and cultured DRG neurons bathed in 250 µM AzoCholine with 460 nm light for 10 s caused a repeatable $[Ca^{2+}]_i$ increase in 77 out of 180 cases, which was higher than that evoked by depolarizing the cells with 30 mM KCl (Fig. 5) and absent in AzoCholine-free media (n = 27 cells, pooled from 4 experiments; Fig. S8a). Measurement of $[Ca^{2+}]_i$ with the calcium-sensitive dye Fura-2 is based upon recording of fluorescence intensity at wavelengths longer than 440 nm. Hence, photoactivation of AzoCholine with 460 nm light interfered with $[Ca^{2+}]_i$ recording for the period of stimulation so that immediate post-stimulation values but not peak height of $[Ca^{2+}]_i$ increase could be determined. This PCL-induced increase in $[Ca^{2+}]_i$ was indeed due to nAChR activation since it was not observed in the presence of the α7 nAChR antagonist MG624 (50 µM; n = 21 cells, pooled from 4 experiments; Fig. S8b). In mammals, MG624 also exhibits antagonistic properties to other nAChR subunits than α7[28], and such nAChRs are also expressed in rat DRG neurons[24, 25]. Thus, this pharmacological profile alone does not allow us to qualify the response as α7 nAChR specific. However, the relative number

of responsive neurons provides additional supportive evidence for selective stimulation of α7 nAChRs by photoactivated AzoCholine. We observed $[Ca^{2+}]_i$ rises in 43 % (77/180) of neurons investigated, which nicely falls into the range of 35-47 % (depending on postnatal age) of rat DRG neurons expressing α7 nAChRs either alone or in combination with other nAChR, whereas the total fraction of nAChRs carrying neurons amounts to 69-78 %[25]. It should be noted, that MG624 (Fig. 1b) closely resembles AzoCholine, but bares a trimethyl ammonium head group instead of a triethyl ammonium moiety.

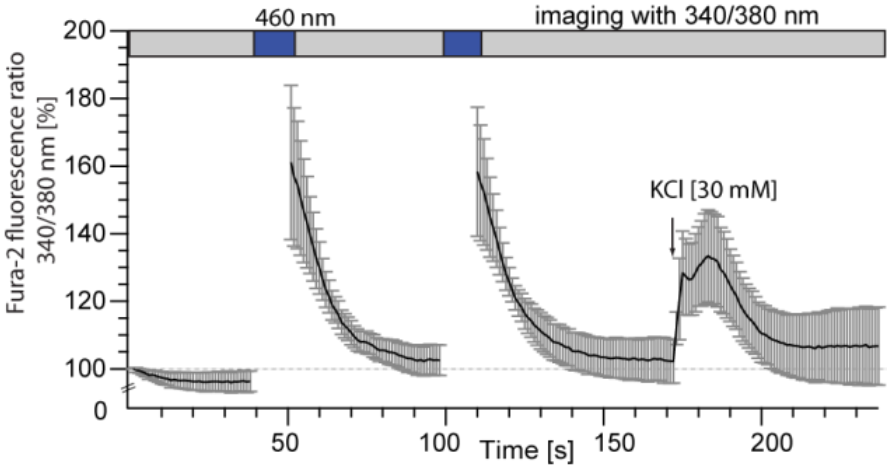

Fig. 5. Light-dependent effect of AzoCholine on rat sensory neurons isolated from dorsal root ganglia. Illumination with 460 nm light in the presence of AzoCholine (250 µM) leads to an increase in $[Ca^{2+}]_i$. Depolarization by application of 30 mM KCl with subsequent increase in $[Ca^{2+}]_i$ served as control for viability of sensory neurons. The graph depicts mean and standard deviation of data recorded from 77 responsive cells; additional 103 cells included in the experiment were unresponsive to AzoCholine.

AzoCholine activates α7 nAChRs in mouse hippocampus. To investigate the effect of AzoCholine on intact neural networks, we performed extracellular electrophysiological recordings in mouse hippocampal brain slices on a multielectrode-array (MEA) (Fig. S9a). As expected, illumination of the brain slice did not alter bursting activity (Fig. S9b). The same is true when washing in AzoCholine (50 µM) in the dark (Fig. S9c). However, in the presence of AzoCholine the neuronal activity could be modulated by toggling between 360 nm and 460 nm (Fig. 6a). In accordance with the HEK cell data, blue light increased and violet light decreased bursting activity. Quantified over all experiments, the switching effect is shown in a correlation plot (Fig. 6c, e; 6 experiments, n = 173 cells, $p<0.001$). To confirm that the α7 nAChR is the target receptor of AzoCholine in hippocampal cells, we co-applied the α7 nAChR specific antagonist MG624 (5 µM). Matching the previous results from rat DRG neurons, changes could not be evoked in the presence of the antagonist (Fig. 6b), however, basal bursting activity could still be detected (Fig. 6d, e; 6 experiments, n = 121 cells, $p>0.05$).

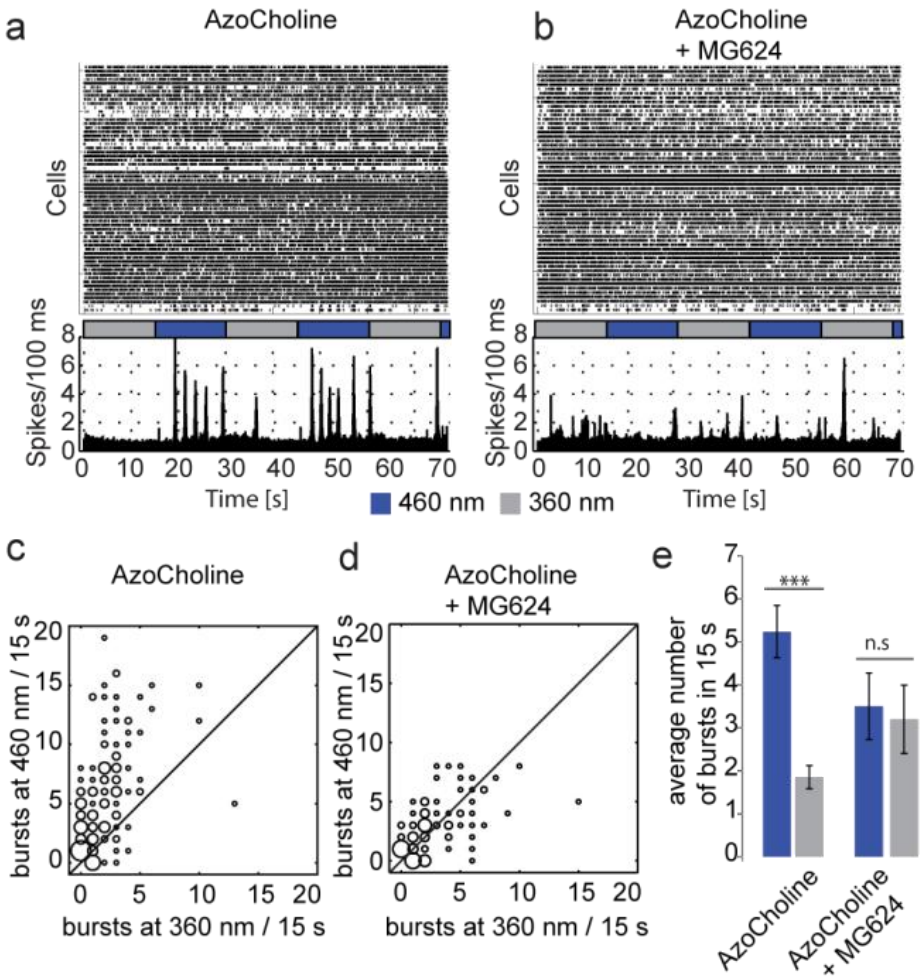

Fig. 6. Bursting activity in mouse hippocampal brain slices. (a) Raster plot of single cell spiking activity in the presence of AzoCholine (50 µM) with the correlating histograms over all cells. Switching light from 360 nm (gray bar) to 460 nm light (blue bar) leads to an increase in bursting activity and *vice versa*. (b) Raster plot in the presence of AzoCholine (50 µM) and MG624 (5 µM) with the correlating histogram. Switching of light has no apparent effect on the spiking activity. (c) Quantification of bursting activity of all experiments with AzoCholine (n = 6 experiments with 173 bursting cells) with the dot size related to the number of cells responding. (d) Quantification of bursting activity of all experiments with AzoCholine and MG624 (n = 6 experiments with 121 bursting cells). (e) Summary of all experiments (n = 6, bars represent mean, error bars represent SEM. t-test: ***p<0.001 for AzoCholine only and p>0.05 with MG624).

AzoCholine evokes light-dependent behavior in *Caenorhabditis elegans*. In liquid medium, the nematode *C. elegans* exhibits a dorso-ventrally alternating c-shaped body posture to achieve swimming locomotion. These thrashing movements can be used to quantify locomotion behavior and motility related phenotypes. Locomotion in the nematode involves neuromuscular as well as neuron-neuron cholinergic synaptic transmission[29]. Furthermore, due to the transparency of the animal, light-based methods like calcium imaging and optogenetics are often used to study neural circuits[30]. As *C. elegans* shows photophobic responses to UV/blue light, mediated by a photosensor, LITE-1[31], mutants lacking this receptor are often used in optogenetic analyses of behavior[32]. Swimming behavior of *lite-1* animals in physiological buffer (M9) was not affected when switching from UV (350 nm) to blue (470 nm) light illumination (Video S1, Fig. 7). Notably, when the buffer was supplemented with 1 mM AzoCholine, the nematodes showed a sharp decline in thrashing frequency upon switching from UV to blue light (Video S2). The thrashing frequency recovered during the second half of the

light pulse and was fully restored after switching to UV-light. This indicates that AzoCholine may have activated nAChRs in the motor nervous system, possibly evoking inhibition, *e.g*. through GABAergic motoneurons. Interestingly, when tested on wild type nematodes (strain N2, with normal LITE-1 function) the light-effect of AzoCholine photoswitching did not appear (Video S3, Fig. S10). This unexpected result is intriguing and difficult to rationalize given the complexity of the system. However, we hypothesize that the UV pre-exposure leads to a LITE-1 dependent signal that could put wildtype animals into a state where AzoCholine cannot exert full effects, *e.g*. because general excitability of the motor system is reduced, or AChRs are modified such that they desensitize more readily upon AzoCholine binding. Given the demonstrated specificity of AzoCholine for α7 nAChRs in mammalian cells, the observed effects in *C. elegans* are likely affected *via* nAChRs. However, the putative target receptor triggered by AzoCholine in *C. elegans* remains to be validated.

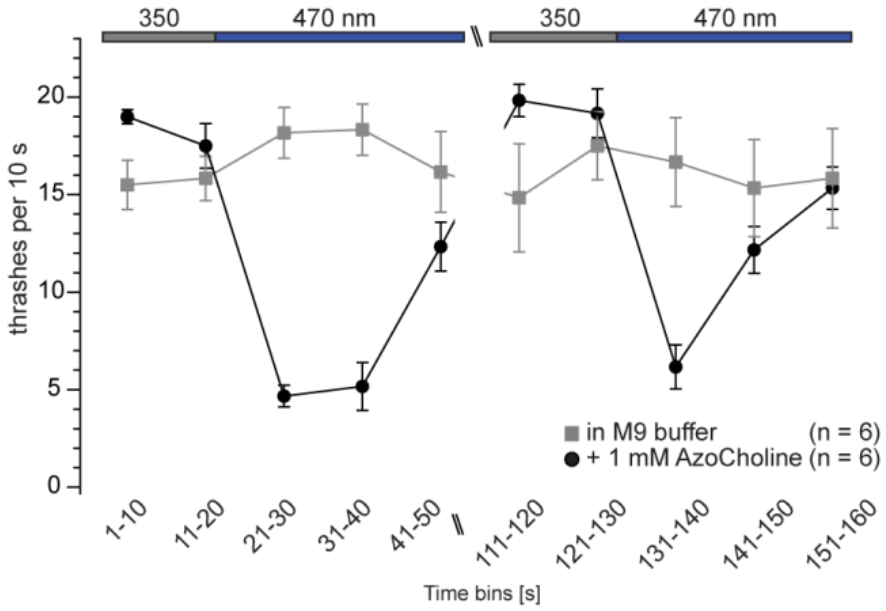

Fig. 7. Quantification of *C. elegans* swimming cycles. Nematodes swimming in M9 buffer (gray boxes) and in M9 with AzoCholine (1 mM, black circles) (n = 6). When switching from UV (350 nm) to blue (470 nm) light (bar), *trans*-AzoCholine induces stopping/freezing behavior in swimming *C. elegans* nematodes.

Conclusion

In summary, we have re-evaluated the first photochromic ligand for ion channels, BisQ, using the methods of modern channel physiology. As expected, BisQ acts on the neuromuscular nAChR but it does not affect neuronal α7 type nAChRs, at least not in a light dependent fashion.

Furthermore, we have developed AzoCholine, a PCL that targets α7 nAChRs, which enables us to control cholinergic systems in various organisms with light. In addition to its photoswitchability, AzoCholine shows faster activation and higher potency than the native ligand ACh. It can be applied in neuronal tissues and works in living animals, as it is able to perturb swimming behavior of *C. elegans* (*lite-1*) in a light-dependent manner.

The main advantage of PCLs when compared to other available tools for light-dependent control of cellular processes is their ease of use. Since no genetic manipulation is required, the compounds can simply be applied like drugs, endowing endogenous receptors with light sensitivity. As such, AzoCholine turns α7 nAChRs into photoreceptors. By varying the wavelengths, the concentration of the active form of AzoCholine can adjusted in a graded fashion ("photodosing"). Thus, it is now feasible to control endogenous nAChRs with high spatiotemporal precision. This will be instrumental for elucidating their roles in the nervous system and may prove to be therapeutically useful.

Methods

Cell culture. HEK293T cells were maintained in Dulbecco's modified Eagle's medium (Biochrom, Merk Millipore, Germany) supplemented with 10 % fetal calf serum (Biochrom, Merk Millipore, Germany) at 37 °C in a 10 % CO_2 atmosphere. Transfections were performed with JetPrime (Polyplus-transfections, France) according to manufacturer's instructions 24 h before measurements. For muscle nAChR expression, cells were transfected with human α_1-GFP, β_1, δ and ε nAChR subunit in pCDNA3.1 plasmid DNA (each 125 ng DNA per coverslip, provided by A. Mourot, Paris). For α7/GlyR expression cells were transfected with α7/GlyR DNA in pMT3 (500 ng per coverslip, provided by T. Grutter, Strasbourg) together with 50 ng per coverslip of yellow fluorescent protein (YFP) plasmid DNA. As controls, not transfected HEK-cells with PCL present and with light switching were used. No photocurrent was detected. Also transfected HEK-cells without the PCL and with light switching gave no photocurrent.

Tissue preparation. Horizontal brain slices preparations from C57Bl6JRj mice (wild type) were prepared as reported elsewhere[29]. Briefly, mice were decapitated, the brain was removed, and 250 µm horizontal slices were prepared using a vibrating microtome (7000smz-2, Campden Instruments, England). Slices were incubated in carbogenated (5 % CO_2, 95 % O_2) sucrose medium (mM: 87 NaCl, 2.5 KCl, 7 $MgCl_2$, 0.5 $CaCl_2$, 25 Gluc, 1.25 NaH_2PO_4, 25 $NaHCO_3$, 75 sucrose) for 30 min at 34°C.

Dorsal root ganglion (DRG) neurons were isolated from male and female Wistar rats (250-300 g body weight) and cultured as described previously[33]. Briefly, DRGs dissected from rat were incubated in an enzyme mixture containing 2 mg/ml collagenase type 1 and 2 mg/ml dispase II (Sigma-Aldrich, Germany) in calcium and magnesium-free Hanks' balanced salt solution (Life Technologies, Germany) for 15 min at 37 °C water bath. Thereafter, DRGs were mechanically dissociated with a glass Pasteur pipette. The process of incubation and mechanical dissociation was repeated 2 times until the DRGs were completely dissociated. Then the cells were suspended in L-15 medium (Life Technologies, Germany) containing 10 % fetal bovine serum (FBS) and 1 % penicillin and streptomycin, and centrifuged at 800x g for 4 min. This wash and centrifugation was repeated 2 times. The cell pellet was then resuspended in the same medium and a small portion (10 µl) of the cell suspension was transferred on poly-D-lysine/laminin (Sigma-Aldrich, Germany) coated glass cover-slips and incubated at 37 °C for 2 hours for the attachment of the neurons to the glass surface. Additional growth medium was added to the wells containing cover slips, and cells were allowed to stabilize for further 2 hours before calcium measurements were performed.

Electrophysiology. Whole cell patch clamp recordings were performed with an EPC10 USB Patch Clamp amplifier and PatchMaster software (HEKA Elektronik, Germany). Cells were maintained at room temperature and held at -60 mV during the experiments. Micropipettes were generated from GB200-F-8P capillaries (Science Products, Germany) using a vertical puller (PC-10, Narishige, Japan). Pipette resistance varied between 5-8 MΩ. Bath solution contained (in mM): 140 NaCl, 2 Cl, 2 $CaCl_2$, 2 $MgCl_2$, 10 *d*-Glucose, 10 HEPES (NaOH to pH 7.4). Pipette solution for muscle nAChR contained (in mM): 140 K-gluconate, 4 NaCl, 12 KCl, 10 HEPES, 4 MgATP, 0.4 Na_2-ATP (KOH to pH 7.3). Pipette solution for α7/GlyR contained (in mM): 140 $CsCl_2$, 10 HEPES 2 Na_2-ATP, 10 EGTA (KOH to pH 7.3).

Multi Electrode Array. Multi Electrode Array (MEA) of mouse horizontal brain slices were recorded with a Multichannel Systems MEA setup (C57Bl6JRj mice aged p7 to p13). Slices were placed and oriented with the hippocampus onto the electrodes (Fig. S9). To increase basal spiking rate we increased extracellular potassium to 7.5 mM. Neural bursting activity is defined as more than two recorded action potentials in two milliseconds.

Calcium measurements. The intracellular calcium concentration measurements were performed on freshly isolated and DRG neurons (wildtype rats weight 250-300 g, this corresponds to 9-10 weeks old animals). All the measurements were performed in oxygenated Locke's buffer (pH 7.4) containing (in mM): 14.3 $NaHCO_3$, 1.2 NaH_2PO_4, 5.6 KCl, 136 NaCl, 1.2 $MgCl_2$, 2.2 $CaCl_2$, 10 D-glucose at constant temperature 34 °C. The cells were loaded with the calcium sensitive dye Fura-2 (1 μM; Life Technologies, Germany) for 30 min at 37 °C in Locke's buffer and were washed for 10 min in dye-free Locke's buffer solution. Fura-2 is a ratiometric calcium sensitive dye. It was excited at 340 and 380 nm wavelengths, and its emission peaks at 510 nm. Recordings were done using a fluorescence microscope (Olympus, Hamburg, Germany) connected to a scan CCD camera with fast monochromator (TiLL Photonics, Gräfelfing, Germany). The barrier filter set allows transmission of wavelengths longer than than 440 nm. Hence, photoactivation of AzoCholine with 460 nm light interfered with recordings for the period of stimulation so that immediate post-stimulation values but not peak height of signal increase could be determined. Each cell was observed separately and fluorescence intensity at the beginning of the experiment ratio was set to 100 %. Light stimulus to activate the photoswitch was applied by a blue light LED.

Swimming assay with *Caenorhabditis elegans* (*C. elegans*). *Caenorhabditis elegans lite-1 (ce314)* strain and wildtype (N2) were reared using standard methods on nematode growth medium (NGM) and fed E. coli strain OP50-1[34]. For the analysis of the behavior of *C. elegans* in liquid, thrashing (swimming) assays of young adult hermaphrodites were carried out in 96-well microtiter plates, containing 100 μL of NGM and 100 μL of M9 saline solution with or without AzoCholine (1 mM) per well. For the control condition (without AzoCholine), M9 was supplemented with 1 % DMSO (carrier solvent for AzoCholine). The animals were incubated in the buffer solution for 15 mins under low intensity UV light. Subsequent UV and blue light illumination of the worms was provided through a 4x magnification objective. Assays were recorded with a Powershot G9 camera (Canon, Krefeld, Germany) and swimming cycles (the worm's body bends forth and back per each cycle) were counted for defined time intervals during the UV and blue light illumination. M9-buffer contained (in mM) 20 KH_2PO_4, 40 Na_2HPO_4, 85 NaCl, 1 $MgSO_4$. Nematode Growth Medium (NGM) contained 1.7 % (w/v) Agar-Agar, 0.25 % (w/v) Trypton/Pepton, 0.3 % (w/v) NaCl, 0.0005 % (w/v) cholesterol (in EtOH), 0.001 % (w/v) nystatin and (in mM) 1 $CaCl_2$, 1 $MgSO_4$, 25 K_3PO_4.

Illumination. For illumination during electrophysiology and UV/Vis experiments a TILL Photonics Polychrome 5000 monochromator was operated with the HEKA patchmaster software *via* the patch clamp amplifier or the PolyCon software, respectively. For MEA and DRG experiments high power LEDs (460 nm with 9 mW/cm^2 and 365 nm, 1.5 mW/cm^2) were operated with the HEKA patchmaster software *via* the patch clamp amplifier. For the Nematode swimming assay a low intensity UV lamp (366 nm, 16 $\mu W/mm^2$, Benda, Wiesloch, Germany) was used for pre-illumination during incubation. During the assay a HBO lamp was used with UV- and blue light filters (Zeiss; 325-375 nm, 0.26 mW/mm^2; 450–490 nm, 0.6 mW/mm^2).

References

1. Kalamida, D., Poulas, K., Avramopoulou, V., Fostieri, E., Lagoumintzis, G., Lazaridis, K., Sideri, A., Zouridakis, M., and Tzartos, S. J. (2007) Muscle and neuronal nicotinic acetylcholine receptors. Structure, function and pathogenicity. *FEBS J 274*, 3799-845.

2. Lemoine, D., Jiang, R., Taly, A., Chataigneau, T., Specht, A., and Grutter, T. (2012) Ligand-gated ion channels: new insights into neurological disorders and ligand recognition. *Chem. Rev. 112*, 6285-318.

3. Bartels, E., Wassermann, N. H., and Erlanger, B. F. (1971) Photochromic activators of the acetylcholine receptor. *Proc. Natl. Acad. Sci. USA 68*, 1820-3.

4. Beith, J., Wassermann, N., Vratsanos, S. M., and Erlanger, B. F. (1970) Photoregulation of Biological Activity by Photochromic Reagents, IV. A Model for Diurnal Variation of Enzymic Activity. *Proc. Natl. Acad. Sci. USA 66*, 850-854.

5. Deal, W. J., Erlanger, B. F., and Nachmansohn, D. (1969) Photoregulation of biological activity by photochromic reagents. 3. Photoregulation of bioelectricity by acetylcholine receptor inhibitors. *Proc. Natl. Acad. Sci. USA 64*, 1230-4.

6. Lester, H. A., Krouse, M. E., Nass, M. M., Wassermann, N. H., and Erlanger, B. C. (1980) A covalently bound photoisomerizable agonist: comparison with reversibly bound agonists at Electrophorus electroplaques. *J. Gen. Physiol 75*, 207-232.

7. Nargeot, J., Lester, H. A., Birdsall, N. J., Stockton, J., Wassermann, N. H., and Erlanger, B. C. (1982) A photoisomerizable muscarinic antagonist. Studies of binding and of conductance relaxations in frog heart. *J. Gen. Physiol 79*, 657-678.

8. Gurney, A. M., and Lester, H. A. (1987) Light-flash physiology with synthetic photosensitive compounds. *Physiol. Rev. 67*, 583-617.

9. Fehrentz, T., Schonberger, M., and Trauner, D. (2011) Optochemical genetics. *Angew. Chem. Int. Ed. Engl. 50*, 12156-82.

10. Velema, W. A., Szymanski, W., and Feringa, B. L. (2014) Photopharmacology: beyond proof of principle. *J. Am. Chem. Soc. 136*, 2178-91.

11. Tochitsky, I., Banghart, M. R., Mourot, A., Yao, J. Z., Gaub, B., Kramer, R. H., and Trauner, D. (2012) Optochemical control of genetically engineered neuronal nicotinic acetylcholine receptors. *Nat. Chem. 4*, 105-11.

12. Banghart, M., Borges, K., Isacoff, E., Trauner, D., and Kramer, R. H. (2004) Light-activated ion channels for remote control of neuronal firing. *Nat. Neurosci. 7*, 1381-6.

13. Stawski, P., Sumser, M., and Trauner, D. (2012) A photochromic agonist of AMPA receptors. *Angew. Chem. Int. Ed. Engl. 51*, 5748-51.

14. Stein, M., Middendorp, S. J., Carta, V., Pejo, E., Raines, D. E., Forman, S. A., Sigel, E., and Trauner, D. (2012) Azo-propofols: photochromic potentiators of GABA(A) receptors. *Angew. Chem. Int. Ed. Engl. 51*, 10500-4.

15. Wyart, C., Del Bene, F., Warp, E., Scott, E. K., Trauner, D., Baier, H., and Isacoff, E. Y. (2009) Optogenetic dissection of a behavioural module in the vertebrate spinal cord. *Nature 461*, 407-10.

16. Mourot, A., Fehrentz, T., Le Feuvre, Y., Smith, C. M., Herold, C., Dalkara, D., Nagy, F., Trauner, D., and Kramer, R. H. (2012) Rapid optical control of nociception with an ion-channel photoswitch. *Nat. Methods 9*, 396-402.

17. Lemoine, D., Habermacher, C., Martz, A., Mery, P. F., Bouquier, N., Diverchy, F., Taly, A., Rassendren, F., Specht, A., and Grutter, T. (2013) Optical control of an ion channel gate. *Proc. Natl. Acad. Sci. USA 110*, 20813-8.

18. Levitz, J., Pantoja, C., Gaub, B., Janovjak, H., Reiner, A., Hoagland, A., Schoppik, D., Kane, B., Stawski, P., Schier, A. F., Trauner, D., and Isacoff, E. Y. (2013) Optical control of metabotropic glutamate receptors. *Nat. Neurosci. 16*, 507-16.

19. Schonberger, M., and Trauner, D. (2014) A photochromic agonist for mu-opioid receptors. *Angew. Chem. Int. Ed. Engl. 53*, 3264-7.

20. Broichhagen, J., Jurastow, I., Iwan, K., Kummer, W., and Trauner, D. (2014) Optical Control of Acetylcholinesterase with a Tacrine Switch. *Angew. Chem. Int. Ed. Engl.*

21. Unwin, N. (2005) Refined structure of the nicotinic acetylcholine receptor at 4A resolution. *J. Mol. Biol. 346*, 967-89.

22. Grutter, T., de Carvalho, L. P., Dufresne, V., Taly, A., Edelstein, S. J., and Changeux, J. P. (2005) Molecular tuning of fast gating in pentameric ligand-gated ion channels. *Proc. Natl. Acad. Sci. USA 102*, 18207-12.

23. Craig, P. J., Bose, S., Zwart, R., Beattie, R. E., Folly, E. A., Johnson, L. R., Bell, E., Evans, N. M., Benedetti, G., Pearson, K. H., McPhie, G. I., Volsen, S. G., Millar, N. S., Sher, E., and Broad, L. M. (2004) Stable expression and characterisation of a human alpha 7 nicotinic subunit chimera: a tool for functional high-throughput screening. *Eur. J. Pharmacol. 502*, 31-40.

24. Haberberger, R. V., Bernardini, N., Kress, M., Hartmann, P., Lips, K. S., and Kummer, W. (2004) Nicotinic acetylcholine receptor subtypes in nociceptive dorsal root ganglion neurons of the adult rat. *Auton. Neurosci. 113*, 32-42.

25. Smith, N. J., Hone, A. J., Memon, T., Bossi, S., Smith, T. E., McIntosh, J. M., Olivera, B. M., and Teichert, R. W. (2013) Comparative functional expression of nAChR subtypes in rodent DRG neurons. *Front. Cell. Neurosci. 7*, 225.

26. Shelukhina, I., Paddenberg, R., Kummer, W., and Tsetlin, V. (2014) Functional expression and axonal transport of alpha7 nAChRs by peptidergic nociceptors of rat dorsal root ganglion. *Brain. Struct. Funct.* Apr 5. [Epub ahead of print]

27. Fucile, S., Sucapane, A., and Eusebi, F. (2005) Ca2+ permeability of nicotinic acetylcholine receptors from rat dorsal root ganglion neurones. *J. Physiol. 565*, 219-28.

28. Gotti, C., Carbonnelle, E., Moretti, M., Zwart, R., and Clementi, F. (2000) Drugs selective for nicotinic receptor subtypes: a real possibility or a dream? *Behav. Brain. Res. 113*, 183-92.

29. Schoenberger, M., Damijonaitis, A., Zhang, Z., Nagel, D., and Trauner, D. (2014) Development of a New Photochromic Ion Channel Blocker via Azologization of Fomocaine. *ACS Chem. Neurosci. 5*, 514-518.

30. de Bono, M., Schafer, W. R., and Gottschalk, A., (2013) Optogenetic actuation, inhibition, modulation and readout for neuronal networks generating behavior in the nematode Caenorhabditis elegans. In *Optogenetics*, (Hegemann, P.and Sigrist, S., Eds.) pp 61-78 De Gruyter

31. Edwards, S. L., Charlie, N. K., Milfort, M. C., Brown, B. S., Gravlin, C. N., Knecht, J. E., and Miller, K. G. (2008) A novel molecular solution for ultraviolet light detection in Caenorhabditis elegans. *PLoS Biol. 6*, e198.

32. Husson, S. J., Costa, W. S., Wabnig, S., Stirman, J. N., Watson, J. D., Spencer, W. C., Akerboom, J., Looger, L. L., Treinin, M., Miller, D. M., 3rd, Lu, H., and Gottschalk, A. (2012) Optogenetic analysis of a nociceptor neuron and network reveals ion channels acting downstream of primary sensors. *Curr. Biol. 22*, 743-52.

33. Nassenstein, C., Taylor-Clark, T. E., Myers, A. C., Ru, F., Nandigama, R., Bettner, W., and Undem, B. J. (2010) Phenotypic distinctions between neural crest and placodal derived vagal C-fibres in mouse lungs. *J. Physiol. 588*, 4769-83.

34. Brenner, S. (1974) The genetics of Caenorhabditis elegans. *Genetics 77*, 71-94.

Acknowledgements

D.T. was supported by an Advanced Grant from the European Research Council (268795). A.D., M.S. and L.L. were supported by the International Max Planck Research School for Molecular and Cellular Life Sciences (IMPRS-LS). J.B. was supported by a PhD fellowship from the Studienstiftung des deutschen Volkes. W.K. was supported by the LOEWE Research Focus Non-neural Cholinergic Systems. The authors gratefully acknowledge Dr. D. Barber for helpful discussions, L. de la Osa de la Rosa for technical assistance and Dr. P. Mayer for crystal structure elucidations. Plasmid containing the α7/GlyR construct was a generous gift from Prof. Dr. T. Grutter. Plasmids for neuromuscular nAChR were generous gifts from Dr. A. Mourot.

Author contributions

D.T., M.P.S., A.G., and A.D. designed the study. J.B., T.U., K.H., D.H.W., and M.S. performed chemical synthesis. M.S., A.D., and K.H. performed UV/Vis experiments. A.D. performed the patch-clamp experiments. L.L. and A.D. designed and performed MEA experiments. A.R. and W.K. designed and performed DRG experiments. J.N., A.D., and A.G. designed and performed *C. elegans* experiments. A.D., J.B., K.H., M.S., and D.T. wrote the manuscript through contributions of all authors. All authors have given approval to the final version of the manuscript.

Additional information

Supporting Information. Synthesis and characterization of organic compounds, additional photochemical and biological characterization. This information is available free of charge via the Internet at http://pubs.acs.org/.

Abbreviations. nAChR, nicotinic acetylcholine receptor; mAChR, muscarinic acetylcholine receptor; RT, room temperature; GlyR, glycine receptor; HEK293T cells, Human Embryonic Kidney cells type 293T; PCL, photochromic ligand; DRG, dorsal root ganglion; UV, ultra violet; MEA, multielectrode array.

Supporting Information (AzoCholine)

Supplementary video material

VideoS1 – C.elegans (lite1) nematodes in M9 buffer (speed = 8x). light switching as indicated.

VideoS2 – C.elegans (lite1) nematodes in M9 buffer with 1 mM Azocholine (speed = 8x). light switching as indicated.

VideoS3 – C.elegans (N2) nematodes in M9 buffer with 1 mM Azocholine (speed = 8x). light switching as indicated.

Supplementary figures

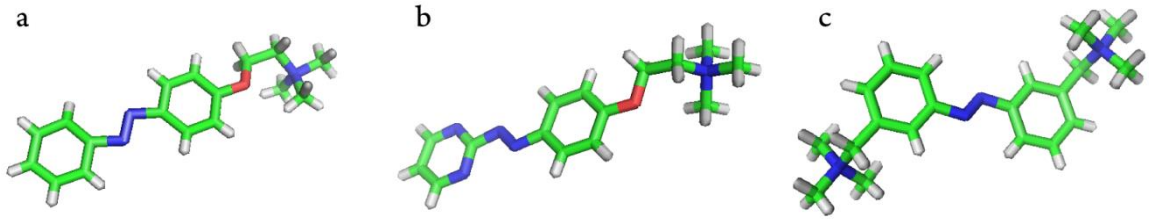

Fig. S1. Crystal structures of (a) AzoCholine (CCDC 1035194), (b) Azocholine-3 (CCDC 1035196) , and (c) BisQ (CCDC 1035195)

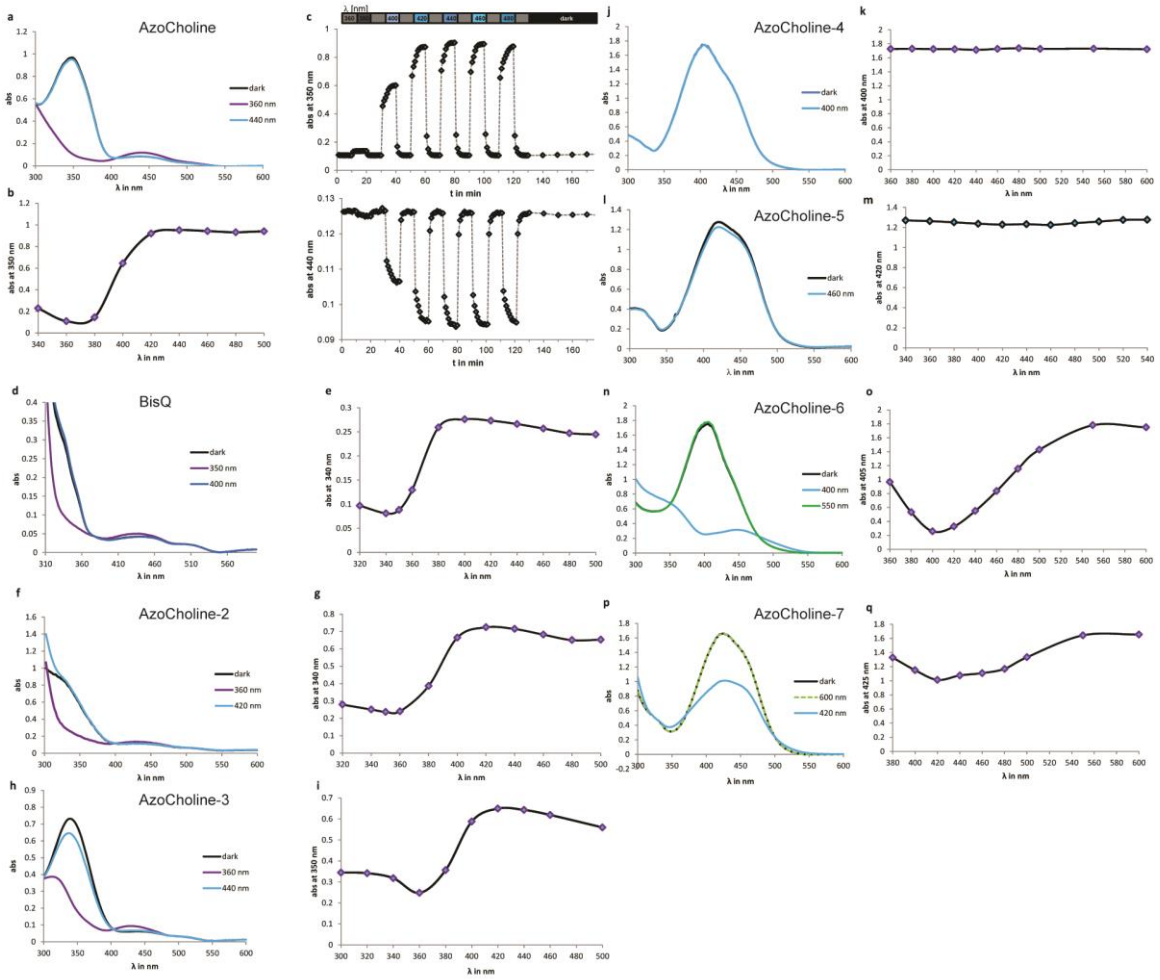

Fig. S2. UV/Vis spectra of PCLs (50 µM in DMSO at 25°C). (a) Absorption spectra of **AzoCholine** in dark, illuminated with 360 nm and with 440 nm (λ_{max} (*trans*, $\pi \rightarrow \pi^*$) = 345 nm; λ_{max}(*cis*, n $\rightarrow \pi^*$) = 440 nm). (b) Absorption of **AzoCholine** at 350 nm when illuminated with indicated wavelength. (c) Action spectrum of **AzoCholine**. Distinct photostationary states are reached by witching to cetrain wavelength. When adapted to violet light **AzoCholine** stays in *cis* configuration for more than 40 min. **AzoCholine** has an extinction coefficient (at 350 nm) of 45789.11 M^{-1} cm^{-1} in PBS and 48925.17 M^{-1} cm^{-1} in DMSO. (d) Absorption spectra of **BisQ** in dark, illuminated with 350 nm and with 400 nm (λ_{max} (*trans*, $\pi \rightarrow \pi^*$) = 324 nm; λ_{max} (*cis*, n $\rightarrow \pi^*$) = 440 nm). (e) Absorption of **BisQ** at 340 nm when illuminated with indicated wavelength.(f) Absorption spectra of **AzoCholine-2** in dark, illuminated with 360 nm and with 420 nm (λ_{max} (*trans*, $\pi \rightarrow \pi^*$) = 320 nm; λ_{max} (*cis*, n $\rightarrow \pi^*$) = 425 nm). (g) Absorption at 340 nm when illuminated with indicated wavelength. (h) Absorption spectra of **AzoCholine-3** in dark, illuminated with 360 nm and with 440 nm (λ_{max} (*trans*, $\pi \rightarrow \pi^*$) = 340 nm; λ_{max} (*cis*, n $\rightarrow \pi^*$) = 435 nm). (i) Absorption of **AzoCholine-3** at 350 nm when illuminated with indicated wavelength. (j) Absorption spectra of **AzoCholine-4** in dark and illuminated with 400 nm (λ_{max} ($\pi \rightarrow \pi^*$) = 403 nm). (k) Absorption of **AzoCholine-4** at 400 nm when illuminated with indicated wavelength. (l) Absorption spectra of **AzoCholine-5** in dark and illuminated with 460 nm (λ_{max} ($\pi \rightarrow \pi^*$) = 420 nm). (m) Absorption of **AzoCholine-5** at 420 nm when illuminated with indicated wavelength. (n) Absorption **AzoCholine-6** spectra in dark, illuminated with 400 nm and with 550 nm (λ_{max} ($\pi \rightarrow \pi^*$) = 408 nm). (o) Absorption **AzoCholine-6** at 405 nm when illuminated with indicated wavelength. (p) Absorption of **AzoCholine-7** spectra in dark, illuminated with 420 nm and with 600 nm (λ_{max} ($\pi \rightarrow \pi^*$) = 422 nm). (q) Absorption of **AzoCholine-7** at 425 nm when illuminated with indicated wavelength.

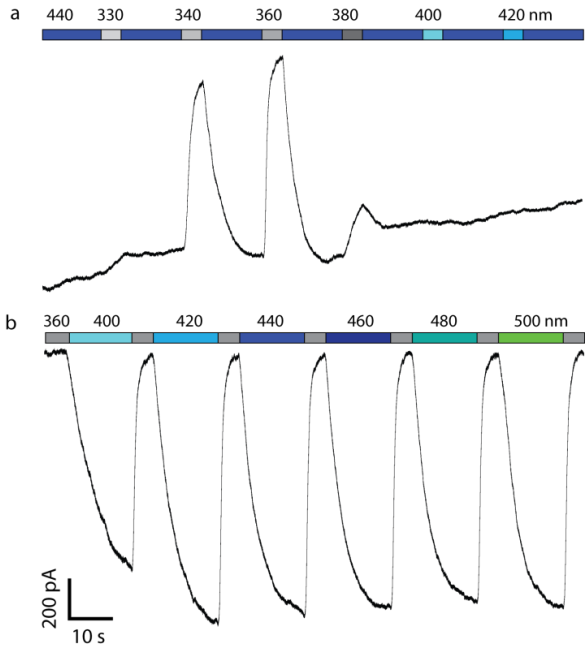

Fig. S3: Action spectrum of **AzoCholine** (50 µM) on α7/GlyR. To determine the optimal wavelengths for activation and deactivation, light was switched between different wavelengths. The optimal wavelengths were determined in (a) λ_{cis} = 340 - 360 nm and in (b) λ_{trans} = 420 - 460 nm. Due to long activation time during the *cis* wavelength screen, the receptor desesitises slowly and a baselinedift accures.

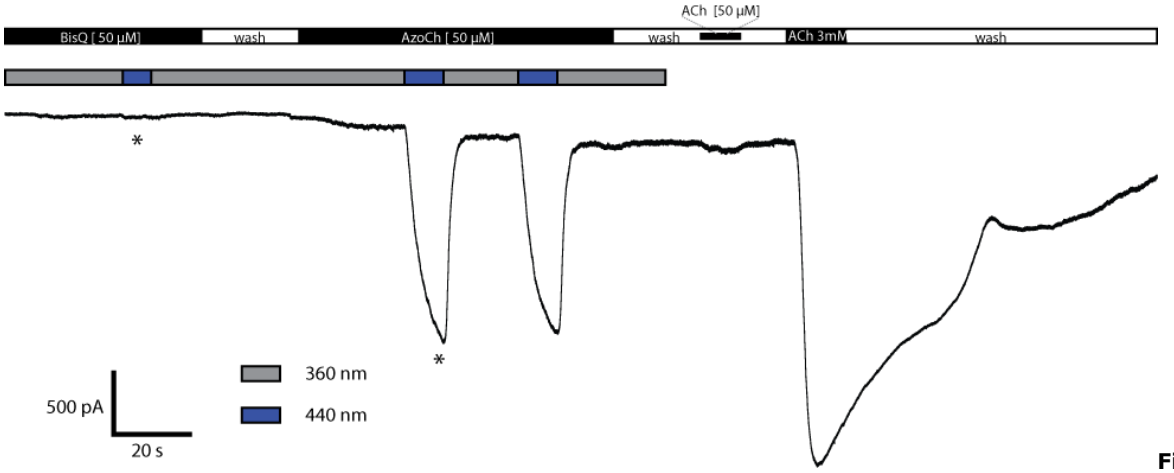

Fig. S4: Typical protocol for electrophysiological characterization of **BisQ** and **AzoCholine** on α7/GlyR. First, **BisQ** is washed in under UV-light irradiation (λ = 360 nm), which shows no effect. After a 25 s wash step with bath solution **AzoCholine** is washed into the application chamber under UV-light irradiation (λ = 360 nm) resulting in a slight increase of baseline current. Changing the light to (λ = 440 nm) results in a strong current, which can be reversed with UV light (λ = 360 nm). Puff application of ACh (50 µM; 10 s) is used to normalize photocurrents (marked *). Finally, for full receptor activation 3 mM ACh is washed in. Due to buffer composition chloride outward currents are recorded.

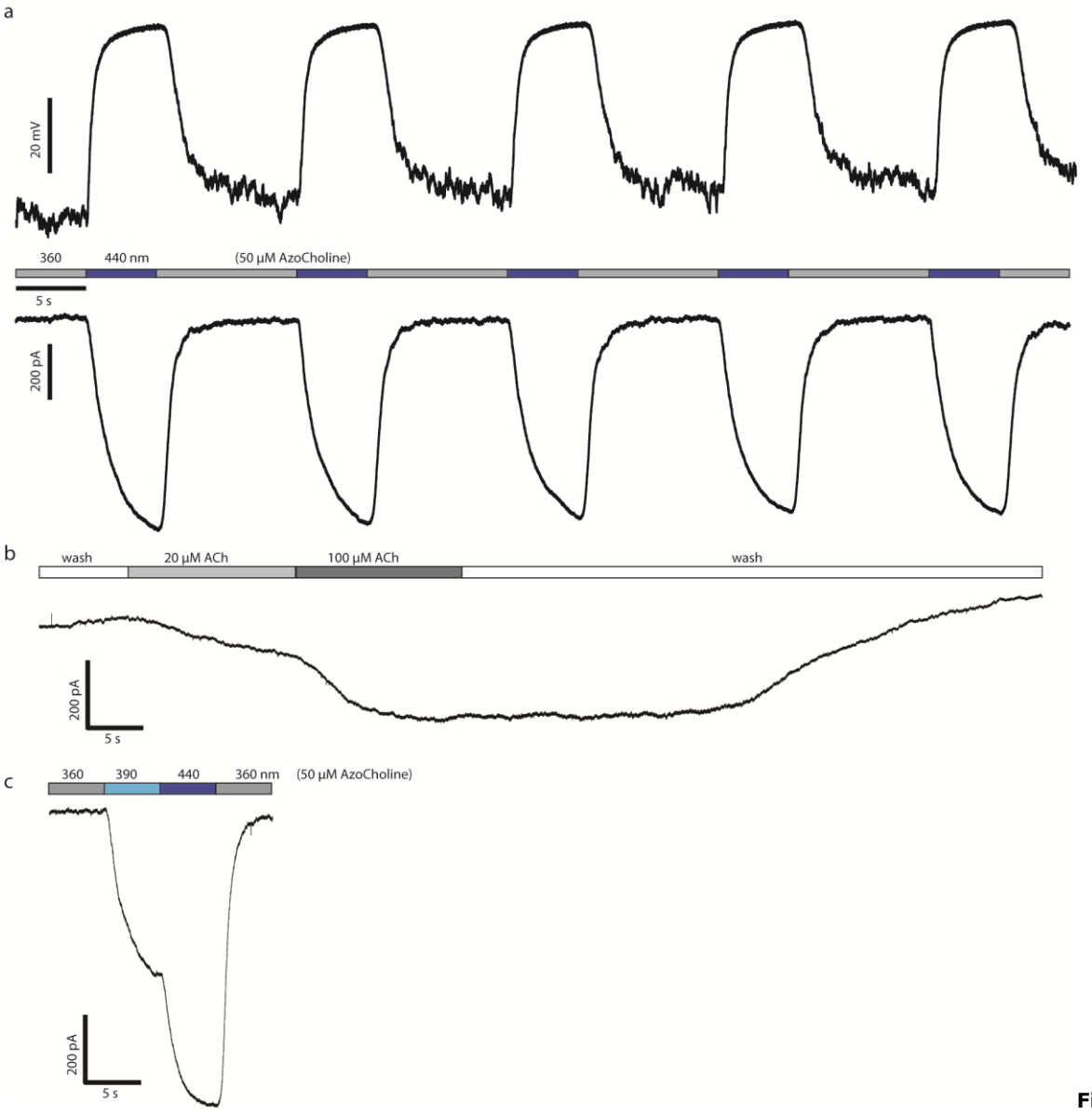

Fig. S5: Reversible switching of **AzoCholine** at α7/GlyR in voltage and current clamp mode and changes in receptor activity by changing agonist concentrations. (a) Holding potential was -60 mV. The wavelengths were λ_{off} = 360 nm and λ_{on} = 440 nm. (b) Two concentrations of acetylcholine (20 µM and 100 µM) were washed in consecutively resulting in a slow stepwise increase of current. (c) Activation of **AzoCholine** (50 µM) with two wavelengths (λ_{trans} = 390 nm and 440 nm) results in a stepwise activation of the receptor by a rapid increase of agonist concentration.

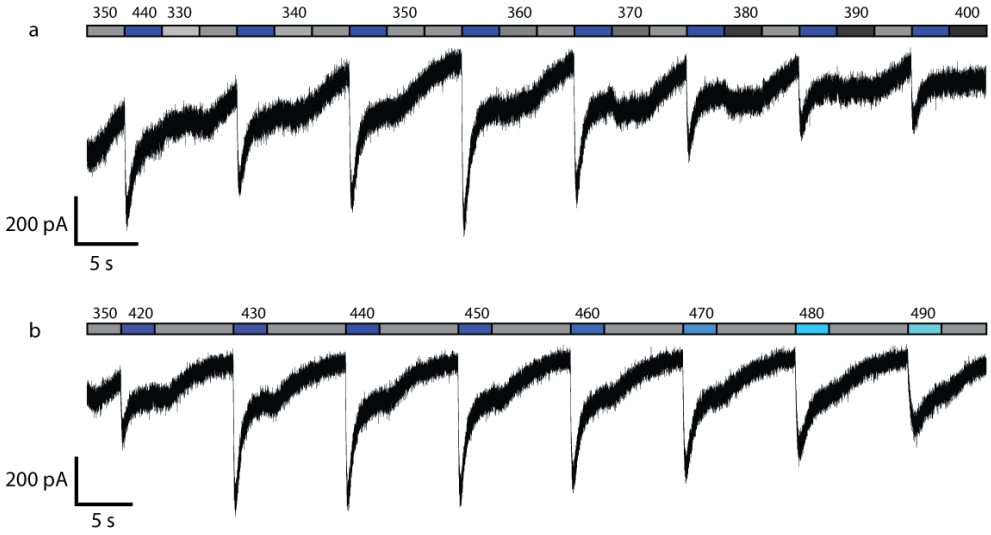

Fig. S6: Action spectrum of **BisQ** (50 µM) on muscle nAChR. To determine the optimal wavelengths for activation and deactivation of the receptor, light was switched between different wavelengths. The optimal wavelengths (a) λ_{cis} = 360 nm and (b) λ_{trans} = 440 nm where found. Even though **BisQ** has a maximal absorbance more in the blue (λ_{max} = 322 nm) in Ringer solution, due to the transmission of the fiber optics in our patch-clamp setup, switching with λ = 360 nm was more effective.

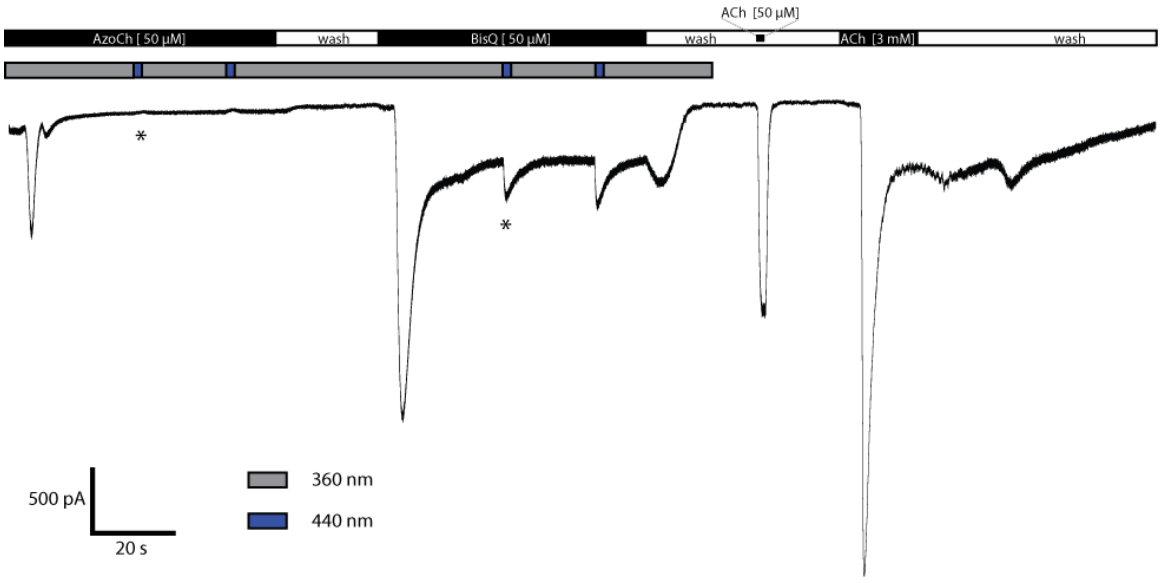

Fig. S7: Typical protocol for electrophysiological characterization of **BisQ** and **AzoCholine** on muscular nAChR. First, 50 µM **AzoCholine** is washed in under 360 nm light. **AzoCholine** evokes a brief peak current followed by rapid desensitization of the receptor. Changing the wavelength to 440 nm has no considerable effect. After a 25 s wash step with bath solution, **BisQ** is washed into the application chamber under UV-light irradiation (λ = 360 nm) resulting in a strong peak current followed by a stationary state current, which can be tuned by changing the wavelength to λ = 440 nm. Puff application of ACh (50 µM; 10 s) is used to normalize photocurrents (marked *). Finally, for full receptor activation 3 mM ACh is washed in.

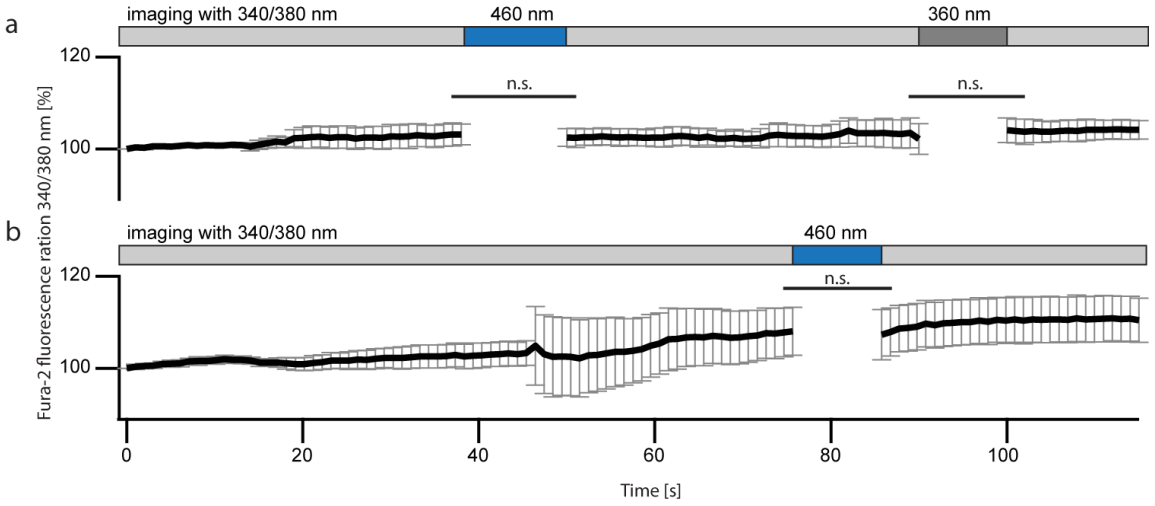

Fig. S8: Calcium imaging with Fura-2 on dorsal root ganglion (DRG) neurons. (a) In the absence of **AzoCholine**, illumination with 460 nm or 360 nm light has no impact upon intracellular [Ca^{2+}] levels in neurons (n = 27 cells, pooled from 4 experiments). (b) Illumination with 460 nm wavelength in the presence of **AzoCholine** (250 µM) and the α7 nAChR antagonist (MG624, 50 µM) does not result in significant increase in intracellular [Ca^{2+}] (n = 21 cells, pooled from 4 experiments). Error bars represent standard deviation. Fluorescence intensity was compared before illumination and at the first time point after illumination and non-parametric Mann–Whitney U-test was used. A significance level of $p \leq 0.05$ was reached in neither of these control experiments (n.s. = non, significant).

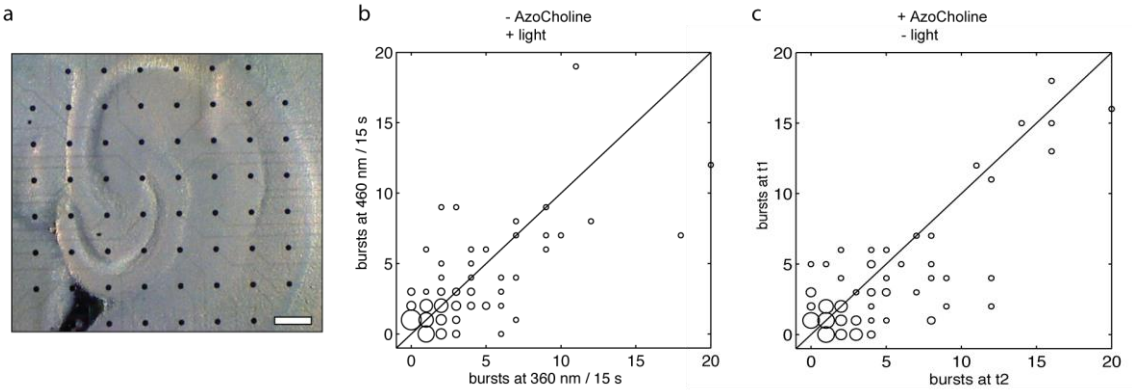

Fig. S9: Murine brain slice on multi-electrode array (MEA) and control experiments. (a) Horizontal murine brain slice positioned with the hippocampus onto the 60 electrodes (black dots) of the MEA (Scale bar represents 200 µm). (b) Quantification of bursting activity of all experiments without **AzoCholine** (dot size related to the number of cells responding). Light switching in absence of **AzoCholine** does not change bursting pattern (n = 103 cells, pooled from 6 experiments, $p>0.05$). (c) Quantification of bursting activity of all experiments without light (dot size related to the number of cells responding). Presence of AzoCholine without switching of light does not change bursting pattern. Bursting was recorded and compared at two time points (t1 and t2) for 15 s (n = 98 cells, pooled from 4 experiments, $p>0.05$).

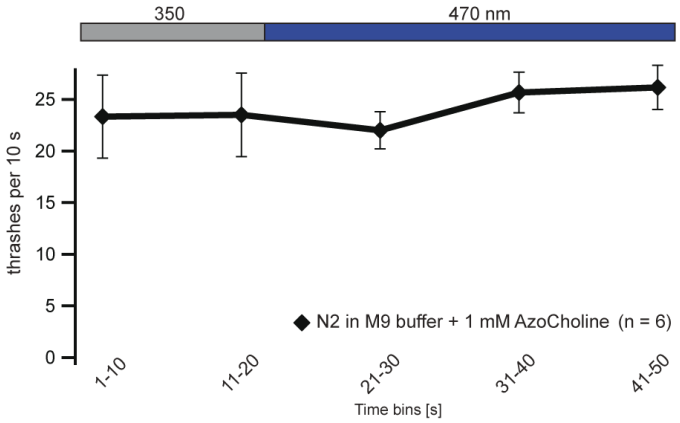

Fig. S10: Quantification of *C. elegans* N2 swimming cycles. Nematodes were swimming in M9 buffer with AzoCholine (1 mM; n = 6). When switching from UV (350 nm) to blue (470 nm) light (bar), stopping/freezing behavior was not induced.

Additional Information (AzoCholine, not included in publication)

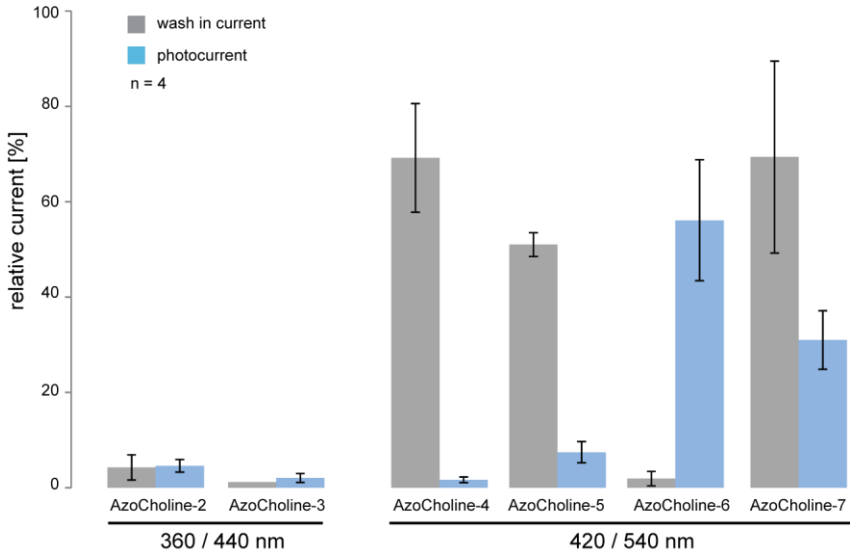

Fig. X1. Effect of **AzoCholines** 2 - 7 (50 µM) on α7/GlyR chimera expressed in HEK293T cells. Light was switched as indicated (between 360 nm and 440 nm or between 420 nm and 540 nm, respectively). Puff application of ACh (50 µM) evoked an inward current and was used for normalization. **AzoCholine** 2 and 3 did exhibit poor receptor activation. **AzoCholine** 4, 5, and 7 triggered large light-independent inward currents, which exceeded the light triggered currents. Only AzoCholine 6 showed a small wash in current and prominent photocurrent. Bars represent mean; error bars represent SEM.

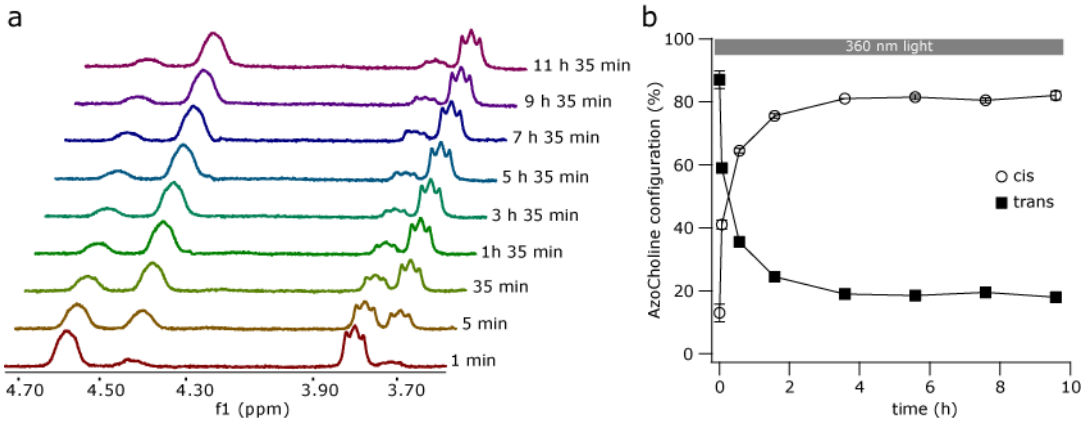

Fig. X2. ^{1}H NMR of **AzoCholine** (5 mM in DMSO). a) A series of ^{1}H NMR measurements of **AzoCholine** recorded within 12 h during illumination with 360 nm light show the transition of the *cis/trans*- ratio over time. b) Before illumination **AzoCholine** is mostly present in the *trans* configuration (96 ± 4 %). At the End of the experiment **AzoCholine** preferably occupies the *cis*-configuration (85 ± 4 %).

III: Azologization of Fomocaine to Fotocaine

Development of a New Photochromic Ion Channel Blocker via Azologization of Fomocaine

Matthias Schoenberger[1], Arunas Damijonaitis[1], Zinan Zhang[2], Daniel Nagel[3], and Dirk Trauner[1]

1 Department of Chemistry, Ludwig-Maximilians-Universitat Munchen, Munich 81377, Germany

2 Department of Chemistry, Princeton University, Princeton, New Jersey 08544, United States

3 Department Molecules-Signaling-Development, Max-Planck Institute of Neurobiology, Martinsried 82152, Germany

ABSTRACT:

Photochromic blockers of voltage-gated ion channels are powerful tools for the control of neuronal systems with high spatial and temporal precision. We now introduce fotocaine, a new type of photochromic channel blocker based on the long-lasting anesthetic fomocaine. Fotocaine is readily taken up by neurons in brain slices and enables the optical control of action potential firing by switching between 350 and 450 nm light. It also provides an instructive example for "azologization", that is, the systematic conversion of an established drug into a photoswitchable one.

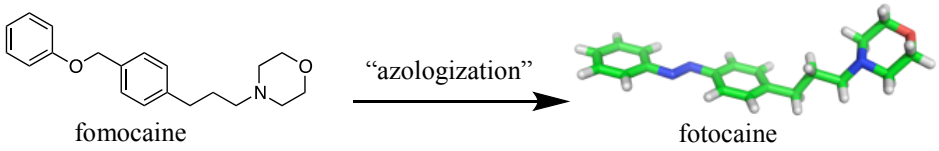

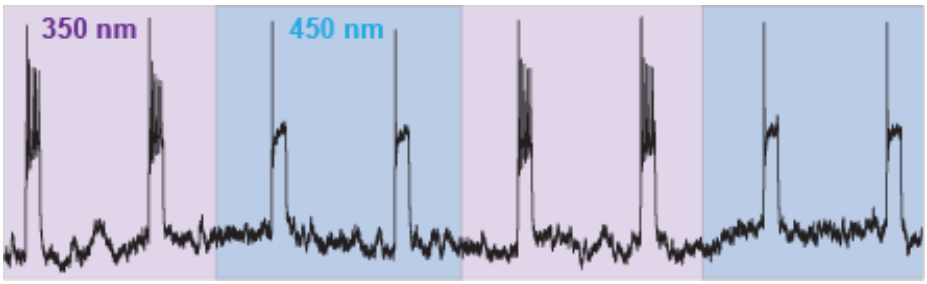

KEYWORDS: Photopharmacology, local anesthetics, fomocaine, action potential firing control, azologization, azobenzene photoswitch

Optical methods for controlling neuronal function have revolutionized neuroscience in recent years.[1-3] For instance, photoswitchable versions of local anesthetics have proven to be powerful tools for addressing native voltage gated ion channels[4,5] and have been used in pain research and vision restoration.[6-8] Two of these compounds, viz. the bis-quaternary ammonium ion QAQ[6] and the quaternary ammonium ion DENAQ[8] are in essence photoswitchable azobenzene derivatives of QX-314, which is a permanently charged version of lidocaine (Figure 1).[9] As is the case for QX-314, their permanent charge may limit their ability to cross biological barriers, such as membranes. In our

ongoing efforts to develop new and improved photoswitchable ion channel blockers, we therefore decided to investigate alternative pharmacophores.

Local anesthetics have a long medical history and are mechanistically reasonably well understood.[10-13] They usually function as use-dependent open channel blockers, in particular of voltage gated-sodium channels (Na_V), but can also have effects on other molecular targets. The alkaloid cocaine, for instance, has been used as a topical anesthetic in ophthalmology since the turn of the last century, despite its well known effects on the central nervous system.[14] Novocaine is a representative of the so-called ester local anesthetics and was initially developed as a simplified analog of cocaine. In the late 1960s, the morpholine fomocaine was introduced, which bears little structural resemblance to cocaine with the exception of a tertiary amine functionality.[14,15] It has been used for decades as a long-lasting topical anesthetic and shows reduced systemic toxicity due to its propensity to bind to plasma proteins.[14] We now describe a photoswitchable version of fomocaine, termed fotocaine, which functions as a photochromic ion channel blocker and can be used to control neuronal activity with light.

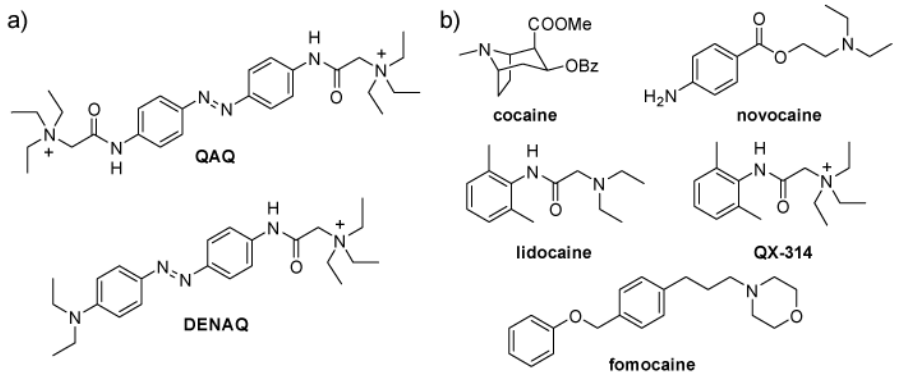

Figure 1. a) Photoswitchable azobenzene derivatives QAQ and DENAQ used as photoswitchable blockers of voltage gated ion channels. b) Structures of local anesthetics. QX-314 is a permanently charged derivative of the local anesthetic lidocaine. Cocaine is a tropane alkaloid, novocaine is an ester local anesthetic. All of these compounds feature a tertiary amine pharmacophore. Fomocaine is an ether local anesthetic with a morpholino group.

Results and Discussion

In addition to its interesting pharmacological properties, fomocaine evoked our interest due to its molecular structure. It features a benzyl-phenyl ether moiety and thus abides to our philosophy of "azologization", i.e. the rational introduction of azobenzenes into drugs (Figure 2). Obvious targets for azologization are compounds that incorporate stilbenes, 1,2-diphenyl ethanes, 1,2-diphenyl hydrazines, N-benzyl anilines, benzyl-phenyl ethers, benzyl-phenyl thioethers, diaryl esters, diaryl amides and heterocyclic derivatives thereof (Figure 2a). A survey of databases shows that many established drugs feature these moieties. Replacing them with azobenzenes yields photoswitchable analogs that resemble their parent compounds in size and shape ("azosters"), but ideally change their efficacy upon irradiation. Application of this logic to fomocaine yields fotocaine, wherein a CH_2-O moiety has been replaced by a diazene unit (N=N) (Figure 2b). We hypothesized that this substitution would provide a photoswitchable ion channel blocker with similar pharmacodynamics and pharmacokinetics. The three-step synthesis of fotocaine from commercially available starting materials is described in the Supporting Information.

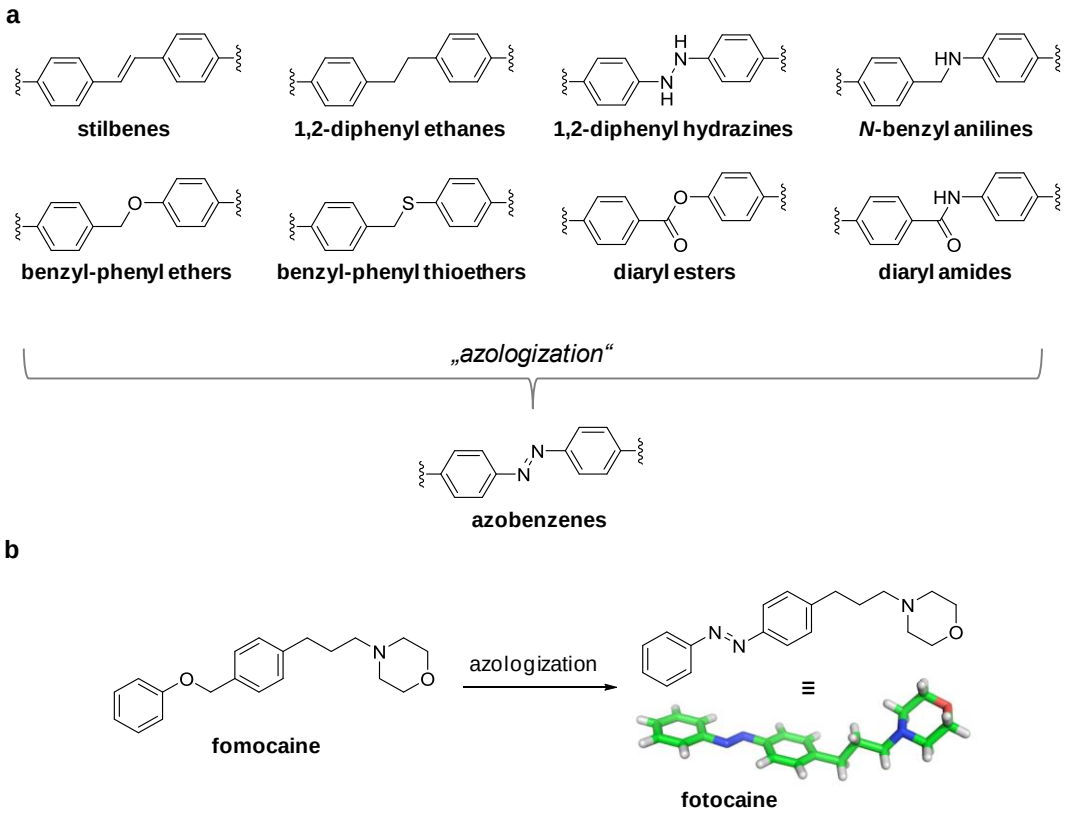

Figure 2. The logic of azologization. a) Prime isosters of azobenzenes, i.e. azosters, are stilbenes, 1,2-diphenyl ethers, 1,2.diphenyl hydrazines, N-benzyl anilines, benzyl-phenyl ethers, benzyl-phenyl thioethers, diaryl esters and diaryl amides. b) Application of the concept of azologization to fomocaine. Replacement of the benzyl-phenyl ether bridge by a diazene yields the azobenzene derivative fotocaine. The X-ray structure of fotocaine is deposited at the Cambridge crystallographic data center, ID: 991565.

To test fotocaine's photoswitching properties, we first utilized UV/Vis spectroscopy (Figure 3). A 50 µM solution of fotocaine in DMSO was placed in a quartz cuvette with 1 cm diameter and illuminated from above using a monochromator. The lightinduced isomerization of fotocaine and the corresponding absorption spectra of *cis*- and *trans*-isomers are depicted in Figure 3a. As a classical azobenzene, isomerization could be followed by monitoring the π to π^* transition at 330 nm over time. Toggling between 350 and 450 nm light switched the molecule into its *cis*- and *trans*-state, respectively (Figure 3c, i). As it is known for regular azobenzenes, photostationary *cis*/*trans* ratios of up to 90:10 can be achieved by irradiation with ultraviolet light.[3] Wavelengths between 400 and 350 nm could be used to install mixtures with different *cis*/*trans* ratios (Figure 3c, ii). As expected from a "classical" azobenzene, the thermodynamically less stable *cis*-state remained stable in the dark (Figure 3c, iii).[16,17] Thus, fotocaine provides the desired reversible light-mediated *cis*/*trans*-isomerization. As an added advantage, it shows bistability and stays in its *cis*-state for severalminutes even without continuous UV-illumination.

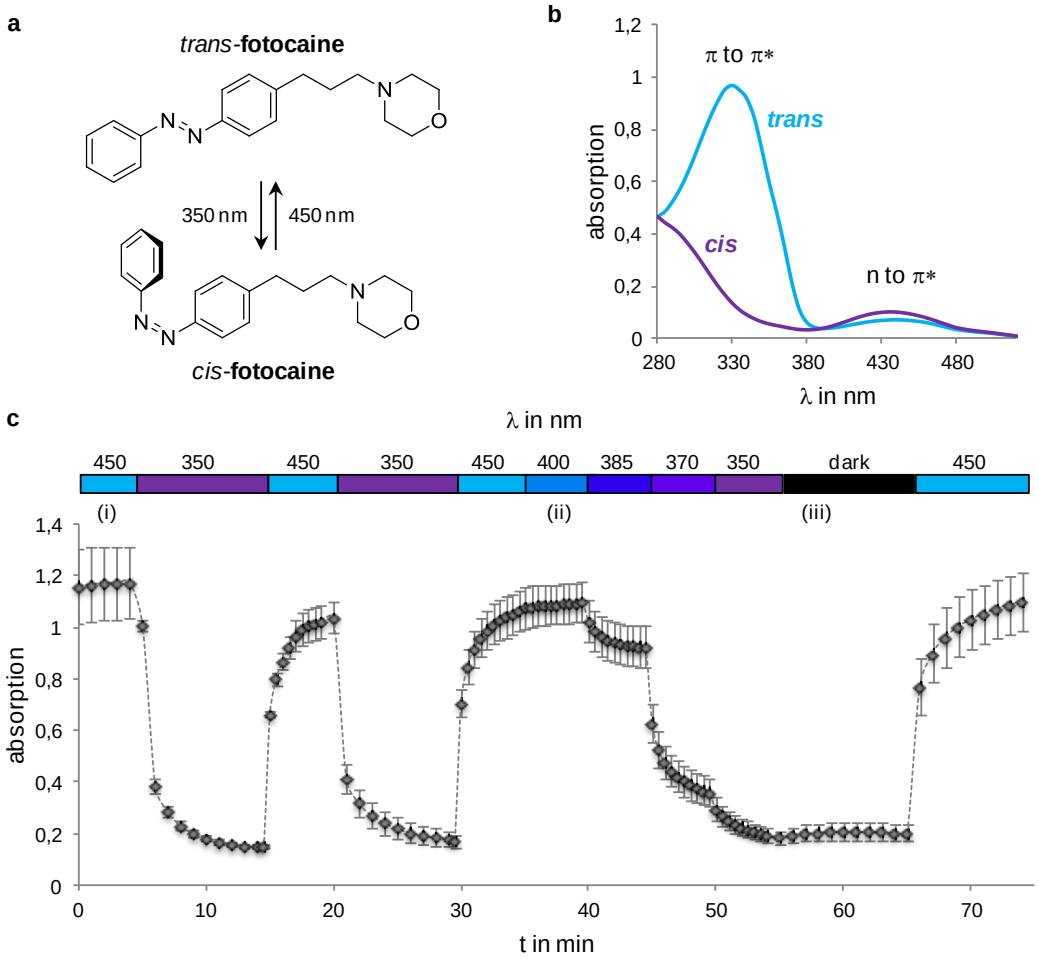

Figure 3. Photoswitching of fotocaine followed by UV/Vis spectroscopy. a) UV-light (e.g. 350 nm) isomerizes the azobenzene functional group in fotocaine to its *cis*-isomer, which is the thermodynamically less stable state. Blue light (e.g. 450 nm) triggers isomerization to *trans*. b) Absorption spectra of *trans*-fotocaine (blue line) and *cis*-fotocaine (purple line) are distinct. The π to π* band decreases starkly upon isomerization to *cis*, while the n to π* band slightly increases. c) In-time photoswitching by following the fotocaine absorption at 330 nm. Fotocaine can be reversibly isomerized by switching between, e.g., 450 and 350 nm (i). Wavelengths between 400 and 350 nm lead to graded effects (ii). Once switched to *cis*, fotocaine stays in its excited state without further illumination (iii). No decay was detected for the investigated time of 10 min. (n = 3, error bar indicates standard deviation).

Next, we investigated the ability of fotocaine to optically control neuronal function. To this end, we resorted to patch clamp electrophysiology using dissociated mouse hippocampal neurons (Figure 4). Fotocaine was applied at 50 µM concentration in the external bath solution. At a starting potential of -80 mV, action potential (AP) firing of neurons was induced by injecting a 50 pA current. When the illumination wavelength was set to 450 nm, AP firing was inhibited. However, when switching to 350 nm, AP firing triggered by the same current took place reliably. This process could be repeated with a variety of different illumination protocols (Figure S1). The same effects were observed at higher concentration (100 µM fotocaine, Figure S1b). The single action potential at the beginning of each current injection under 450 nm indicates that *trans*-fotocaine acts as an open channel blocker as is the case for its permanently charged relatives.[9,18]

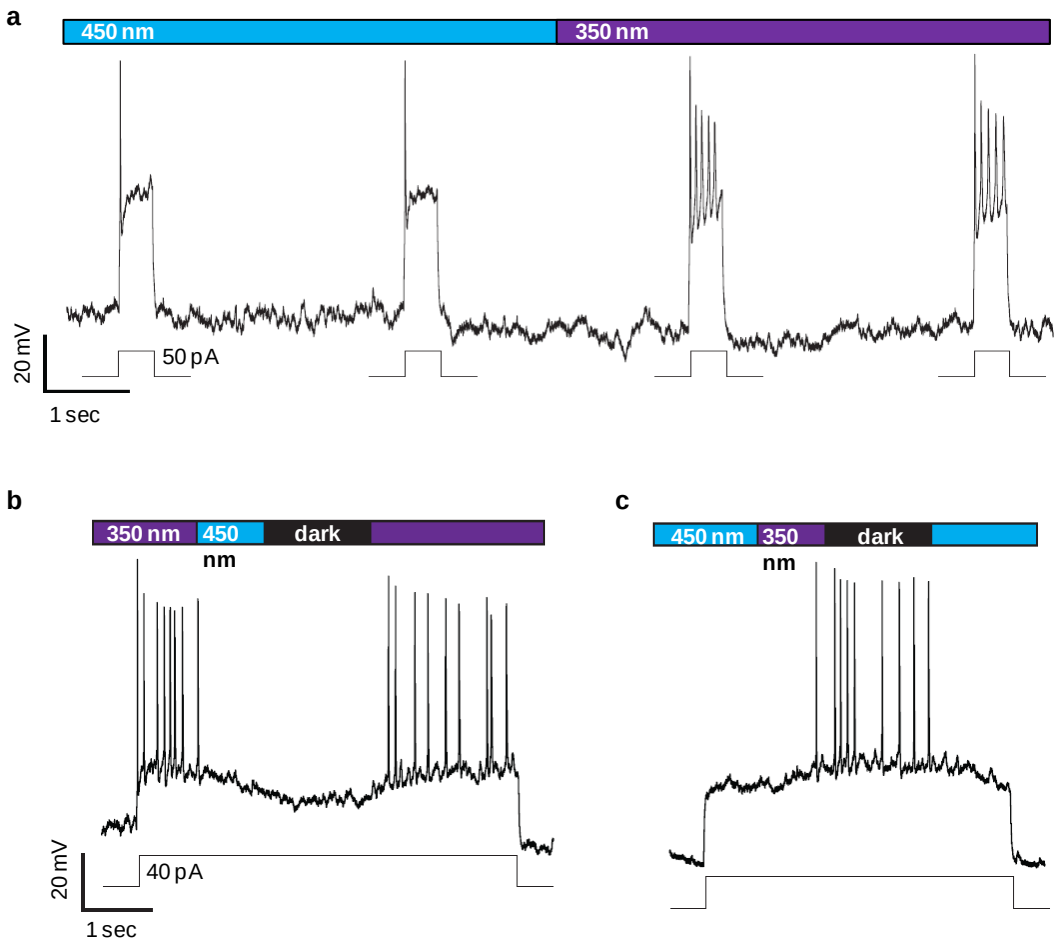

Figure 4. Photocontrol of action potential (AP) firing mediated by fotocaine investigated in whole cell patch clamp experiments (representative traces). a) Dissociated mouse hippocampal neurons, current clamp mode, 50 µM fotocaine. AP-firing was triggered by injecting 50 pA for 300 ms (cells were held at -80 mV). Under 450 nm (*trans*-fotocaine), AP-firing was suppressed, while and 350 nm illumination (*cis*-fotocaine), allowed AP-firing. The initial AP under 450 nm is indicative of the action of an open channel blocker. b & c) Acute mouse brain slice, hippocampal CA1 neurons, current clamp mode, after 10 min wash-out of fotocaine. 40 pA currents were injected and illumination wavelengths were changed simultaneously. Effects of *cis*- and *trans*-fotocaine were identical to a). In addition, when 350 nm or 450 nm were turned off after short application, the thereby installed effect maintained.

To test the action of fotocaine in a functional neuronal circuit and assess its distribution in tissues, we performed further patch clamp experiments using acute hippocampal mouse brain slices. First, the tissue preparation was treated with 100 µM fotocaine for 5 minutes to allow the cells to take up the photochromic drug. Then, buffered ringer solution was perfused for 10 min to remove the photoswitchable blocker from the extracellular solution. As expected for a long-lasting open channel blocker, photocontrol of AP firing was possible without continuous supply of extracellular fotocaine (Figure 4b). AP firing was triggered by injecting a 40 pA current for several seconds and illumination wavelengths where switched during this activation period. In line with our observations using dissociated neurons, AP firing was inhibited by 450 nm illumination and enabled by 350 nm. Furthermore, the bistability of fotocaine, which was established with UV/Vis-spectroscopy (Figure 3c), also applied to this physiological experiment. Neuronal silencing triggered by 450 nm light was sustained in the dark but could be lifted with 350

nm light (Figure 4b). Conversely, AP-firing activated with 350 nm light continued after the light was tuned off but could be abrogated by switching to 450 nm (Figure 4c).

In summary, we have applied the logic of azologization to the local anesthetic fomocaine thus establishing a novel photochromic ion channel blocker, fotocaine. We demonstrated that fotocaine gets readily taken up by neurons in brain slices, can be used to control their action potential firing with light, and has long-lasting effects. Its relatively simple structure could facilitate the design and synthesis of improved versions with desirable properties, such as red-shifted action spectra. These investigations and the application of fotocaine in neurophysiology, in particular as an analgesic for the photopharmacological control of pain, will be reported in due course.

METHODS

UV/Vis Spectroscopy was performed using a VARIAN Cary 50 Scan UV/Vis spectrometer. PCL solution was placed in a standard quartz cuvette (d = 1 cm) illuminated by a light fibre cable from above.

Cell and Tissue Preparation. Dissociated mouse hippocampal neurons were prepared and cultured using an astrocyte feeder layer as reported elsewhere.19 For acute mouse hippocampal brain slices, BL6 wild type mice (postnatal days 9 to 13) of either sex, were quickly decapitated, the brain was removed, and 250 µm horizontal slices were prepared using a vibrating microtome (7000smz-2, Campden Instruments). Slices were incubated for 30 min at 34°C in carbogenated (5 % CO2, 95 % O2) sucrose medium (mM: 87 NaCl, 2.5 KCl, 7 $MgCl_2$, 0.5 $CaCl_2$, 25 Gluc, 1.25 NaH_2PO_4, 25 $NaHCO_3$, 75 sucrose, (319 mOsm)). Slices were perfused with 100 µM Fotocaine in bath solution for 5 min, followed by 10 min perfusion with bath solution. Whole cell patch clamp recordings where performed on CA1 hippocampal neurons.

Electrophysiology. Whole cell patch clamp recordings where performed using a standard electrophysiology setup equipped with a HEKA Patch Clamp EPC10 USB amplifier and patch master software. Micropipettes were generated from "Science Products GB200-F-8P with filament" pipettes using a vertical puller (PC-10, Narishige). Resistance varied between 5-7 MΩ. Bath solution for dissociated hippocampal neurons contained in mM: 140 NaCl, 3 KCl, 2 $CaCl_2$, 1 $MgCl_2$, D-Gluc 10, 20 HEPES (NaOH to pH 7.4). Pipette solution for dissociated hippocampal neurons contained in mM: 107 KCl, 1.2 $MgCl_2$, 1 $CaCl_2$, 10 EGTA, 5 HEPES, 2 MgATP, 0.3 Na_2GTP (KOH to pH 7.2). Bath solution for acute brain slice contained in mM: 125 NaCl, 2.5 KCl, 1 $MgCl_2$, 2 $CaCl_2$, 10 Glucose, 1.25 NaH_2PO_4, 26 $NaHCO_3$, (290 - 295 mOsm). Pipette solution for acute brain slice contained in mM: 140 K-gluconate, 4 NaCl, 12 KCl, 10 HEPES, 4 MgATP, 0.4 Na_2ATP (KOH to pH 7.3). Action Potentials (APs) were induced with 50 pA current injection. Fotocaine was dissolved in bath solution from a 1000 x DMSO stock for either tissue preparation.

Illumination. Irradiation during electrophysiology and UV/Vis experiments was performed using a TILL Photonics Polychrome 5000 monochromator operated by the PolyCon software or by the patch clamp amplifier, respectively.

ASSOCIATED CONTENT

Representative traces of AP-firing using different concentrations of fotocaine and illumination timing (Figure S1). Synthesis and characterization of organic compounds. This material is available free of charge via the Internet at http://pubs.acs.org.

Author Contributions

D.T. supervised the study. M.S. conceived of the study, planed the chemical synthesis, performed the electrophysiology on dissociated neurons and wrote the manuscript together with D.T. and A.D. A.D. performed the electrophysiology on acute mouse brain slice. Z.Z. performed the chemical synthesis, D.N. prepared the dissociated mouse hippocampal neurons.

Acknowledgements

The authors thank Dr. Peter Mayer (LMU Munich) for X-ray structure elucidation and Dr. David Barber for helpful discussions. M.S. is grateful for financial support from the German National Study Foundation. A.D. and M.S. thank the International Max Planck Research School for Life Sciences (IMPRS-LS).

References

1. Deisseroth, K. (2011) Optogenetics. Nat. Methods 8, 26-29.

2. Zemelman, B. V., Lee, G. A., Ng, M., and Miesenbock, G. (2002) Selective photostimulation of genetically chARGed neurons. Neuron 33, 15-22.

3. Fehrentz, T., Schonberger, M., and Trauner, D. (2011) Optochemical genetics. Angew. Chem., Int. Ed. Engl. 50, 12156-12182.

4. Banghart, M. R., Mourot, A., Fortin, D. L., Yao, J. Z., Kramer, R. H., and Trauner, D. (2009) Photochromic blockers of voltage-gated potassium channels. Angew. Chem., Int. Ed. Engl. 48, 9097-10001.

5. Banghart, M., Borges, K., Isacoff, E., Trauner, D., and Kramer, R. H. (2004) Light-activated ion channels for remote control of neuronal firing. Nat. Neurosci. 7, 1381-1386.

6. Mourot, A., Fehrentz, T., Le Feuvre, Y., Smith, C. M., Herold, C., Dalkara, D., Nagy, F., Trauner, D., and Kramer, R. H. (2012) Rapid optical control of nociception with an ion-channel photoswitch. Nat. Methods 9, 396-402.

7. Polosukhina, A., Litt, J., Tochitsky, I., Nemargut, J., Sychev, Y., De Kouchkovsky, I., Huang, T., Borges, K., Trauner, D., Van Gelder, R. N., and Kramer, R. H. (2012) Photochemical restoration of visual responses in blind mice. Neuron 75, 271-282.

8. Tochitsky, I., Polosukhina, A., Degtyar, V. E., Gallerani, N., Smith, C. M., Friedman, A., Van Gelder, R. N., Trauner, D., Kaufer, D., and Kramer, R. H. (2014) Restoring Visual Function to Blind Mice with a Photoswitch that Exploits Electrophysiological Remodeling of Retinal Ganglion Cells. Neuron 81, 800-813.

9. Mourot, A., Kienzler, M. A., Banghart, M. R., Fehrentz, T., Huber, F. M., Stein, M., Kramer, R. H., and Trauner, D. (2011) Tuning photochromic ion channel blockers. ACS Chem. Neurosci. 2, 536-543.

10. Moldovan, M., Alvarez, S., Romer Rosberg, M., and Krarup, C. (2013) Axonal voltage-gated ion channels as pharmacological targets for pain. Eur. J. Pharmacol. 708, 105-112.

11. Wulff, H., Castle, N. A., and Pardo, L. A. (2009) Voltage-gated potassium channels as therapeutic targets. Nat. Rev. Drug Discovery 8, 982-1001.

12. Wang, Y., Park, K. D., SalomeÌ, C., Wilson, S. M., Stables, J. P., Liu, R., Khanna, R., and Kohn, H. (2011) Development and Characterization of Novel Derivatives of the Antiepileptic Drug Lacosamide That Exhibit Far Greater Enhancement in Slow Inactivation of Voltage-Gated Sodium Channels. ACS Chem. Neurosci. 2, 90-106.

13. Wang, Y., Wilson, S. M., Brittain, J. M., Ripsch, M. S., SalomeÌ□, C., Park, K. D., White, F. A., Khanna, R., and Kohn, H. (2011) Merging Structural Motifs of Functionalized Amino Acids and □-Aminoamides Results in Novel Anticonvulsant Compounds with Significant Effects on Slow and Fast Inactivation of Voltage-Gated Sodium Channels and in the Treatment of Neuropathic Pain. ACS Chem. Neurosci. 2, 317-332.

14. Oelschlager, H. (2000) Fomocaine from the chemical, pharmacokinetic and pharmacologic viewpoint: current status and overview. Pharm. Unserer Zeit 29, 358-364.

15. Oelschlager, H., Iglesias-Meier, J., Gotze, G., and Schatton, W. (1977) On a novel Fomocaine synthesis/10th communication: on syntheses of new compounds with local anaesthetic activity. Arzneimittelforschung 27, 1625-8.

16. Sadovski, O., Beharry, A. A., Zhang, F., and Woolley, G. A. (2009) Spectral tuning of azobenzene photoswitches for biological applications. Angew. Chem., Int. Ed. Engl. 48, 1484-6.

17. Schonberger, M., and Trauner, D. (2014) A Photochromic Agonist for mu-Opioid Receptors. Angew. Chem., Int. Ed. Engl.

18. Nau, C., and Wang, G. K. (2004) Interactions of local anesthetics with voltage-gated Na+ channels. J. Membr. Biol. 201, 1-8.

19. Kaech, S., and Banker, G. (2006) Culturing hippocampal neurons. Nat. Protoc. 1, 2406-2415.

IV: Ethylene bridged azobenzene QAQ

Ethylene bridged azobenzene equips *trans*-active photochromic ligands with a dark-adapted *cis*-configuration

Arunas Damijonaitis, David H. Woodmansee, Dirk Trauner

Department of Chemistry, Ludwig-Maximilians-University Munich and Center of Integrated Protein Science Munich; Butenandtstr. 13, 81377 Munich, Germany

Photochromic ligands (PCLs) that contain conventional azobenzenes are typically thermally stable in their *trans*-configuration. This can result in complications when the activity of the molecule also originates from the *trans*-configuration, i.e. the PCL acts on its target protein in the dark. In this case continuous illumination, to keep the PCL in its inactive *cis* configuration has to be applied, which because of phototoxic effects is not desirable. Here, we describe the application of ethylene bridged azobenzenes that are thermally stable in their *cis*-configuration and therefore preferentially occupy this configuration in the dark. This concept was applied to the PCL QAQ to yield the Bridged Azobenzene QAQ (BAQ).

Introduction

Potassium channels, and more specifically, voltage-gated potassium channels (K_V) are essential for the repetitive firing of action potentials and are primary carriers in neural signaling. For instance, many local anesthetics block these channels to reduce nociception and thus suppress pain sensation. Within the last decade, photochromic ligands (PCLs) have emerged as tools to enable the exploration of neuronal systems with the spatiotemporal precision of light (Figure 1).[1] These PCLs are based on known ion channel blockers like lidocaine and fomocaine.[2, 3] The recent development of photochromic ion channels blockers has focused on altering the pharmacological and spectral properties of the azobenzene-containing molecules. In particular, the electronic environment of the azobenzene was modified by the addition of different electron-donating or withdrawing groups to shift the absorption spectrum towards the visible range.[4]

In practice, it is desirable to introduce the PCL to the system in a non-active configuration. This allows the operator to selectively activate the function of the molecule at a chosen time. One way to achieve this is to illuminate the molecule with light of the wavelength that puts it into the inactive state, or to design the molecule in such a way that it is inactive in the dark-adapted state. This would mean the molecule should ideally be active in its *cis*-configuration (*cis*-active). It is difficult to predict if the molecule will be active in its *trans*- or *cis*-configuration, because the binding mode of the PCL is determined by the binding pocket. Many existing PCLs, for instance the ion channel blocker QAQ (Figure 1b), are *trans*-active, which greatly limits their usefulness as a research tool because they remain active in their dark-adapted state.

One possible solution to this problem is rather simple. The molecule can be modified in such a way, that its thermodynamically more stable state is the *cis*-configuration. Azobenzene-containing molecules where the two aryl groups of the azobenzene are bridged by an ethylene unit are a class of compounds that exhibit this property.[5, 6] Herein, we demonstrate that we can change the dark-adapted state of the PCL from the *trans*- to the *cis*-configuration. This concept can be applied to many *trans*-active PCLs, allowing them to be inactive in the dark, and only activated upon photostimulation. The PCL QAQ was therefore endowed with a *cis*-stable photoswitch to yield a Bridged Azobenzene QAQ (BAQ, Figure 1c).

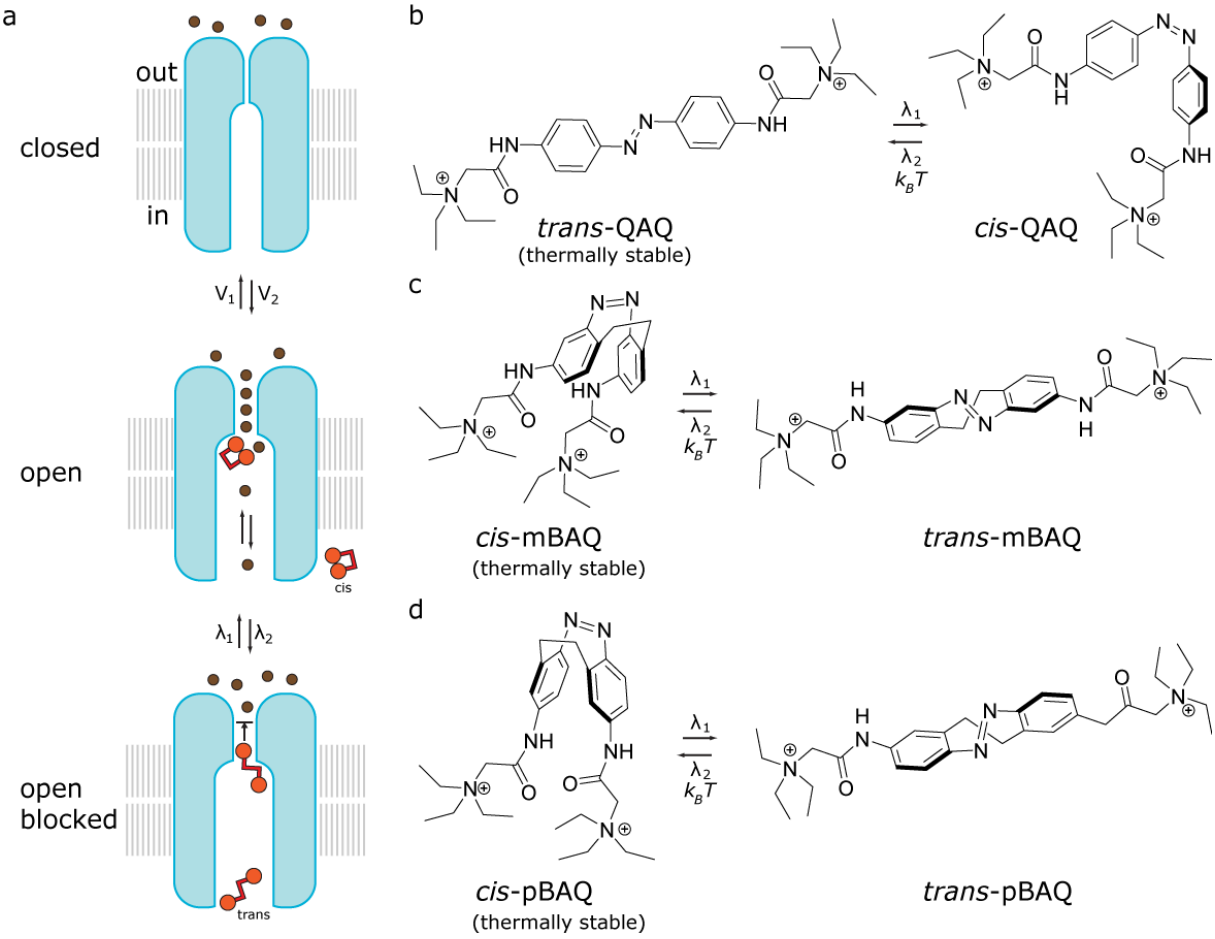

Figure 1. Photochromic potassium channel blockers. a) Putative mechanism of the light-dependent open-channel-block of K_V-channels by photochromic ligands. b) Chemical structure of quaternary ammonium-azobenzene-quaternary ammonium (QAQ) in its thermally stable *trans* and the light induced *cis* configuration. c-d) Chemical structure of (c) *meta*-bridged QAQ (mBAQ) and (d) *para*-bridged QAQ (pBAQ) in their thermally stable *cis*- and the light induced *trans*-configurations.

Results and discussion

The PCLs mBAQ and pBAQ are switchable with $\lambda_{(trans)}$ = 400 nm and $\lambda_{(cis)}$ = 480 nm light.

For the photochromic characterization absorption spectra of the PCLs (50 µM in DMSO) were recorded at ambient temperature (Figure 2). Both, *meta*- and *para*-BAQ exhibited the characteristic n- π^* band at 408 nm (*cis*-isomer).[5, 6] Illumination with light at 400 nm promoted the isomerization of the molecules from the *cis*- to the *trans*-configuration. When switched to *trans*, the n– π^* transition of both molecules shifted to approximately 500 nm. Therefore, illumination with 460–600 nm light converted the *trans*-isomer back to the thermally stable *cis*-form (Figure 2). Notably, *meta*- and *para*-BAQ experienced a faster *trans* to *cis* isomerization (τ = 60 s and τ = 35 s, respectively) than *cis* to *trans* isomerization (τ = 115 s and τ = 100 s, respectively) (Figure 2c).

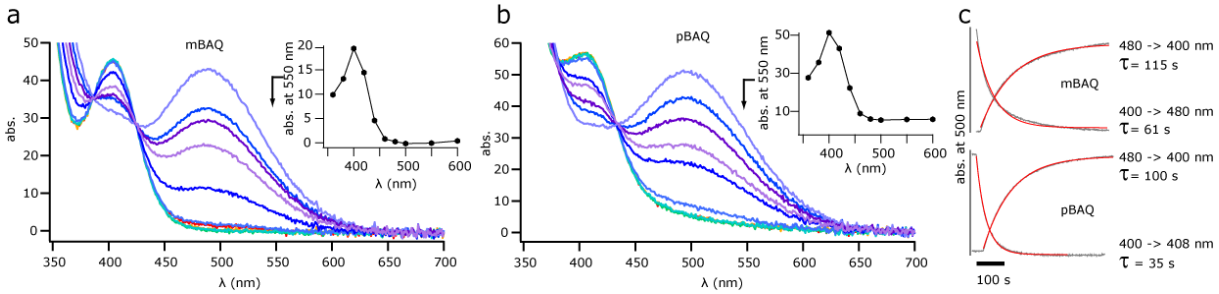

Figure 2. Spectroscopic characterization of mBAQ and pBAQ. UV-Vis spectrum of mBAQ (a) and pBAQ (b) (50 µM in DMSO, RT) in dark and illuminated with different wavelengths. Inlet shows absorption at 550 nm when illuminated with indicated wavelength. c) Kinetic measurement of photoswitching (absorption at 500 nm over time) of mBAQ and pBAQ. *Cis* to *trans* switching was achieved by changing illumination from 480 nm to 400 nm light. *Trans* to *cis* switching was achieved by changing illumination from 400 nm to 480 nm light

The PCL mBAQ blocks K^+ currents in a light-dependent manner.

Using whole-cell patch-clamp electrophysiology mBAQ was tested for its capability to block ion channels. Thus, the voltage-gated potassium channel Shaker-IR was expressed in HEK293T cells. As a doubly charged PCL, mBAQ is not membrane permeable and therefore was applied intracellularly through the patch pipette. Indeed, mBAQ (200 µM) showed a light-dependent block of depolarization-induced K-currents (Figure 3a) in its *trans*-state (38 ± 4 %, *n* = 3, Figure 3b) and a release of the block in the dark-adapted *cis*-state. This process was repeatable for many cycles (Figure 3c).

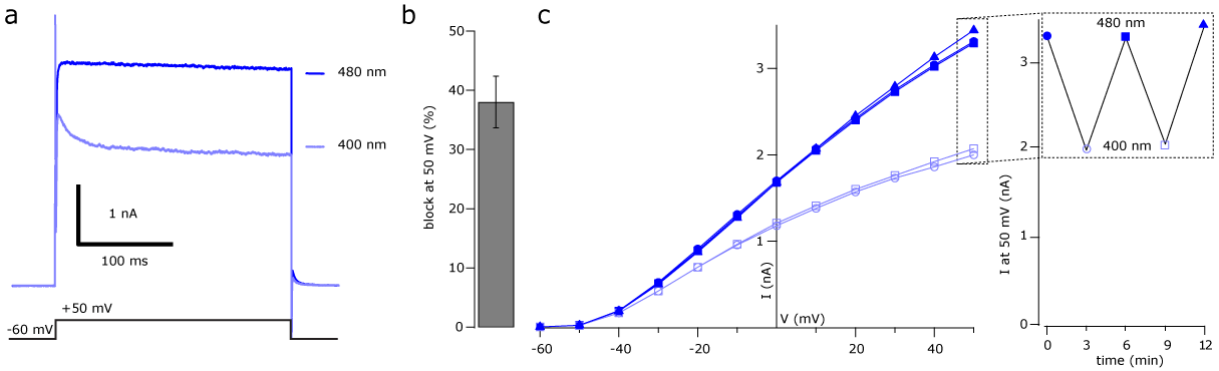

Figure 3. Light controlled Shaker K^+ channel current using intracellular mBAQ (200 µM). a) Depolarization (from -60 to +50 mV) induced K-currents, while illuminated with either 480 nm or 400 nm light. b) Light-dependent block (38 ± 4 %, *n* = 3 cells). c) Current–voltage relationship of depolarization induced currents with reversible light-dependent reduction of currents. Inlet shows K^+ current at +50 mV over two photoswitching cycles.

Photoswitching of mBAQ enables control of membrane potential in naive neural tissue.

Finally, the activity of mBAQ was tested in acute mouse brain slices (Figure 4). Electrophysiological recordings in layer 2/3 cortical neurons were performed with intracellular mBAQ (200 µM). To activate the voltage gated receptors, the membrane potential was changed from -60 mV to +50 mV. During the voltage pulse the wavelength was changed (Figure 4a). When screening for the best *cis* to *trans* isomerization wavelength, the light was switched from 480 nm to a wavelength between 370 and 440 nm (Figure 4b). For the *trans* to *cis* transition, the light was kept at 370 nm and switched to a wavelength between 470 and 560 nm (Figure 4c). In accordance with the data

obtained from UV-Vis and HEK cell experiments, the greatest difference in response was observed when switching between 480 and 400 nm light (Figure 4d). mBAQ exhibits fast switching kinetics for the blocking (τ_{block} = 27.47 ± 0.05 ms) and unblocking ($\tau_{unblock}$ = 38.20 ± 1.53 ms) of the channel (Figure 4e).

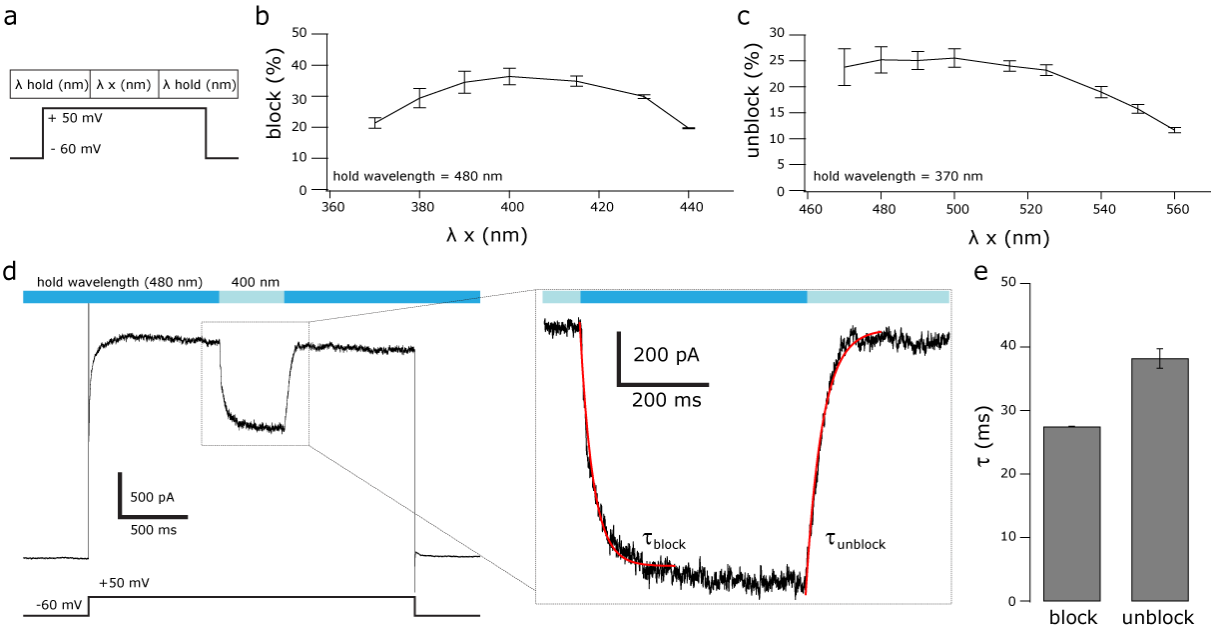

Figure 4. Intracellular mQBAQ (200 µM) quickly modulates membrane potentials in mouse brain slice. a) Voltage step and illumination protocol. b) Wavelength screen displayed as relative photo-block at indicated wavelength normalized to maximal current when holing wavelength is 480 nm. c) Same as (b) for unblock with 370 nm as holing wavelength. d) Depolarizing pulse from −60 mV to +50 mV with light switch between 480 nm and 400 nm. Inlet shows switching with exponential fit (red line) to obtain the kinetics. e) Measurement of photoswitching kinetics (n = 2). *Cis* to *trans* switching (block) was achieved by changing illumination from 480 nm to 400 nm light (τ_{block} = 27.47 ± 0.05 ms). *Trans* to *cis* switching (unblock) was achieved by switching from 400 nm to 480 nm light ($\tau_{unblock}$ = 38.20 ± 1.53 ms).

Outlook

In summary, we developed an efficient photoswitchable ion channel blocker that is inactive in the dark and can be activated by light. The fast switching kinetics and strong blocking effect make mBAQ a promising candidate for the optical control of neural activity. Electrophysiological evaluation of pBAQ will show if the positioning of the quaternary ammonium group has an effect on the efficiency of the light-dependent block.

Methods:

Cell culture and tissue preparation. HEK-293T cells were maintained at 37°C in a 10 % CO_2 atmosphere in Dulbecco's modified Eagle medium (DMEM, Biochrom, Merk Millipore, Germany) containing 10 % FBS (Biochrom, Merk Millipore, Germany). For electrophysiological measurements cells were plated on coverslips treated with 0.1 mg/ml poly-L-lysine (Sigma-Aldrich, Germany) in a density of 40,000 cells per coverslip. HEK-293T cells were transfected using JetPrime (Polyplus-transfections, France) according to manufacturer's instructions 24 h before measurements. Acute mouse coronal brain slices were obtained from BL6 wild type mice (postnatal days 9 to 13) of either sex. Mice were decapitated, the brain was isolated, and 250 µm coronal slices were prepared using a microtome (7000smz-2, Campden

Instruments). Slices were incubated for 30 minutes at 34°C in carbogenated (5 % CO_2, 95 % O_2) sucrose medium (mM: 87 NaCl, 2.5 KCl, 7 $MgCl_2$, 0.5 $CaCl_2$, 25 glucose, 1.25 NaH_2PO_4, 25 $NaHCO_3$, 75 sucrose, (319 mOsm)).

Electrophysiology. Patch clamp measurements were performed in whole-cell modus at ambient temperature and recorded using the EPC10 USB patch Clamp amplifier and PatchMaster software (HEKA Elektronik, Germany). Bath solution for HEK-293T cells contained in mM: 138 NaCl, 1.5 KCl, 1.2 $MgCl_2$, 2.5 $CaCl_2$, 5 HEPES, 10 glucose. Bath solution for brain slices contained in mM: 125 NaCl, 2.5 KCl, 1.25 NaH_2PO_4, 25 $NaHCO_3$, 2 $CaCl_2$, 1 $MgCl_2$, 25 glucose, and 0.5 ascorbic acid saturated with 95 % O_2 / 5 % CO_2. PCLs were added to the pipette solution for HEK-293T cells (in mM: 135 K^+ gluconate, 10 NaCl, 10 HEPES, 2 $MgCl_2$, 2 MgATP, 1 EGTA) or brain slice (in mM: 140 K^+ gluconate, 4 NaCl, 12 KCl, 10 HEPES, 4 $MgCl_2$, 0.4 MgATP), respectively.

Illumination. Illumination during electrophysiology and UV/Vis experiments was achieved using a monochromator (TILL Photonics, Polychrome 5000) operated with the patch clamp amplifier or the PolyCon software, respectively.

Chemical synthesis. The chemical synthesis and compound characterization was conducted by D. H. Woodmansee and is reported in the postdoc report (Trauner group 2013).

Author Contributions

D.T. and A.D designed the study. D.H.W. performed chemical synthesis. A.D. performed UV-Vis and patch−clamp experiments.

ACKNOWLEDGMENTS

The authors gratefully acknowledge M. Sumser for helpful discussions and L. de la Osa de la Rosa for excellent technical assistance.

References:

1. Fehrentz, T., Schonberger, M., and Trauner, D. (2011) Optochemical genetics. *Angew. Chem. Int. Ed. Engl. 50*, 12156-82.
2. Mourot, A., Fehrentz, T., Le Feuvre, Y., Smith, C. M., Herold, C., Dalkara, D., Nagy, F., Trauner, D., and Kramer, R. H. (2012) Rapid optical control of nociception with an ion-channel photoswitch. *Nat. Methods 9*, 396-402.
3. Schoenberger, M., Damijonaitis, A., Zhang, Z., Nagel, D., and Trauner, D. (2014) Development of a New Photochromic Ion Channel Blocker via Azologization of Fomocaine. *ACS Chem. Neurosci. 5*, 514-518.
4. Fehrentz, T., Kuttruff, C. A., Huber, F. M., Kienzler, M. A., Mayer, P., and Trauner, D. (2012) Exploring the pharmacology and action spectra of photochromic open-channel blockers. *Chembiochem 13*, 1746-9.
5. Samanta, S., Qin, C., Lough, A. J., and Woolley, G. A. (2012) Bidirectional photocontrol of peptide conformation with a bridged azobenzene derivative. *Angew. Chem. Int. Ed. Engl. 51*, 6452-5.
6. Sell, H., Nather, C., and Herges, R. (2013) Amino-substituted diazocines as pincer-type photochromic switches. *Beilstein J Org Chem 9*, 1-7.

V: AzoAPG – a PCL for the Glutamate-Gated Chloride Channel

Rational design of photoswitchable antagonists for the glutamate-gated chloride channel

Arunas Damijonaitis[1], David Konrad[1], Jatin Nagpal[2], Simon Veth[1], Alexander Gottschalk[2] and Dirk Trauner[1]

[1] Department of Chemistry, Ludwig-Maximilians-University Munich and Center of Integrated Protein Science Munich, Butenandtstr. 13; 81377 Munich, Germany;

[2] Institute of Biochemistry and Buchmann Institute for Molecular Life Sciences, Johann Wolfgang Goethe-University, Max-von-Laue-Straße 15; 60438 Frankfurt, Germany;

Abstract

Controlling biological function with the spatiotemporal precision of light has become a standard technique in many neuroscience laboratories. These optogenetic tools are based on light sensitive proteins, e.g. Channelrhodopsin 2, which can be genetically targeted to a specific population of cells enabling the light-dependent control of cellular function. This approach for instance is the method of choice, if neural connections are the object of interest. However, the effect of intrinsic receptors cannot be addressed with this method. Photopharmacology, on the other hand, utilizes small molecules, i.e. photochromic ligands (PCL) to endow native target proteins with sensitivity towards light. There are several ways to design a PCL. One approach, azologization, is the incorporation of a light switchable domain, usually an azobenzene into the structure of a known ligand. Upon illumination with different wavelengths the PCL then can be reversibly switched between its active and inactive form. Here, we introduce the rational design of a photoswitchable antagonist for the glutamate-gated chloride channel.

Introduction

The glutamate-gated chloride channel (GluCl) is an anion-selective pentameric ligand-gated ion channel (pLGIC) and a member of the 'Cys-loop' receptor superfamily. GluCls are found in the neurons and muscles of nematodes and other invertebrates where they mediate sensory inputs to control behavior.[1] In neurons, chloride influx leads to the hyperpolarization of the membrane thereby generating an inhibitory postsynaptic potential (IPSP). In the nematode *Caenorhabditis elegans*, for instance, six genes encoding GluCls have been identified. Molecular cloning and *in vitro* expression have shown that the majority of these channels form homopentamers. In 2011 Hibbs and Gouaux solved the three-dimensional structure of monomeric GLC-1 (GluClα), which was the first crystal structure of a eukaryotic ligand-gated ion channel (Figure 1a).[2] The obtained structural model revealed the architecture of the ligand binding site, which is located between the extracellular domains of two subunits. It is formed by loops of one subunit and β strands of the adjacent subunit.

Because of the vital function of these receptors, GluCl agonists, potentiators or blockers can interrupt or modify signal transduction in these animals. Since some invertebrate species can be pathogenic to mammals, e.g. parasitic helminthes, identification and development of GluCl ligands are of great interest. Therefore they are enormously relevant for human- and animal-health. The most widely used GluCl potentiator is the macrocyclic lactone Ivermectine (IVM) which, beside its tremendous success in curing river blindness in humans, is of great value in treating nematode infested livestock.[3] Until recently, serious consideration had not been given to protecting efficacy of these compounds by implementing control programs that use these medicines in a more targeted manner.[4] IVM resistance is now a serious problem for parasite control in livestock and there is a concern about resistance development and spread in nematode parasites of humans.[5, 6]

Therefore, the development of competitive GluCl (ant)agonists would not only provide new potential drugs, but also offer an alternative mode of (de)activation compared to the existing channel blockers and allosteric modulators. In addition, changing the function/efficacy of the molecule reversibly with the spatiotemporal precision of light would enable accurate control over the receptor, ultimately contributing to the understanding of GluCl function and inhibitory neural signaling.

The lack of 'azologable' targets[7] and the complexity of the photochromic ligand (PCL) design require a structure-function based PCL synthesis strategy in which the target molecule would be modified and tested for biological functionality after each structural change with regard to the lead compound.

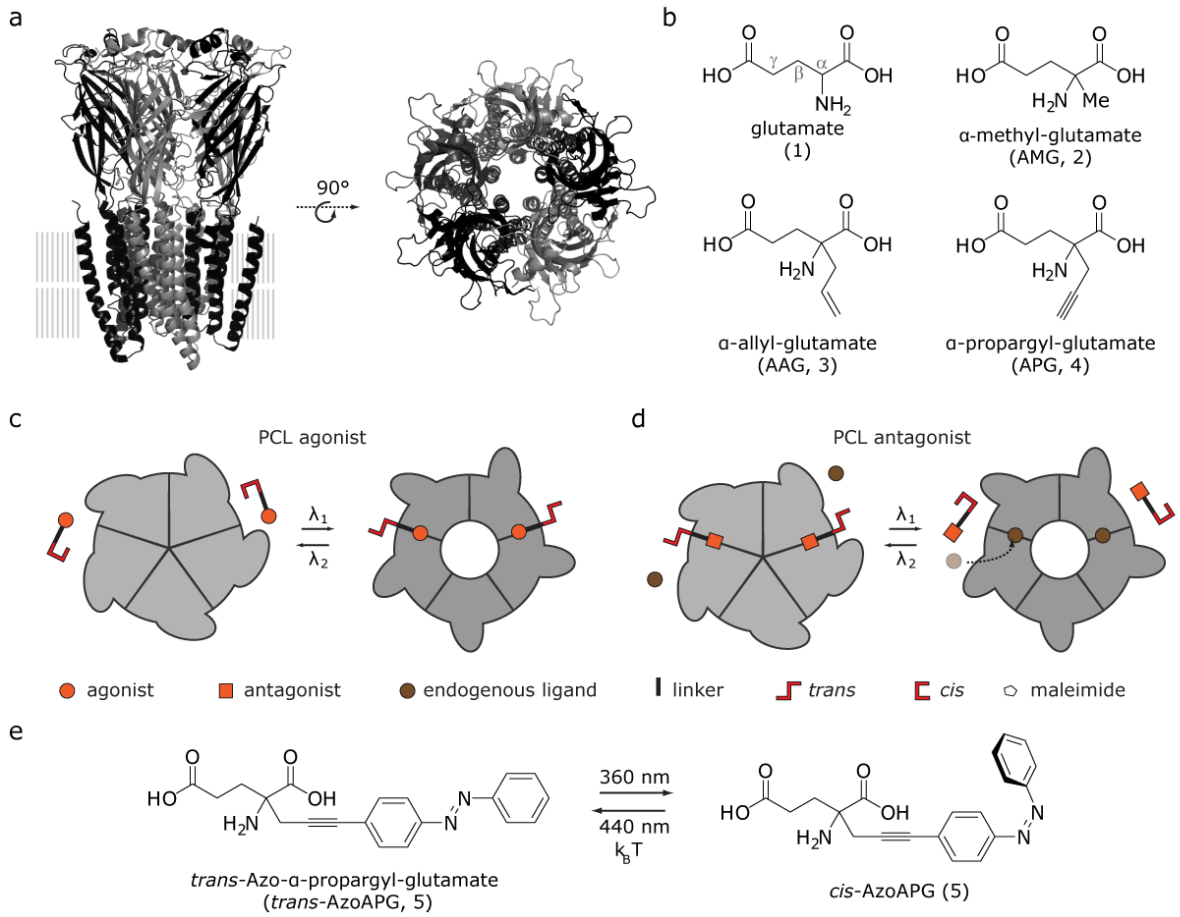

Figure 1. Structure of the GluCl with a selection of ligands. a) Structural model derived from X-ray crystallography (pdb:4TNW). b) GluCl ligands. Putative mechanism of photoswitchable agonists (c) and antagonists (d). e) The PCL AzoAPG depicted in its *cis* and *trans* configurations.

Results and Discussion

Starting with the endogenous GluCl agonist glutamate (**1**) we evaluated different substitution patterns. As β- and γ-carbon substituted glutamate PCLs did not show (agonistic) function, we turned our attention to the α-carbon position. We envisaged to gradually elongate the α-substituent to find a suitable linker length and form to attach an azobenzene moiety. Due to the fact that both, D-glutamate and L-glutamate, are agonists for the GluCl we tested a racemic mixture of the derivative with the smallest possible substitution, namely α-methyl-glutamate (AMG, **2**) (Figure 1b). We evaluated biological functionality of the molecules using electrophysiology. For this, the homopentameric α-glutamate-gated chloride channel (GLC-1) was expressed in HEK293T cells. GLC-1 was modified to contain a point mutation (T309P) allowing for glutamate activation in the absence of ivermectine.[8] In the initial electrophysiological evaluation AMG (**2**) proved to be an agonist of GLC-1 (-229 ± 74 pA; Figure 2). Inspired by these results, we prepared AAG (**3**) via a Petasis-Mannich reaction from α-ketoglutarate (**6**) and allylboronic acid pinacol ester (**7**) (Figure 2b).[9] Applying AAG (**3**) resulted in poor channel activation (-27 ± 1 pA; Figure 2a).

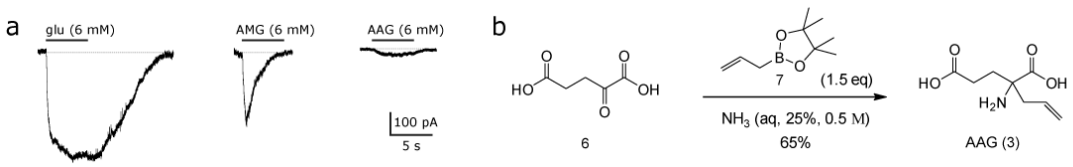

Figure 2. Electrophysiological evaluation of glutamate, AMG, and AAG and synthesis of AAG. a) Representative patch-clamp recording of local application of AAG (6 mM) to GLC-1 expressed in HEK293T cells. b) Petasis-Mannich reaction of α-ketoglutarate (**6**) and allylboronic acid pinacol ester (**7**) yielding AAG (**3**).

To increase the ligand binding interaction we aimed to introduce a linker bearing a different functional group, which logically led us to design APG (**4**). For its synthesis, nitroester **10** was prepared via a Michael reaction of nitroacetate **8** with ethyl acrylate (**9**).[10] Thereafter, **10** was reacted with TMS-propargyl bromide (**11**) under phase-transfer conditions[11] to give **12**. Nitro propargyl **12** was then converted to α-propargyl pyroglutamate **14** via a two-step reduction sequence[12]. Zinc reduction to hydroxylamine **13** followed by SmI_2 mediated cleavage of the N-O bond as well as cyclization obtained **14**. The TMS group was removed using TBAF. Boc-protection of the Lactam **15** enabled LiOH mediated ring opening to yield **17**. α-propargyl-glutamate **4** was then finalized via a Boc-deprotection using HCl in EtOAc.

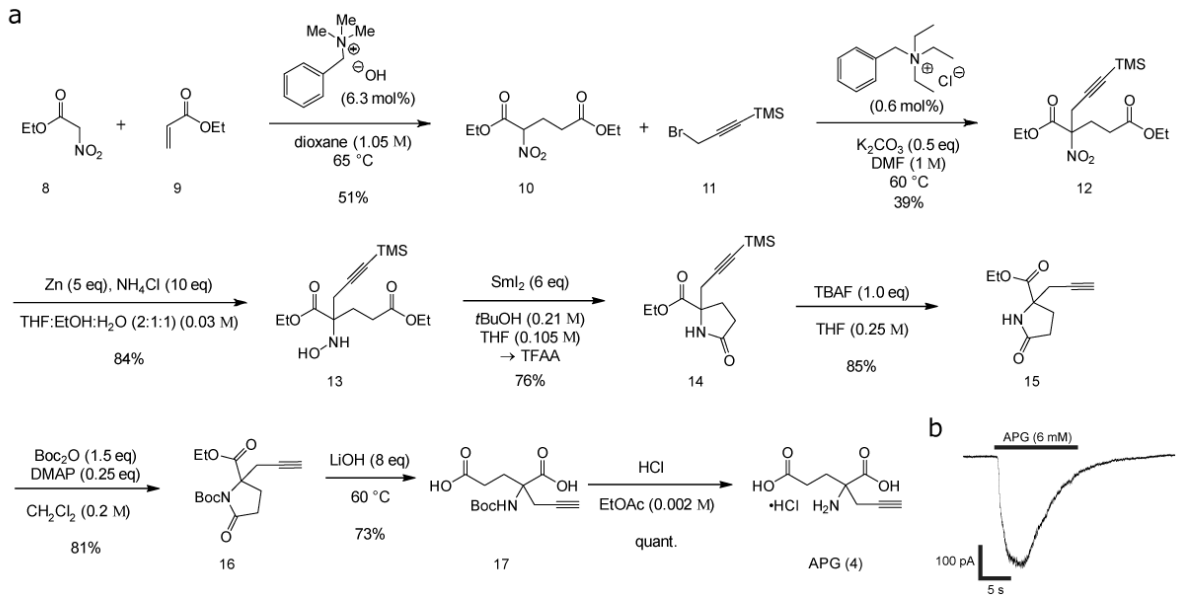

Figure 3. Synthesis and electrophysiological evaluation of α-propargyl-glutamate (APG). a) Synthesis of APG (**4**). b) Representative patch-clamp recording of GLC-1 activation by APG (6 mM) application.

Electrophysiological evaluation revealed that APG (4) is a potent GLC-1 agonist (-406 ± 61 pA; Figure 4). Therefore, we decided to attach an azobenzene group to obtain a potential photoswitchable agonist version for the GLC-1, namely AzoAPG (**5**).

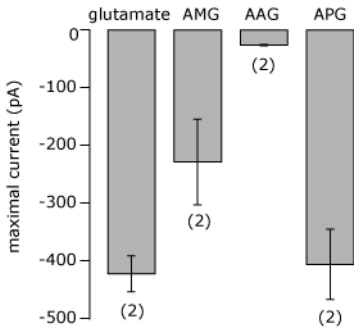

Figure 4. Summary of the electrophysiological evaluation of glutamate (6 mM) and the □-substituted glutamate derivatives (6 mM) activating GLC-1. Application of glutamate for 5 seconds resulted in -423 ± 31 pA current. Application of AMG resulted in -229 ± 74 pA current. Application of AAG resulted in -27 ± 1 pA current. Application of APG resulted in -406 ± 61 pA current. Error bars represent SEM; numbers of cells tested are in parentheses.

The azobenzene was attached to the Boc-pyroglutamate building block **16** via a Sonogashira coupling with iodoazobenzene (**18**, Figure 5a). A subsequent two-step deprotection sequence consisting of a basic hydrolysis of the Lactam **19** and HCl-mediated cleavage of the Boc group afforded the desired photoswitch AzoAPG (**5**).

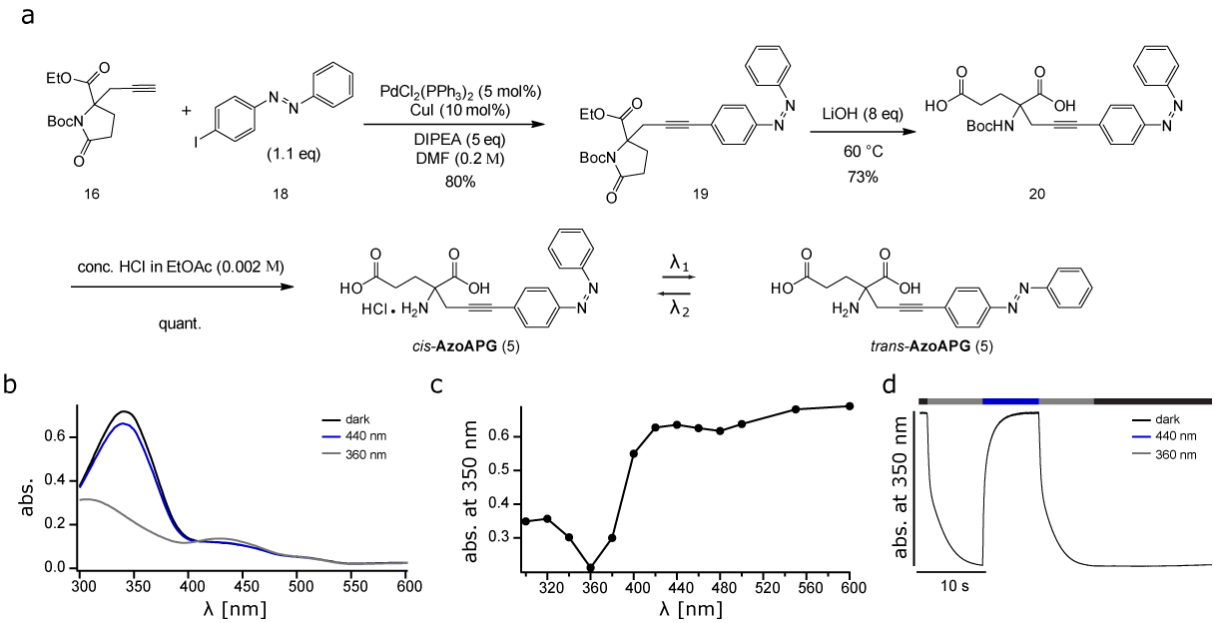

Figure 5. Synthesis and photoswitching of AzoAPG. a) Synthesis of AzoAPG and azobenzene isomerization. b) UV-Vis spectra of AzoAPG in dark, illuminated with 440 nm or 360 nm light, respectively. c) Absorbance at 350 nm when illuminated with the indicated wavelength. d) Kinetic measurement of photoswitching in buffered solution at room temperature (absorbance at 350 nm over time). *Trans* to *cis* switching was achieved by changing illumination from 440 nm to 360 nm light. *Cis* to *trans* switching was achieved by changing illumination from 360 nm to 440 nm light.

The photoswitching ability was tested via UV-Vis spectroscopy by recording the absorption spectra when illuminating the sample with different wavelengths (Figure 5b). The optimum photoswitching was achieved with 440 nm (*trans*-AzoAPG) and 360 nm (*cis*-AzoAPG) light (Figure 5b). In buffer AzoAPG (100 µM) showed double exponential photoswitching kinetics (Figure 5d). The *cis* to *trans* photoswitching was faster ($\tau_{(cis\ to\ trans)1}$ = 0.157 ± 0.0003 s and $\tau_{(cis\ to\ trans)2}$ =1.22 ± 0.0013 s) than the switching from *trans* to *cis* ($\tau_{(trans\ to\ cis)1}$ = 0.182 ± 0.001 and $\tau_{(trans\ to\ cis)2}$ = 2.234 ± 0.004 s).

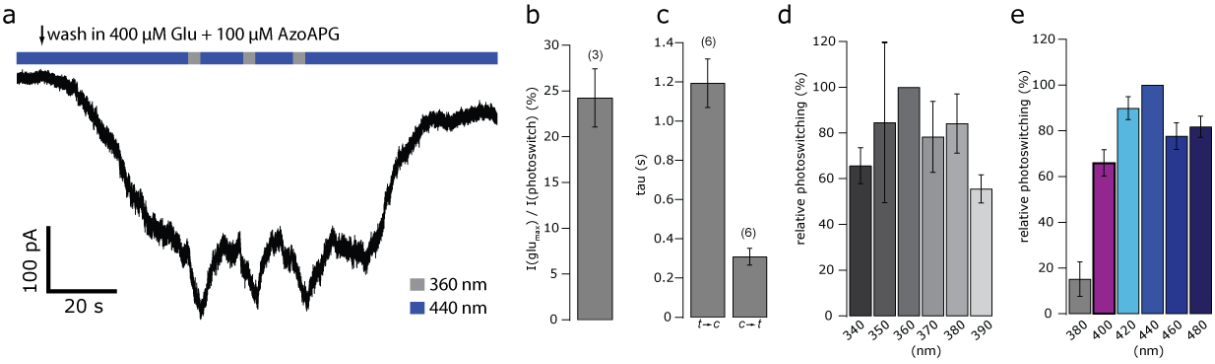

Figure 6. Electrophysiological evaluation of AzoAPG photoswitching at GLC-1. a) Photodependent antagonism of AzoAPG (100 µM) when competing with glutamate (400 µM). b) Statistical analysis of the photo-antagonism relative to overall activation (24.24 ± 3.17 %, n=3). c) Kinetics of photoswitching $\tau_{trans\ to\ cis}$ = 1.19 ± 0.12 s (n=6); $\tau_{cis\ to\ trans}$ = 0.31 ± 0.04 s (n=6). d) Wavelength screen displayed as relative photoswitching at indicated wavelengths normalized to maximal switching when holding wavelength is 440 nm. e) As in (d) with 360 nm as holding wavelength. Error bars represent SEM; numbers of cells tested are in parentheses.

When tested for biological functionality, AzoAPG (**5**) did not show agonistic effects but surprisingly acted as an antagonist when competing with glutamate (Figure 6). The

electrophysiological data suggests, that AzoAPG is a competitive antagonist in its *trans* configuration. The PCL effectively blocks up to 25 % (24.24 ± 3.17 %, n=3) of the glutamate-induced current in a reversible manner (Figure 6a,b). In accordance with the UV-Vis spectroscopy data, illumination with 440 nm and 360 nm light resulted in optimal switching of the receptor (Figure 6d,e). The *cis* to *trans* photoswitching kinetics ($\tau_{cis \text{ to } trans}$ = 0.31 ± 0.04 s) were faster than the *trans* to *cis* isomerization ($\tau_{trans \text{ to } cis}$ = 1.19 ± 0.12 s, n=6) (Figure 6c) confirming the results obtained by UV-Vis.

Outlook

In conclusion, we have developed a photochromic antagonist for the glutamate-gated chloride channel, namely AzoAPG. This molecule has proven to effectively block up to 25 % of a glutamate-induced current at the GLC-1. Evaluation of AzoAPG in *C. elegans* will reveal, if 25 % block is enough to modulate for example feeding behavior or movement of the nematode. Finally, starting from the developed building blocks, further synthetic effort will yield new molecules with an extended linker domain between the glutamate and the azobenzene, to allow for more flexibility and presumably better ligand binding. Also, attempts to red-shift the absorption spectrum of the PCL by attaching electron donating groups will be undertaken. The addition of these groups, might contribute to the photoswitching effect because of the steric effect of bulky groups.

Methods:

Cell culture. HEK293T cells were maintained at 37°C in a 10 % CO2 atmosphere in Dulbecco's modified Eagle medium (DMEM, Merk Millipore, Germany) containing 10 % FBS (Merk Millipore, Germany). For electrophysiological measurements cells were plated on coverslips treated with 0.1 mg/ml poly-L-lysine (Sigma-Aldrich, Germany) in a density of 40,000 cells per coverslip. HEK293T cells were transfected using JetPrime (Polyplus-transfections, France) according to manufacturer's instructions 24 h before measurements.

Electrophysiology. Patch clamp measurements were performed in whole-cell modus at room temperature and recorded using the EPC10 USB patch clamp amplifier and PatchMaster software (HEKA Elektronik, Germany). Bath solution for HEK-293T cells contained in mM: 140 NaCl, 2 KCl, 2 $MgCl_2$, 2 $CaCl_2$, 10 HEPES, 10 glucose (NaOH to pH 7.3). Pipette solution contained in mM: 140 $CsCl_2$, 10 HEPES, 2 Na_2ATP, 10 EGTA (CsOH to pH 7.3).

Illumination. Illumination during UV-Vis and electrophysiology experiments was performed using a TILL Photonics monochromator (Polychrome 5000) operated with the patch clamp amplifier or the PolyCon software (HEKA Elektronik, Germany), respectively.

Chemical synthesis. The chemical synthesis and compound characterization was conducted by David Konrad.

Author Contributions

D.T. and A.D. designed the study. D.K. and S.V. performed chemical synthesis. A.D. and D.K. performed UV-Vis and patch−clamp experiments. J.N. performed the molecular cloning of GLC-1.

ACKNOWLEDGMENTS

The authors gratefully acknowledge Dr. D. M. Barber for helpful discussions and L. de la Osa de la Rosa for technical assistance.

References:

1. Wolstenholme, A. J. (2012) Glutamate-gated chloride channels. *J Biol Chem 287*, 40232-8.
2. Hibbs, R. E., and Gouaux, E. (2011) Principles of activation and permeation in an anion-selective Cys-loop receptor. *Nature 474*, 54-60.
3. Raymond, V., and Sattelle, D. B. (2002) Novel animal-health drug targets from ligand-gated chloride channels. *Nat Rev Drug Discov 1*, 427-36.
4. Matthews, J. B. (2014) Anthelmintic resistance in equine nematodes. *Int J Parasitol Drugs Drug Resist 4*, 310-5.
5. Prichard, R. K. (2007) Ivermectin resistance and overview of the Consortium for Anthelmintic Resistance SNPs. *Expert Opin Drug Discov 2*, S41-52.
6. Janssen, I. J., Krucken, J., Demeler, J., and von Samson-Himmelstjerna, G. (2015) Transgenically expressed Parascaris P-glycoprotein-11 can modulate ivermectin susceptibility in Caenorhabditis elegans. *Int J Parasitol Drugs Drug Resist 5*, 44-7.
7. Schoenberger, M., Damijonaitis, A., Zhang, Z., Nagel, D., and Trauner, D. (2014) Development of a New Photochromic Ion Channel Blocker via Azologization of Fomocaine. *ACS Chem. Neurosci. 5*, 514-518.
8. Etter, A., Cully, D. F., Schaeffer, J. M., Liu, K. K., and Arena, J. P. (1996) An amino acid substitution in the pore region of a glutamate-gated chloride channel enables the coupling of ligand binding to channel gating. *J Biol Chem 271*, 16035-9.
9. Sugiura, M., Hirano, K., and Kobayashi, S., (2006) ALLYLBORONATION OF IMINES: 1-PHENYLHEX-5-EN-3-AMINE. In *Organic Syntheses, Vol 83*, (Curran, D. P., Ed. Vol. 83, pp 170-176.
10. Baldwin, N. J. (1989) The archive of the Society for the Protection of Science and Learning. *History of science; an annual review of literature, research and teaching 27*, 103-5.
11. Gogte, V. N., Natu, A. A., and Pore, V. S. (1987) ALKYLATION OF ALKYL NITROACETATES UNDER PTC CONDITIONS. *Synthetic Communications 17*, 1421-1429.
12. Fernandez Gonzalez, D., Brand, J. P., and Waser, J. (2010) Ethynyl-1,2-benziodoxol-3(1H)-one (EBX): an exceptional reagent for the ethynylation of keto, cyano, and nitro esters. *Chemistry 16*, 9457-61.

VI: Photoswitchable Orthogonal Remotely Tethered Ligand

Orthogonal optical control of a G protein-coupled receptor with a SNAP-tethered photochromic ligand

Johannes Broichhagen[1*], Arunas Damijonaitis[1*], Joshua Levitz[2*], Kevin R. Sokol[1], Philipp Leippe[1], David Konrad[1], Ehud Y. Isacoff[2,3,4], and Dirk Trauner[1,#]

*=equal contribution

[1] Department of Chemistry, Ludwig-Maximilians-Universität München, and Munich Center for Integrated Protein Science, Butenandtstrasse 5-13, 81377 München, Germany

[2] Department of Molecular and Cell Biology, University of California, Berkeley, California, USA

[3] Helen Wills Neuroscience Institute, University of California, Berkeley, CA, USA

[4] Physical Bioscience Division, Lawrence Berkeley National Laboratory, Berkeley, California, USA

Abstract

The covalent attachment of synthetic photoswitches is a general approach to impart light-sensitivity onto native receptors. It mimics the logic of natural photoreceptors and significantly expands the reach of optogenetics. Here we describe a novel photoswitch design – the Photoswitchable Orthogonal Remotely Tethered Ligand (PORTL) – that combines the genetically encoded SNAP-tag with photochromic ligands connected to a benzylguanine *via* a long flexible linker. We use the method to convert the G protein-coupled receptor mGluR2, a metabotropic glutamate receptor, into a photoreceptor (SNAG-mGluR2) that provides efficient optical control over the neuronal functions of mGluR2: presynaptic inhibition and control of excitability. The PORTL approach enables multiplexed optical control of different native receptors using distinct bioconjugation methods. It should be broadly applicable since SNAP-tags have proven to be reliable, many SNAP-tagged receptors are already available, and photochromic ligands on a long leash are readily designed and synthesized.

Introduction

The ability to covalently link synthetic molecules with proteins has significantly increased the power of molecular biology and has provided new therapeutic approaches *via* antibody drug conjugates. In recent years, chemical biologists have developed methods that can be used not only *in vitro* and in cell cultures, but can be also applied *in vivo*, even in large animals and, potentially, in humans.[1]

Important issues in bioconjugation are the speed, selectivity and orthogonality of the reaction and the extent to which the target protein needs to be modified to enable covalent attachment. Engineered cysteines have proved popular since they represent a minimal change in the protein structure and reliably react with certain electrophiles, such as maleimides.[1] More selective methods depend on the expansion of the genetic code[2,3] and otherwise inert molecules that specifically react with protein motifs[4]. These include self-labeling "tags", such as the SNAP-tag[5,6], the CLIP-tag[7] or the Halo-tag[8], and amino acid sequences that can be modified using external enzymes[9,10].

Bioconjugation has also played an important role in photopharmacology, which is an effort to control biological activity with synthetic photoswitches[11,12]. While soluble photochromic ligands (PCLs) are diffusion limited, photoswitchable tethered ligands (PTLs) covalently attach to an engineered site in the target protein. This places the ligand in the vicinity of its binding pocket, so that light maneuvers it in and out of a position where it can bind[13]. The PTL approach allows for precise targeting since the bioconjugation motif, which is usually an engineered cysteine for maleimide conjugation, can be genetically encoded and selectively expressed in cells of interest. By contrast, PCLs act on native receptors, making for easier use, especially in therapeutic settings, albeit with less precision.

Although PTLs have proven to be powerful for controlling neural signaling and animal behavior[14-21], they have faced the disadvantages of cysteine/maleimide chemistry. Maleimides hydrolyze under physiological conditions and conjugate to glutathione, making them incompatible with the intracellular environment. Moreover, both in the cell and on the cell surface, they are likely to react with accessible native cysteines that are not at the designed PTL anchoring site. Although attachment to the introduced cysteine can be enhanced by affinity labeling due to increased times of proximity when the ligand binds in the binding pocket[22], the susceptibility of maleimides to unwanted nucleophiles, including water, makes them less than ideal for applications in photopharmacology.

A solution to these challenges could be the introduction of electrophiles that react with very high selectivity and yet are stable toward water. Under normal circumstances, this requires a larger protein tag, moving the site of attachment far away from the ligand-binding site, typically in the range of several nanometers. Although tethers with photoswitches placed in series could be designed, multiple isomerization states of the tether and the spread of conformations of the long entropic spring[23] could complicate control and prevent clean changes in biological activity upon irradiation.

Here we introduce a new concept, termed PORTL (**P**hotoswitchable **O**rthogonal **R**emotely **T**ethered **L**igand), that overcomes the limitations of maleimide chemistry and lays to rest concerns about off-target attachment (**Fig. 1**). Like a PTL, a PORTL consists of a bioconjugation handle, a photoswitchable group, and a ligand. In this case, however, the switch does not primarily impact the overall length, pointing angle and flexibility of the tether, but rather the pharmacology of the tethered ligand. As such, the switch becomes

an integral part of the pharmacophore and the change in biological activity is designed to result not from a change in the relative position of the ligand with respect to its binding site, but rather from a change in the efficacy of the ligand, as it does in a PCL. Therefore, the tether can be long and flexible, allowing for the use of larger bioconjugation motifs, such as a SNAP-tag, which provide an anchoring site at a more remote location with respect to the ligand-binding site. The SNAP-tag is a modified DNA repair enzyme that functions as a self-labeling domain by selectively and quickly reacting with benzylguanine (**BG**) electrophiles[5,6]. It enables specific and efficient labeling with BG fluorophores in cultured cells and in brain slice[24,25]. Importantly, unlike maleimides, BGs are essentially inert toward water, regular cysteines and glutathione making them ideal for labeling in physiological systems that include extracellular and intracellular targets[6,26,27].

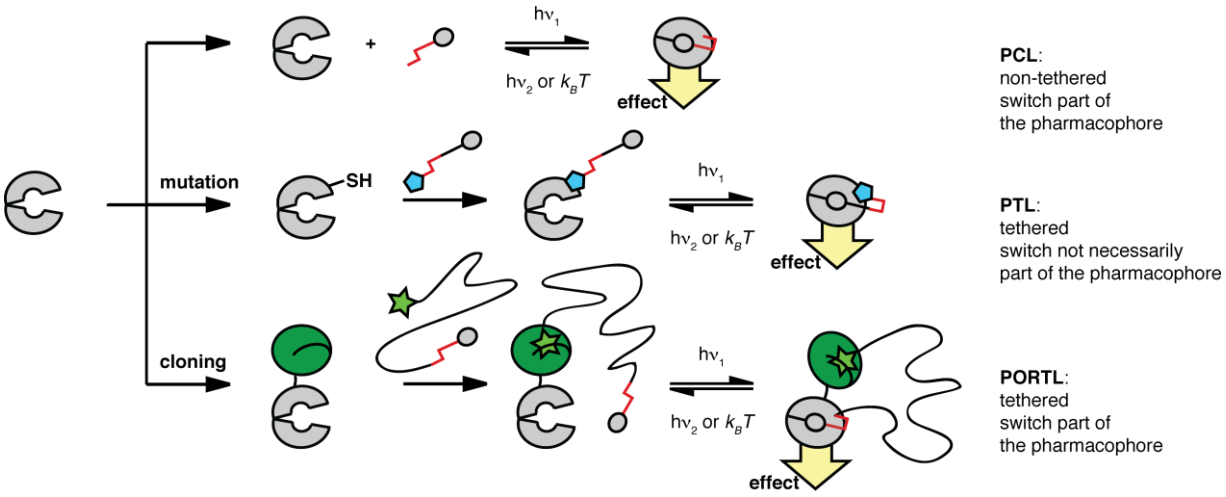

Figure 1: The PORTL concept. A photochromic ligand (PCL) is freely diffusible and the switch is part of the pharmacophore (top). This is not necessarily the case in a photoswitchable tethered ligand (PTL) (middle). The photoswitchable orthogonal remotely tethered ligand approach (PORTL, bottom) combines the switch as part of the pharmacophore with a long, flexible tether that allows for anchoring on a remote site.

We demonstrate the validity of the PORTL concept by fusing the class C G protein-coupled receptor (GPCR), mGluR2, with a SNAP-tag and endowing it with a synthetic azobenzene photoswitch through benzylguanine chemistry. The resulting photoreceptor, termed SNAG-mGluR2 (**SN**AP-tagged-**A**zobenzene-**G**lutamate receptor), permits rapid, repeatable, high-efficacy photoagonism of mGluR2 with thermally bistable and fast relaxing photoswitches. SNAG-mGluR2 allows for optical manipulation of neuronal excitability and synaptic transmission in hippocampal neurons. We also show that the SNAG approach may be combined with the cysteine attachment of a conventional PTL to allow for orthogonal optical control of two glutamate receptors within the same cell, paving the way for other multiplexing strategies.

Results

Design of PORTL photoswitches for metabotropic glutamate receptors

mGluRs are class C GPCRs that mediate many aspects of glutamatergic signaling in the brain and serve as drug targets for a number of neurological disorders[28,29]. The defining structural feature of class C GPCRs is a large, bi-lobed extracellular ligand-binding domain (LBD) that assembles as a dimer and mediates receptor activation. We previously developed photoswitchable versions of mGluR2, 3, and 6, termed "LimGluRs", via cysteine-conjugation of D-Maleimide-Azobenzene Glutamate ("D-MAG") molecules to the LBD near the glutamate binding site[20,30]. This work indicated that mGluRs are amenable to agonism by azobenzene-conjugated glutamate compounds. In addition, previous work has shown that *N*-terminal SNAP-tagged mGluRs retain normal function and may be efficiently labeled in living cells[31]. In order to take advantage of the many attractive properties of the SNAP-tag linkage relative to that of cysteine-maleimide, we sought to optically control the LBD of mGluR2 via PORTL conjugation to a genetically-encoded SNAP-tag fused to the LBD.

To design a new family of photoswitches we first analyzed SNAP and mGluR crystal structures to determine the dimensions required to permit a compound conjugated to an *N*-terminal SNAP-tag via a BG group at one end to reach the orthosteric binding site within the mGluR LBD via a glutamate at the other end (**Fig. 2a**). We decided to place the central photoswitchable azobenzene unit close to the glutamate ligand based on the logic that the ability of the glutamate moiety to dock in the binding pocket and activate mGluR2 would be altered by photo-isomerization of the azobenzene, as achieved earlier for soluble photochromic ligands[32-40] rather than a length-dependent change in the ability to reach the binding site. Furthermore, we hypothesized that a long, flexible polyethylene glycol linker between the BG and azobenzene units would span the necessary distance between the SNAP domain and the mGluR2 LBD and permit the glutamate moiety to reach the binding site (**Fig. 2b**).

Based on our previous work, which indicated that agonism of mGluR2 via glutamate-azobenzene molecules requires 4' D stereochemistry, which we refer to as "D-MAG"[20], we decided to maintain this feature in our new SNAP-tag photoswitches. We opted to construct the linker between BG and azobenzene out of monodisperse PEG-polymers of different sizes. PEG polymers do not strongly adhere to protein surfaces and are known to be conformationally very flexible[1]. To allow this system to be adopted for other pharmacophores in the future, we designed the synthetic chemistry to be flexible as well, using amide bond formation and click chemistry for rapid assembly. Alkyne-azide click chemistry has been extensively used for bioorthogonal reactions and can be employed in presence of benzylguanines[41-43]. Both the Cu(I)-catalyzed click chemistry or the cyclooctyne strain promoted version, which can be used *in vivo,* are available.

Together, these considerations led to the design of two families of benzylguanine-azoglutamates with either a diacyl azidianiline switch (**BGAG$_n$**), as used in the original set of D-MAGs for a 2-wavelength on/off bistable optical control of mGluRs[20], or a red-shifted azobenzene switch (**BGAG$_{n(460)}$**), as used more recently for single wavelength single or two-photon control of an mGluR[30,44] (**Fig. 2c**). In these molecules, the first index denotes the number of ethylene glycol repeat units and the tether length, whereas the number in brackets indicated the wavelength that results in maximum *cis*-azobenzene content upon irradiation.

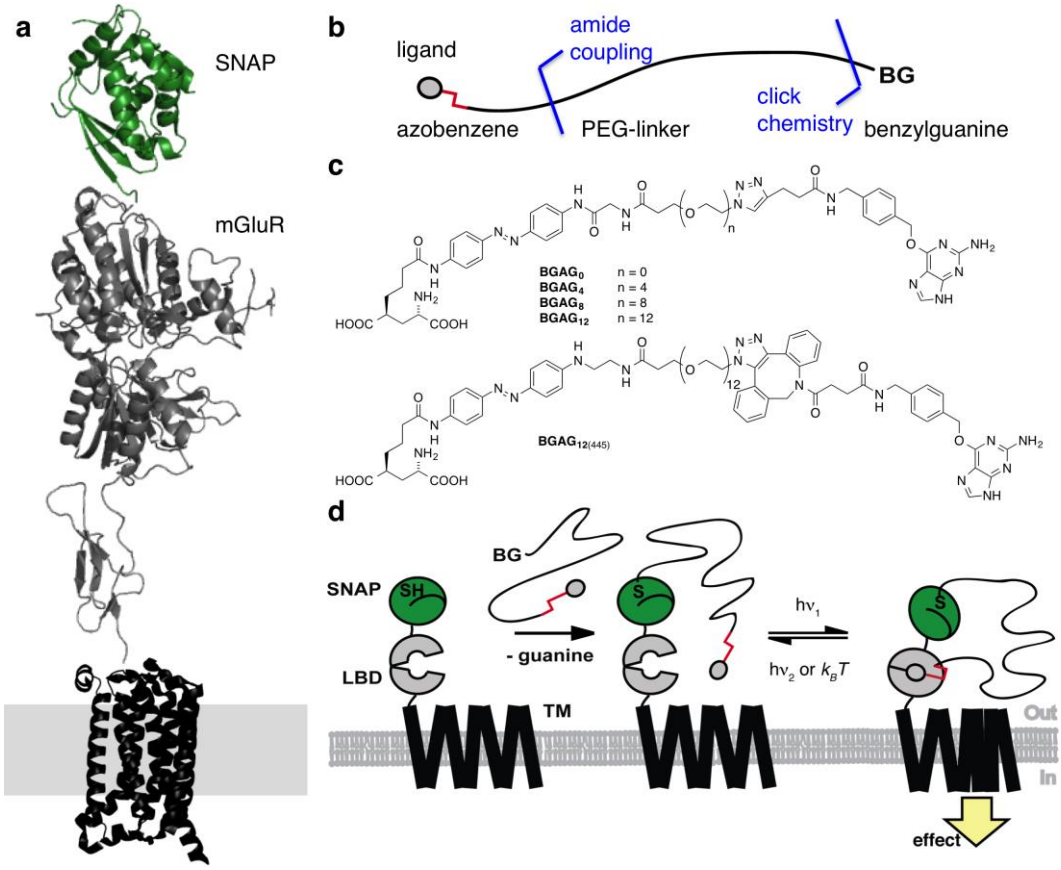

Figure 2: Concept and Design of PORTL compounds for SNAP-tag conjugation. **a**) Model of a SNAP-mGluR subunit showing the relative dimensions of the domains (SNAP pdb: 3kzy, mGluR3-LBD pdb: 2e4u, mGluR5-7TM pdb: 4oo9). The mGluR extracellular domains are shown in gray and the transmembrane domains are shown in black while the SNAP tag is shown in green. **b**) Schematic design of a photoswitchable orthogonal remotely tethered ligand (PORTL) using amide coupling and click chemistry to ensure synthetic modularity. **c**) PORTL consisting of a ligand connected to an azobenzene a flexible linker (PEG-chain) of various length and a benzylguanine (**BG**). Only one regioisomer is shown in **$BGAG_{12(460)}$**. Depending on the substitution pattern on the azobenzene the switching wavelength can be tuned. **d**) Schematic showing the logic of PORTL-mediated reversible activation and deactivation of a target receptor with two orthogonal wavelengths of light.

Synthesis of Benzylguanines-Azobenzenes-Glutamates (BGAGs)

Our synthesis of BGAGs started with guanine derivative **1**, which was converted into the known benzylguanine (**BG**) in 5 steps[5] (**Fig. 3a**). Coupling with pent-3-yenoic acid (**2**) then yielded BG-alkyne **4**. Alternatively, cyclooctyne **4** was linked to **BG** by amidation to obtain BG-DBCO, **5**. On the ligand side, we utilized several steps from the reported synthesis of D-MAGs starting from L-glutamate[20] to synthesize glutamate azobenzene **6**. Acylation with glycine derivative **7**, followed by deprotection, gave primary amine **8**, whereas reductive amination with aldehyde **9**[45] and deprotection yielded diamine **10**. (**Fig. 3b**). Coupling of both **8** and **10** with bifunctional PEG-O-Su esters of varying length yielded azides **15**-**18** (whereas **14** was obtained by HBTU-mediated coupling) that were ready for click chemistry (**Fig. 3c**).

BGAGs with a "regular" azobenzene switch were synthesized by Cu(I) catalyzed azide alkyne click chemistry, followed by deprotection, which yielded **BGAG$_0$**, **4**, **8** and **12** (**Fig. 3d**). It should be noted, that high temperatures and high catalyst loadings were needed to drive the click-reaction to completion and that red-shifted version could not be obtained from **18** and **3** under these conditions. Therefore, strain promoted reaction of **18** with **5**, followed by deprotection of the amino acid moiety, was used instead, which gave the red-shifted photoswitch **BGAG$_{12}$**$_{(460)}$.

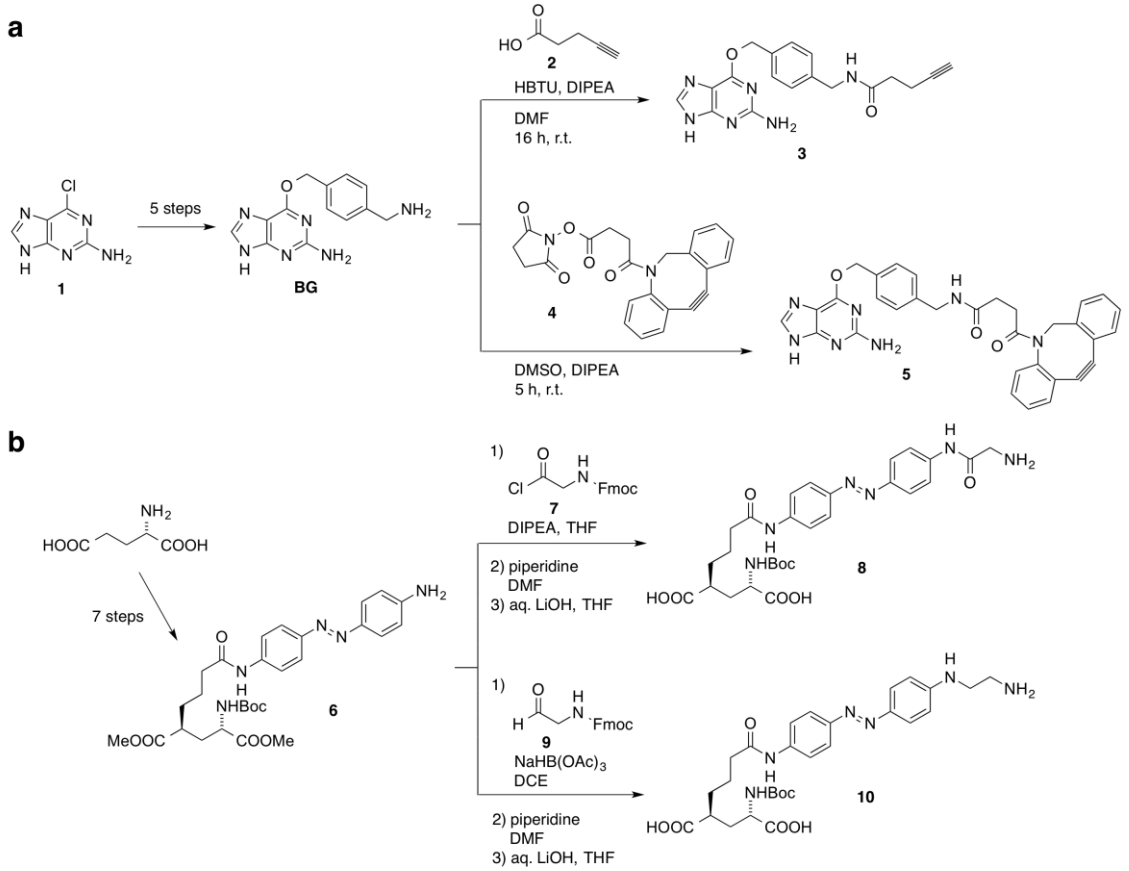

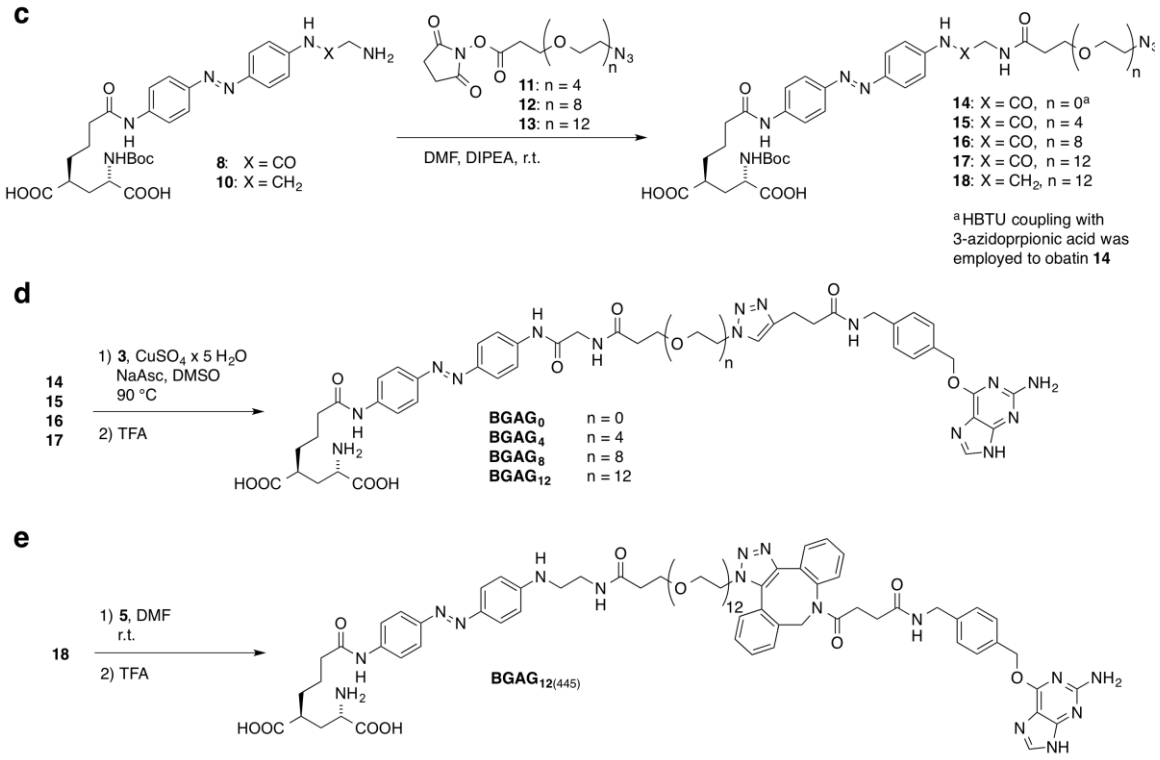

Figure 3: Synthesis of BGAGs. **a**) Synthesis of BG-alkynes **3** and **5** for click chemistry. **b**) Diversification of previously described **6** to give blue azobenzene glutamate **8** and red-shifted azobenzene glutamate **10**. **c**) PEG-chain installation. **d**) Cu(I)-catalyzed alkyne azide click to obtain **BGAG**s. e) PEG-Linker implementation. **e**) Strain promoted alkyne azide click to obtain **$BGAG_{12(460)}$**.

Optical control of SNAG-mGluR2 in HEK293T cells

After synthesizing the set of BGAG molecules, we next sought to test whether they could be efficiently conjugated to SNAP-mGluR2 and used to optically manipulate mGluR2 function (**Fig. 2d**). We first expressed a GFP-fusion construct (SNAP-mGluR2-GFP) in HEK293T cells and saw efficient labeling with a BG-conjugated Alexa dye that was limited to the cell surface (**Fig. S1**), as previously reported[31,46]. This indicated that BG-conjugated compounds are unlikely to cross the membrane and will, thus, primarily target receptors on the cell surface.

We next tested the ability of BGAGs to photoactivate SNAP-mGluR2 using whole cell patch-clamp in HEK293T cells co-transfected with the G protein-activated inward rectifier potassium (GIRK) channel. Cells expressing SNAP-mGluR2 were initially incubated with 10 µM **$BGAG_{12}$** for 45 minutes at 37 °C. Following extensive washing to remove excess, non-attached photoswitches, photoisomerization to the *cis* configuration with a brief (<1 s) bout of illumination at 380 nm produced robust photoactivation that persisted in the dark and was reversed by a brief (~1 s) bout of illumination at 500 nm to isomerize the azobenzene back to the *trans* state (**Fig. 4a, S2a**). mGluR2 photoactivation *via* **$BGAG_{12}$** was highly reproducible. In the photoswitch "off" state (i.e. in the dark or following illumination at 500 nm), responses to the native neurotransmitter ligand glutamate was intact. Photocurrents were abolished at high glutamate concentrations, suggesting that **$BGAG_{12}$** does not function as a partial agonist (**Fig. 4a**). Light responses were ~60 % of the responses to saturating glutamate (59.3 ± 2.8 %, n=10 cells), consistent with both efficient conjugation and receptor activation. Importantly, cells expressing wild type mGluR2 (*i.e.* with no SNAP tag) and incubated with **$BGAG_{12}$** showed no light responses (**Fig. S2b**). Given the successful optical control of mGluR2, we termed the tool that

combines SNAP-mGluR2 and BGAG "SNAG-mGluR2". SNAG-mGluR2 showed similar photocurrent efficacy and kinetics to the previously reported LimGluR2[20]. SNAG-mGluR2 photoactivation was fully blocked by the competitive mGluR2 antagonist LY341495, without altering the baseline current, supporting the interpretation that **BGAG$_{12}$** activates mGluR2 *via* its native, orthosteric binding site and does not significantly activate in the *trans* configuration of the azobenzene (**Fig. S2c**). The apparent affinity for glutamate of SNAG-mGluR2 was comparable to that of both SNAP-mGluR2 not labeled by **BGAG$_{12}$** and, indeed, of wild type mGluR2 (**Fig. S2d**), indicating that normal mGluR2 function is maintained.

We next tested different labeling conditions of **BGAG$_{12}$** and found that 45 minute incubation with $\geq$ 1 μM **BGAG$_{12}$** showed optimal labeling (**Fig. S3a, b**). However, photocurrents were still observed with 100 nM labeling for 45 minutes (**Fig. S3c**) and these were increased with overnight labeling at 100 nM and could even be observed with concentrations as low as 10 nm with overnight labeling (**Fig. S3d-f**). Remarkably, the labeling solution could be reused for multiple experiments for one week following dilution in aqueous buffer at room temperature, without a decline in efficacy of optical activation (**Fig. 4b, c**). This result is in stark contrast to maleimide-based MAG photoswitches, which typically need to be applied at concentrations up to 100-200 μM[20,22] and are hydrolyzed in water with a half-life in the range of minutes to hours[1].

To further explore the mechanism of photoswitching in SNAG-mGluR2, we synthesized a PCL version of **BGAG$_{12}$** where the BG group was omitted ("AG$_{12}$"; **Fig. S4a**). AG$_{12}$ photoagonized SNAP-mGluR2 with the same directionality as **BGAG$_{12}$** (**Fig. S4b**), supporting the hypothesis that photoswitching is based on the relative efficacy of the azobenzene-glutamate moiety in *cis* versus *trans*, rather than a length or geometry-dependent change in the ability to reach the binding site. We also tested BGAG variants ranging in length from 0 to 8 PEG repeats and found comparable photoactivation of SNAG-mGluR2 to **BGAG$_{12}$** for all versions (**Fig. S5**), suggesting similar effective concentrations of the ligand near the binding pocket.

We next tested the red-shifted version of **BGAG$_{12}$**, **BGAG$_{12(460)}$**, to see if we could develop a SNAG-mGluR2 variant that is controlled with a single wavelength of visible light. Following labeling with 10 μM **BGAG$_{12(460)}$** photoactivation of SNAP-mGluR2 was achieved reproducibly in response to illumination with blue light (420-470 nm bandpass) (**Fig. 4d**). Relaxation occurred rapidly in the dark following illumination, as expected, and the photoactivation was ~35 % relative to saturating glutamate (34.9 ± 4.2 %, n=18 cells). We termed the combination of SNAP-mGluR2 and **BGAG$_{12(460)}$** "SNAG$_{460}$-mGluR2".

Having developed multiple versions of SNAG-mGluR2 that were able to efficiently photo-activate mGluR2, we next wondered if this toolset could be used to optically manipulate mGluR2 in its native neuronal setting.

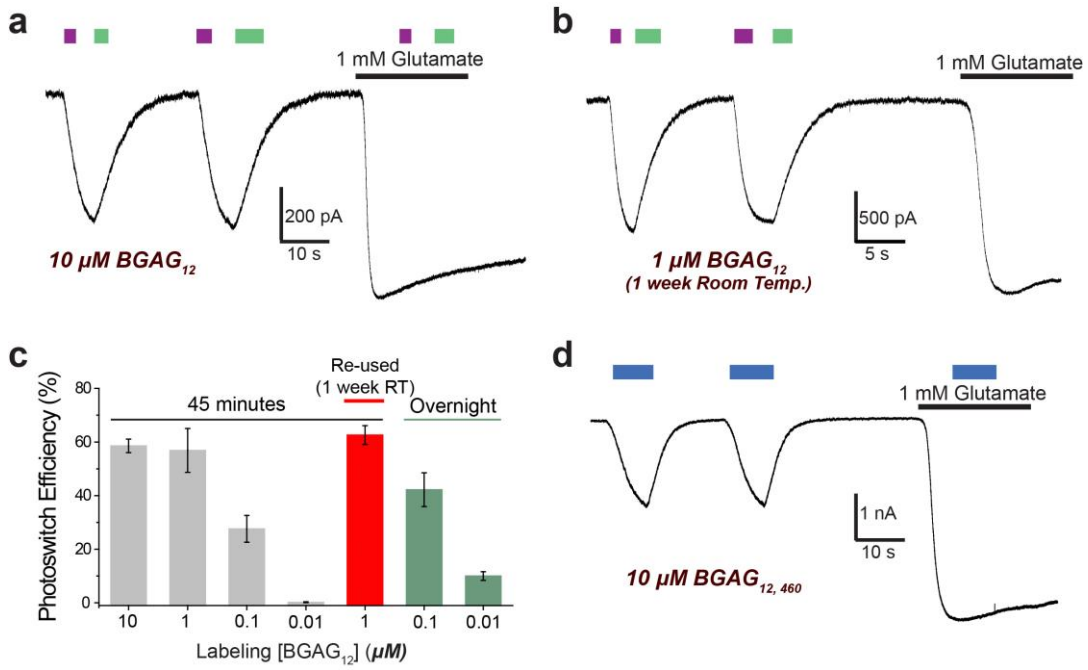

Figure 4: Optical control of SNAG-mGluR2 in HEK 293T cells co-expressing SNAP-mGluR2 and GIRK. **a**) Representative patch-clamp trace demonstrating the reversible optical control of SNAG-mGluR2 (SNAP-mGluR2 + $BGAG_{12(460)}$). Photoactivation is achieved with a brief pulse of UV light (λ = 380 nm, purple) and reversed by a brief pulse of green light (λ = 500 nm, green). Application of saturating 1 mM glutamate gives full activation and prevents further photoswitching. **b**) Representative trace showing photoactivation of SNAG-mGluR2 using 1 μM **$BGAG_{12}$** after it was incubated for 1 week in aqueous buffer. **c**) Summary of the efficiency of photoactivation of SNAG-mGluR2 (compared to 1 mM glutamate) following different **$BGAG_{12}$** labeling conditions. Error bars represent SEM. **d**) Representative trace showing photoactivation of $SNAG_{460}$-mGluR2 (SNAP-mGluR2 + **$BGAG_{12(460)}$**) with blue light (λ = 445 nm). Relaxation occurs spontaneously in the dark.

Optical manipulation of excitability and synaptic transmission via SNAG-mGluR2 in hippocampal neurons

mGluR2, like other neuronal Gi/o-coupled GPCRs, primarily signals either somatodendritically, to hyperpolarize membranes through the activation of GIRK channels, or presynaptically, to inhibit neurotransmitter release by a number of mechanisms, including inhibition of voltage-gated calcium channels[28]. We hypothesized that SNAG-mGluR2 would efficiently gate both of those canonical functions in neurons.

We first expressed SNAP-mGluR2-GFP in dissociated hippocampal neurons and labeled with BG-Alexa-647 to determine if SNAP-BG conjugation could occur efficiently in neuronal cultures, which are considerably denser than HEK 293T cell cultures. We observed strong SNAP-mGluR2-GFP expression and surface labeling with Alexa-647 **(Fig. 5a)**, indicating that the SNAP tethering approach is suitable to neurons. Importantly, untransfected cells did not show BG-Alexa-647 fluorescence (**Fig. S6**), confirming the specificity of the labeling chemistry. Next, instead of labeling with BG-Alexa-647, we labeled with **$BGAG_{12}$** and observed rapid membrane hyperpolarization (~2-8 mV) in response to illumination at 380 nm, which was reversed by illumination at 500 nm (**Fig. 5b**). When the neurons were at depolarized potentials that induced firing, the light-induced hyperpolarization was sufficient to inhibit the action potentials (**Fig. 5c**).

To test for presynaptic inhibition, we cultured hippocampal neurons at low density to promote the formation of autapses, *i.e.* synapses between the axon and dendrites of the

same neuron. In autaptic neurons, photoactivation of SNAG-mGluR2 reversibly decreased excitatory post synaptic current (EPSC) amplitude by up to 70 % (average = 48.3 ± 7.3 %, n=5 cells) (**Fig. 5d, e**). Optical inhibition of EPSC amplitude was accompanied by an increase in paired pulse ratio (**Fig. 5f, g**) and a decrease in synaptic depression during high frequency trains (**Fig. S7**), consistent with a presynaptic reduction in the probability of transmitter release. Together, these observations demonstrate that the SNAG system is well suited for neuronal cells and that SNAG-mGluR2 itself is a powerful tool for optical manipulation of neuronal inhibition *via* native mGluR2-mediated mechanisms that control neural firing and transmitter release.

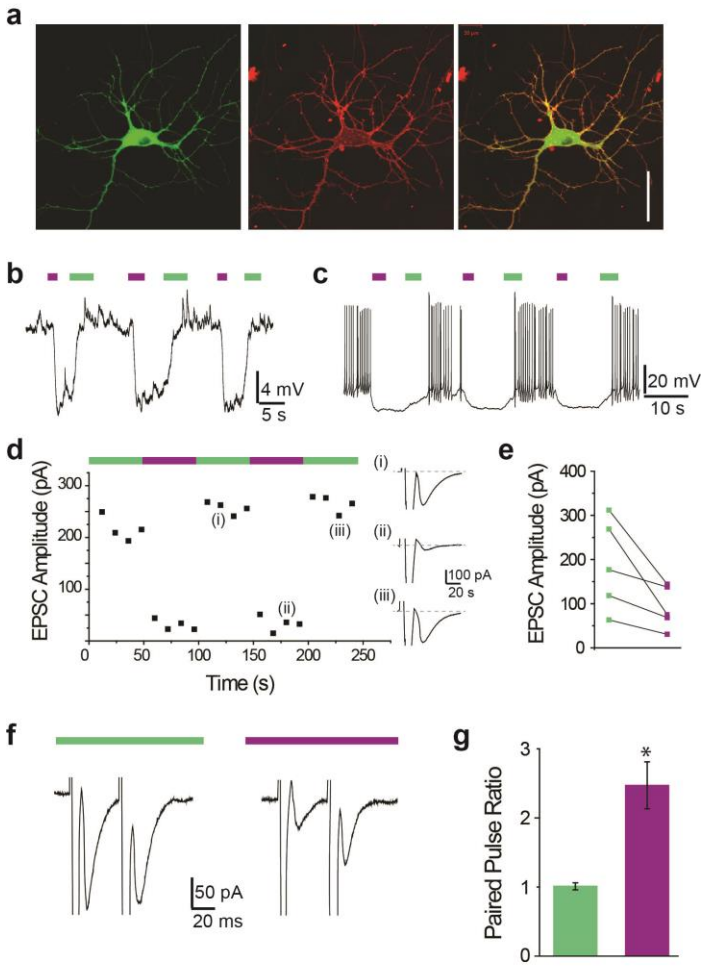

Figure 5: Optical control of SNAG-mGluR2 in hippocampal neurons. **a**) Representative confocal images showing the expression of SNAP-mGluR2-GFP (left) and its labeling with BG-Alexa-647 (middle) in hippocampal neurons. In the merge (right) of the two images it is clear that dye labeling occurs on the surface of the neuron only. **b-c**) Representative recording showing SNAG-mGluR2 mediated hyperpolarization (b) and silencing (c) of hippocampal neurons in whole cell patch-clamp recordings. Violet bars indicate 380 nm illumination and green bars indicate 500 nm illumination. **d**) Time course of autaptic EPSC amplitude for a representative neuron showing rapid, reversible inhibition of synaptic transmission by SNAG-mGluR2. (i), (ii), and (iii) show individual traces associated with data points. **e**) Summary of SNAG-mGluR2 mediated optical synaptic inhibition by 380 nm light in all cells tested. **f**) Representative recording showing an increase in paired pulse ratio in response to SNAG-mGluR2 activation using an

interstimulus interval of 50 ms. g) Summary of paired pulse ratio in 500 nm (green) or 380 nm (violet) for the same cell as in f).

Dual optical control of SNAG-mGluR2 and LiGluR via orthogonal photoswitch labeling

A major goal in physiology is to be able to manipulate independently different receptors within the same preparation using different wavelengths of light. This type of experiment could be extremely powerful for deciphering the different roles, and potential cross-talk, of different signaling pathways within a cell or neural circuit. With this goal in mind, we wondered if SNAG-mGluR2 could be used in conjunction with a previous generation photoswitchable receptor to provide individual optical control of two receptors within the same cell. We turned to LiGluR, a GluK2 ionotropic glutamate receptor that is photoactivated by molecules of the maleimide-azobenzene-glutamate (MAG) family through cysteine-maleimide linkage[32,47]. To test this, we co-expressed SNAP-mGluR2 along with its GIRK channel effector and LiGluR (GluK2-L439C) in HEK293T cells. We labeled the cells with $BGAG_{12}$ for 30 minutes, and then with L-$MAG0_{460}$, a blue light-activated, spontaneously relaxing version of MAG with similar spectral properties to **$BGAG_{12(460)}$**[44]. Due to the spectral and light sensitivity differences between the two photoswitches, we were able to independently and sequentially activate SNAG-mGluR2 and LiGluR (**Fig. 6a**). Photoactivation of SNAG-mGluR2 with dim illumination at 380 nm induced slow inward photocurrents, which were deactivated by illumination at 590 nm, as shown above. 590 nm yellow light was used to ensure orthogonality to L-$MAG0_{460}$. In contrast, photoactivation of LiGluR-L-$MAG0_{460}$ by illumination at 500 nm induced rapid, spontaneously-relaxing photocurrents, as shown earlier[44]. When only one of the receptors was expressed, only its characteristic photo-response was seen. In the case of SNAG-mGluR2 this was a slow ON, slow OFF photocurrent induced by illumination at 380 nm and 500 nm, respectively, whereas in the case of LiGluR-L-$MAG0_{460}$ this was a rapid, spontaneously-relaxing photocurrent, which was triggered by illumination at 500 nm, which turned off spontaneously in the dark (**Fig. 6b, c**). Together these experiments show that the PORTL approach based on conjugation of BGAGs to SNAP-tagged receptors allows for independent, dual optical control within the same preparation, a major step forward for chemical optogenetics.

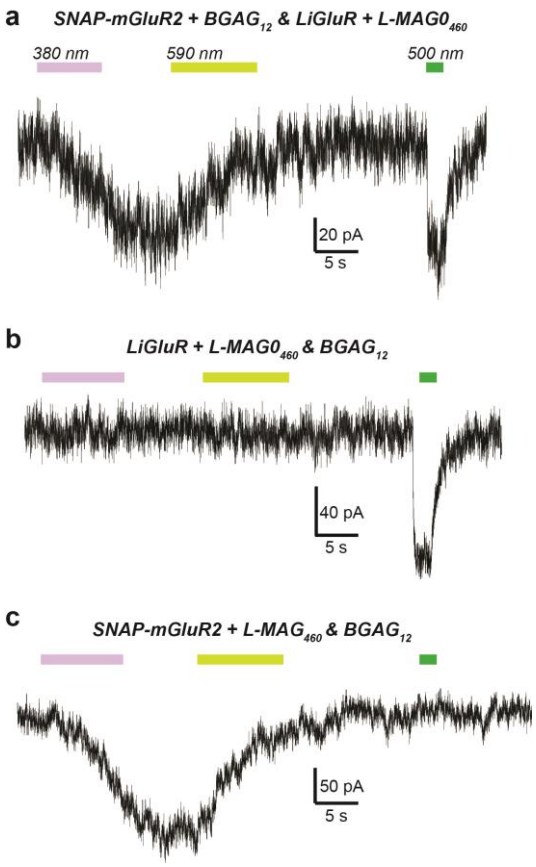

Figure 6: Dual optical control of SNAG-mGluR2 and LiGluR in HEK 293T cells *via* orthogonal labeling of **$BGAG_{12}$** and MAG_{460}. **a-c**) Representative traces showing the responses to dim 380 nm light (<.01 mW/mm^2; purple bars), 590 nm light (~1 mW/mm^2; yellow bars), and 500 nm light (~1 mW/mm^2; green bars) in cells treated with **$BGAG_{12}$** and L-$MAG0_{460}$. Cells expressing both SNAP-mGluR2 and LiGluR show a slow SNAG-mGluR2-mediated response to 380 nm light that is reversed by 590 nm light and a fast LiGluR-mediated response to 500 nm light (a). In the absence of SNAP-mGluR2, the slow response to 380 nm is not seen (b) and in the absence of LiGluR, the fast response to 500 nm is not seen (c), confirming the origins of each current.

Discussion

Photoswitchable tethered ligands (PTLs) provide a powerful component of the optogenetic arsenal for biophysical, synaptic, neural circuit, behavioral and disease treatment applications[11,12,47]. Unlike opsin-based approaches, which rely on the exogenous expression of non-native light-gated membrane proteins, PTLs offer target-specific control of native signaling proteins through the bioconjugation of synthetic light-controlled compounds. They allow one to study the physiological roles of individual proteins with a high subtype specificity and spatiotemporal and genetic precision compared to classical pharmacological or genetic techniques. Until the present, PTL anchoring to the signaling protein of interest has been almost exclusively based on the covalent attachment of a maleimide group on the PTL to an engineered cysteine positioned near the pore or ligand binding pocket of the protein[48]. Even on extracellular parts of proteins, where most native cysteines are disulfide bonded and not subject to attack by a maleimide, there are many free cysteines where PTLs will attach. As a result, the specificity of action of cysteine-reactive PTLs relies not on unique targeting, but on the insensitivity of other proteins to the minor repositioning of tethered ligands[14,32,49]. Still, there would be a major advantage if protein attachment could be bio-orthogonal and so highly specific. Maleimide-cysteine attachment has proven viable in small animals, such as zebrafish and easily accessible tissues, such as the outer retina of mouse. However, it may be inefficient in larger systems due to slow diffusion and competition with hydrolysis, and is restricted to the extracellular environment, since inside the cell competition for the target cysteine by glutathione at millimolar concentrations would be forbidding. In addition, attachment to a native accessible cysteine, such as in enzyme active site, could be deadly. Our goal was to create a new orthogonal and efficient strategy for specific PTL attachment that is easy to generalize. We present a solution to these challenges in the form of a second generation PTL, termed PORTL, an approach built around the conjugation of BG-labeled photoswitches to genetically encoded SNAP tags.

The PORTL approach takes advantage of the fact that the SNAP-tag reacts with BGs in a very efficient and selective way that is fully orthogonal to native chemical reactions[5,6]. Unlike first-generation PTLs, which need to be tethered near the site of ligand binding[14,20,32,49-51], PORTL tethers the photoswitch farther away, on a separate domain, providing a useful separation between the attachment point and functional head group of the compound by a long linker. In principle, the photoswitch could also be attached to a separate transmembrane protein, an antibody or a membrane anchor. This physical separation is expected to place the ligand head group of a PORTL at a relatively lower local concentration than a conventional PTL. The head group would then be photoswitched between active and active states like a photochromic ligand, and should be ideally inactive in the dark. Aspects of this logic were previously applied to a photoswitchable ligand attached via a long flexible tether to a $GABA_A$ receptor, although in that case the ligand was a potentiator, not an agonist, the ligand was active in the dark, and the attachment was to an introduced cysteine[52]. A further feature to our design is that the predicted relatively low local concentration of PORTL head groups may help ensure the lack of basal modulation of receptor activity by the relaxed state of the photoswitch.

With these considerations in mind, we designed and synthesized benzylguanine-azoglutamate (BGAG) PORTL compounds that may be attached to a SNAP-tagged version of the class C GPCR mGluR2 to produce the chemical optogenetic tool termed "SNAG-mGluR2". SNAG-mGluR2 permits the high-efficacy, rapid, repeatable photoactivation of

mGluR2 with a 2-color, bistable BGAG (SNAG-mGluR2) or a 1-color, spontaneously relaxing **BGAG$_{12(460)}$** (SNAG$_{460}$-mGluR2). In both cases, SNAG-mGluR2 remains inactive in the dark and is activated in the high-energy state in response to either near UV (~380 nm, **BGAG$_n$**) or visible light (~460 nm, **BGAG$_{12(460)}$**). Consistent with our predictions about the mechanism of PORTL photoactivation, untethered photoswitches that mimic the azobenzene-glutamate part of BGAG showed the same directionality of photoswitching on mGluR2, suggesting that the efficacy of the photoswitchable ligand is higher in *cis* than *trans* and independent of the tether. Importantly, since it maintains the entire full-length sequence of mGluR2, SNAG-mGluR2 should also retain all native signaling properties ranging from ligand binding to G protein coupling to downstream regulation. Consistent with this, SNAG-mGluR2 permitted efficient optical manipulation of two distinct native downstream targets of mGluR2 in neurons: a somato-dendritic control of excitability and a presynaptic control of synaptic transmission.

In line with the attractive properties of SNAP-tag conjugation, BGAG photosensitizes SNAP-mGluR2 at concentrations 100-1000x lower than typically used for maleimide-based PTLs, minimizing potential activation of glutamate receptors during photoswitch incubation. Furthermore, owing to its insensitivity to hydrolysis by water, BGAG remains reactive over not minutes but days, and stocks diluted in aqueous buffer may be re-used without a loss of labeling efficiency. Taken together, these properties should make the PORTL approach ideally suited for labeling in intact tissue or *in vivo*, as was recently shown for fluorophore conjugation to a SNAP-tag in the nervous system of mouse[25].

Another major advantage of the PORTL approach is its modularity, which will allow it to be widely applicable to many protein targets with a variety of photoswitches. The SNAP-tag is well characterized and has been used extensively to label fusion proteins with fluorophores or to create semisynthetic probes for the sensing of small molecules[24]. Like GFP, the SNAP tag can be fused to proteins of interest without significantly altering their activity. Indeed, several SNAP-tagged transmembrane class A and class C GPCRs, including all of the mGluRs[53,54], have been described and many of these are commercially available.

To facilitate the application of this approach to a wide range of target proteins, we designed our synthetic strategy to be as modular and efficient as possible, taking advantage of the power of click chemistry. Building on existing pharmacology and the growing repertoire of PCLs, PORTL compounds may be synthesized with different head groups for many other target proteins of interest. These compounds may include photoswitchable agonists, antagonists, or allosteric modulators. The ability to change linker lengths may aid in the engineering of other photoswitchable proteins. Relative to the challenge of finding optimal cysteine residues for maleimide-based photoswitch conjugation with first-generation PTLs, the PORTL system will greatly facilitate the design and implementation of new photoswitchable proteins. In addition, the PORTL system with the SNAP tag will enable the optical control of intracellular proteins because, unlike maleimide, the benzylguanine-labeling motif is unaffected by the reducing environment of the cell.

Finally, a major breakthrough in this study that is made possible by the PORTL system is the demonstration of the ability to orthogonally optically manipulate SNAG-mGluR2 and the maleimide-based LiGluR in the same cell. The ability to separately label and manipulate multiple receptor populations may be especially useful for probing crosstalk between proteins at the molecular, cellular, or circuit level. In the future, combination of SNAP-tethered photoswitches with PORTL compounds targeting the

orthogonal SNAP-variant CLIP[7] or the unrelated Halo tag[8] may greatly expand the ability to optically control multiple receptor populations independently in the same preparation. Tuning of the spectral properties of the azobenzene photoswitch will further facilitate the ability to complex multiple tools within the same preparation. Overall, the PORTL approach brings us closer toward the overarching goal of obtaining the ability to individually and precisely photo-activate or inhibit the fundamental signaling molecules of the brain in concert in behaving animals.

Methods

Chemical Synthesis of Photoswitches

Details on the chemical synthesis of BGAGs and their precursors and characterization data can be found in the Supporting Information.

HEK293T and Hippocampal Neuron Electrophysiology

HEK 293T cell recordings were performed as described previously[20]. Cells were seeded on 18 mm glass coverslips and transfected with 0.7 µg/well SNAP-mGluR2 (and/or LiGluR: GluK2-L439C) and GIRK1-F137S DNA, along with 0.1 µg/well tdTomato as a transfection marker, using Lipofectamine 2000 (Invitrogen). Whole-cell HEK cell recordings were performed 24-48 hrs later at room temperature (22–24 °C) using an Axopatch 200B headstage/amplifier (Molecular Devices) on an inverted microscope (Olympus IX series) or a EPC10 USB patch clamp amplifier (HEKA) and PatchMaster software (HEKA) on a Leica DM IL LED. Recordings were performed in high potassium (HK) extracellular solution containing (in mM): 120 KCl, 29 NaCl, 1 $MgCl_2$, 2 $CaCl_2$, 10 Hepes, pH 7.4. Glass pipettes of resistance between 4 and 8 Ω M were filled with intracellular solution containing (in mM): 140 KCl, 10 Hepes, 3 Na_2ATP, 0.2 Na_2GTP, 5 EGTA, 3 $MgCl_2$, pH 7.4. Voltage-clamp recordings were typically performed at -60 mV. Drugs were purchased from Tocris, diluted in HK solution and applied using a gravity-driven perfusion system. Data were analyzed with Clampfit (Molecular Devices) or IgorPro (v6.22, wavemetrics).

Prior to recording, cells were washed with extracellular labeling solution and labeled with BGAG variants at the reported concentrations for 45-50 minutes in an incubator at 37 °C. The extracellular labeling solution contained (in mM): 138 NaCl, 1.5 KCl, 1 $MgCl_2$, 2 $CaCl_2$, 10 HEPES, pH 7.4. For overnight labeling experiments, BGAG was diluted in HEK cell culture media (DMEM + 5 % FBS). For experiments involving LiGluR, following BGAG incubation cells were incubated for 5 minutes at room temperature with 0.3 mg/mL concavalin A to prevent receptor desensitization followed by 50 µM L-$MAG0_{460}$ for 30 minutes at room temperature. Illumination was mediated by Xe-lamp (DG4, Sutter) in combination with excitation filters. Neutral density filters (Omegafilters) were used to vary the light intensity.

Dissociated hippocampal neuron cultures were prepared from postnatal P0 or P1 mice on 12 mm glass coverslips as previously described[20]. Neurons were transfected with SNAP-mGluR2 (1.5 µg/well) and tdTomato (0.25 µg/well as a transfection marker) using the calcium phosphate method at DIV9. Whole cell patch clamp experiments were performed 3-6 days after transfection (DIV 12-15). Labeling was performed using the same protocol as HEK cells except BGAG was diluted in extracellular recording solution containing (in mM): 138 NaCl, 1.5 KCl, 1.2 $MgCl_2$, 2.5 $CaCl_2$, 10 glucose, 5 HEPES, pH 7.4. Glass pipettes of resistance 4-8 MΩ were filled with an intracellular solution containing (in mM):

140 K-gluconate, 10 NaCl, 5 EGTA, 2 $MgCl_2$, 1 $CaCl_2$, 10 HEPES, 2 MgATP and 0.3 Na_2GTP, pH 7.2. Autaptic neurons were voltage clamped at -60 mV and a 2-3 ms voltage step to +20 mV was used to evoke a spike followed (~3-5 ms later) by an EPSC. Stimulation was performed once every 12 s to prevent rundown.

Confocal imaging of SNAP-mGluR2-GFP and Alexa dye-labeled constructs was performed on a Zeiss LSM780 AxioExaminer. Dye labeling was performed in appropriate extracellular solutions for 45 minutes at 1 µM in an incubator at 37 °C and extensively washed before imaging.

Acknowledgements

We gratefully acknowledge S. Nadal for synthetic work and L. de la Osa de la Rosa for technical assistance. We thank Prof. Dr. J.-P. Pin for providing plasmids encoding for SNAP-tagged mGluRs. The work was supported by a Studienstiftung des deutschen Volkes PhD fellowship (J.B.), the International Max Planck Research School for Molecular and Cellular Life Sciences (IMPRS-LS) (A.D.), the National Institutes of Health Nanomedicine Developmental Center for the Optical Control of Biological Function (2PN2EY018241) (E.Y.I. and D.T.), the National Science Foundation EAGER Award (IOS-1451027) (E.Y.I.) and an Advanced Grant from the European Research Commission (268795) (D.T.).

References

1 Hermanson, G. T. *Bioconjugate Techniques*. 3rd ed., (Academic Press, 2013).
2 Wang, L. & Schultz, P. G. Expanding the genetic code. *Angew Chem Int Ed Engl* **44**, 34-66, doi:10.1002/anie.200460627 (2004).
3 Tsai, Y. H., Essig, S., James, J. R., Lang, K. & Chin, J. W. Selective, rapid and optically switchable regulation of protein function in live mammalian cells. *Nat Chem* **7**, 554-561, doi:10.1038/nchem.2253 (2015).
4 Hinner, M. J. & Johnsson, K. How to obtain labeled proteins and what to do with them. *Curr Opin Biotechnol* **21**, 766-776, doi:10.1016/j.copbio.2010.09.011 (2010).
5 Keppler, A. *et al.* A general method for the covalent labeling of fusion proteins with small molecules in vivo. *Nat Biotechnol* **21**, 86-89, doi:10.1038/nbt765 (2003).
6 Keppler, A. *et al.* Labeling of fusion proteins of O6-alkylguanine-DNA alkyltransferase with small molecules in vivo and in vitro. *Methods* **32**, 437-444, doi:10.1016/j.ymeth.2003.10.007 (2004).
7 Gautier, A. *et al.* An engineered protein tag for multiprotein labeling in living cells. *Chemistry & Biology* **15**, 128-136, doi:10.1016/j.chembiol.2008.01.007 (2008).
8 Los, G. V. *et al.* HaloTag: a novel protein labeling technology for cell imaging and protein analysis. *ACS chemical biology* **3**, 373-382, doi:10.1021/cb800025k (2008).
9 Chen, I., Howarth, M., Lin, W. & Ting, A. Y. Site-specific labeling of cell surface proteins with biophysical probes using biotin ligase. *Nat Methods* **2**, 99-104, doi:10.1038/nmeth735 (2005).
10 Spicer, C. D. & Davis, B. G. Selective chemical protein modification. *Nat Commun* **5**, 4740, doi:10.1038/ncomms5740 (2014).
11 Fehrentz, T., Schonberger, M. & Trauner, D. Optochemical genetics. *Angew Chem Int Ed Engl* **50**, 12156-12182, doi:10.1002/anie.201103236 (2011).
12 Broichhagen, J., Frank, J. A. & Trauner, D. A Roadmap to Success in Photopharmacology. *Accounts of chemical research*, doi:10.1021/acs.accounts.5b00129 (2015).
13 Broichhagen, J. & Trauner, D. The in vivo chemistry of photochromic tethered ligands. *Current Opinion in Chemical Biology* **21**, 121-127 (2014).
14 Banghart, M., Borges, K., Isacoff, E., Trauner, D. & Kramer, R. H. Light-activated ion channels for remote control of neuronal firing. *Nat Neurosci* **7**, 1381-1386, doi:10.1038/nn1356 (2004).

15 Szobota, S. *et al.* Remote control of neuronal activity with a light-gated glutamate receptor. *Neuron* **54**, 535-545, doi:10.1016/j.neuron.2007.05.010 (2007).
16 Wyart, C. *et al.* Optogenetic dissection of a behavioural module in the vertebrate spinal cord. *Nature* **461**, 407-410, doi:10.1038/nature08323 (2009).
17 Janovjak, H., Szobota, S., Wyart, C., Trauner, D. & Isacoff, E. Y. A light-gated, potassium-selective glutamate receptor for the optical inhibition of neuronal firing. *Nature Neuroscience* **13**, 1027-1032, doi:10.1038/nn.2589 (2010).
18 Caporale, N. *et al.* LiGluR restores visual responses in rodent models of inherited blindness. *Mol Ther* **19**, 1212-1219, doi:10.1038/mt.2011.103 (2011).
19 Kauwe, G. & Isacoff, E. Y. Rapid feedback regulation of synaptic efficacy during high-frequency activity at the Drosophila larval neuromuscular junction. *Proc Natl Acad Sci U S A* **110**, 9142-9147, doi:10.1073/pnas.1221314110 (2013).
20 Levitz, J. *et al.* Optical control of metabotropic glutamate receptors. *Nat Neurosci* **16**, 507-516, doi:10.1038/nn.3346 (2013).
21 Gaub, B. M. *et al.* Restoration of visual function by expression of a light-gated mammalian ion channel in retinal ganglion cells or ON-bipolar cells. *Proc Natl Acad Sci U S A* **111**, E5574-5583, doi:10.1073/pnas.1414162111 (2014).
22 Gorostiza, P. *et al.* Mechanisms of photoswitch conjugation and light activation of an ionotropic glutamate receptor. *Proc Natl Acad Sci U S A* **104**, 10865-10870, doi:10.1073/pnas.0701274104 (2007).
23 Schafer, L. V., Muller, E. M., Gaub, H. E. & Grubmuller, H. Elastic properties of photoswitchable azobenzene polymers from molecular dynamics simulations. *Angew Chem Int Ed Engl* **46**, 2232-2237, doi:10.1002/anie.200604595 (2007).
24 Reymond, L. *et al.* Visualizing biochemical activities in living cells through chemistry. *Chimia (Aarau)* **65**, 868-871, doi:10.2533/chimia.2011.868 (2011).
25 Yang, G. *et al.* Genetic targeting of chemical indicators in vivo. *Nat Methods* **12**, 137-139, doi:10.1038/nmeth.3207 (2015).
26 Juillerat, A. *et al.* Directed evolution of O6-alkylguanine-DNA alkyltransferase for efficient labeling of fusion proteins with small molecules in vivo. *Chemistry & biology* **10**, 313-317 (2003).
27 Bojkowska, K. *et al.* Measuring in vivo protein half-life. *Chemistry & biology* **18**, 805-815, doi:10.1016/j.chembiol.2011.03.014 (2011).
28 Conn, P. J. & Pin, J. P. Pharmacology and functions of metabotropic glutamate receptors. *Annu Rev Pharmacol Toxicol* **37**, 205-237, doi:10.1146/annurev.pharmtox.37.1.205 (1997).
29 Niswender, C. M. & Conn, P. J. Metabotropic glutamate receptors: physiology, pharmacology, and disease. *Annu Rev Pharmacol Toxicol* **50**, 295-322, doi:10.1146/annurev.pharmtox.011008.145533 (2010).
30 Carroll, E. C. *et al.* Two-photon brightness of azobenzene photoswitches designed for glutamate receptor optogenetics. *Proc Natl Acad Sci U S A* **112**, E776-785, doi:10.1073/pnas.1416942112 (2015).
31 Doumazane, E. *et al.* Illuminating the activation mechanisms and allosteric properties of metabotropic glutamate receptors. *Proc Natl Acad Sci U S A* **110**, E1416-1425, doi:10.1073/pnas.1215615110 (2013).
32 Volgraf, M. *et al.* Allosteric control of an ionotropic glutamate receptor with an optical switch. *Nat Chem Biol* **2**, 47-52, doi:nchembio756 [pii]
10.1038/nchembio756 (2006).
33 Broichhagen, J., Jurastow, I., Iwan, K., Kummer, W. & Trauner, D. Optical control of acetylcholinesterase with a tacrine switch. *Angew Chem Int Ed Engl* **53**, 7657-7660, doi:10.1002/anie.201403666 (2014).
34 Stawski, P., Sumser, M. & Trauner, D. A photochromic agonist of AMPA receptors. *Angew Chem Int Ed Engl* **51**, 5748-5751, doi:10.1002/anie.201109265 (2012).
35 Stein, M. *et al.* Azo-propofols: photochromic potentiators of GABA(A) receptors. *Angew Chem Int Ed Engl* **51**, 10500-10504, doi:10.1002/anie.201205475 (2012).
36 Stein, M., Breit, A., Fehrentz, T., Gudermann, T. & Trauner, D. Optical control of TRPV1 channels. *Angew Chem Int Ed Engl* **52**, 9845-9848, doi:10.1002/anie.201302530 (2013).

37 Schonberger, M. & Trauner, D. A photochromic agonist for mu-opioid receptors. *Angew Chem Int Ed Engl* **53**, 3264-3267, doi:10.1002/anie.201309633 (2014).
38 Schonberger, M., Althaus, M., Fronius, M., Clauss, W. & Trauner, D. Controlling epithelial sodium channels with light using photoswitchable amilorides. *Nat Chem* **6**, 712-719, doi:10.1038/nchem.2004 (2014).
39 Broichhagen, J. *et al.* Optical control of insulin release using a photoswitchable sulfonylurea. *Nat Commun* **5**, 5116, doi:10.1038/ncomms6116 (2014).
40 Damijonaitis, A. *et al.* AzoCholine enables optical control of alpha 7 nicotinic acetylcholine receptors in neural networks. *ACS Chem Neurosci*, doi:10.1021/acschemneuro.5b00030 (2015).
41 Prescher, J. A. & Bertozzi, C. R. Chemistry in living systems. *Nat Chem Biol* **1**, 13-21, doi:10.1038/nchembio0605-13 (2005).
42 Hong, V., Steinmetz, N. F., Manchester, M. & Finn, M. G. Labeling live cells by copper-catalyzed alkyne--azide click chemistry. *Bioconjug Chem* **21**, 1912-1916, doi:10.1021/bc100272z (2010).
43 Song, X., Wang, C., Han, Z., Xu, Y. & Xiao, Y. Terminal alkyne substituted O6-benzylguanine for versatile and effective syntheses of fluorescent labels to genetically encoded SNAP-tags. *RSC Advances* **5**, 23646-23649, doi:10.1039/C4RA17072E (2015).
44 Kienzler, M. A. *et al.* A red-shifted, fast-relaxing azobenzene photoswitch for visible light control of an ionotropic glutamate receptor. *J Am Chem Soc* **135**, 17683-17686, doi:10.1021/ja408104w (2013).
45 Chen, J. J. & Aduda, V. DMSO-aided o-iodoxybenzoic acid (IBX) oxidation of Fmoc-protected amino alcohols. *Synthetic Commun* **37**, 3493-3499, doi:Doi 10.1080/00397910701555469 (2007).
46 Vafabakhsh, R., Levitz, J. & Isacoff, E. Y. Conformational Dynamics of a Class C GPCR. *Nature* **in press** (2015).
47 Reiner, A., Levitz, J. & Isacoff, E. Y. Controlling ionotropic and metabotropic glutamate receptors with light: principles and potential. *Curr Opin Pharmacol* **20**, 135-143, doi:10.1016/j.coph.2014.12.008 (2015).
48 Lemoine, D. *et al.* Optical control of an ion channel gate. *Proc Natl Acad Sci U S A* **110**, 20813-20818, doi:10.1073/pnas.1318715110 (2013).
49 Lin, W. C. *et al.* Engineering a light-regulated GABAA receptor for optical control of neural inhibition. *ACS chemical biology* **9**, 1414-1419, doi:10.1021/cb500167u (2014).
50 Fortin, D. L. *et al.* Photochemical control of endogenous ion channels and cellular excitability. *Nat Methods* **5**, 331-338, doi:10.1038/nmeth.1187 (2008).
51 Sandoz, G., Levitz, J., Kramer, R. H. & Isacoff, E. Y. Optical control of endogenous proteins with a photoswitchable conditional subunit reveals a role for TREK1 in GABA(B) signaling. *Neuron* **74**, 1005-1014, doi:S0896-6273(12)00423-0 [pii] 10.1016/j.neuron.2012.04.026 (2012).
52 Yue, L. *et al.* Robust photoregulation of GABA(A) receptors by allosteric modulation with a propofol analogue. *Nat Commun* **3**, 1095, doi:10.1038/ncomms2094 (2012).
53 Maurel, D. *et al.* Cell-surface protein-protein interaction analysis with time-resolved FRET and snap-tag technologies: application to GPCR oligomerization. *Nat Methods* **5**, 561-567, doi:10.1038/nmeth.1213 (2008).
54 Doumazane, E. *et al.* A new approach to analyze cell surface protein complexes reveals specific heterodimeric metabotropic glutamate receptors. *Faseb J* **25**, 66-77, doi:10.1096/fj.10-163147 (2011).

VII: Chemistry and Biology of Loline Alkaloids

Towards the elucidation of the bioactivity of loline alkaloids

Arunas Damijonaitis[1], Peter Schulz[1], Marion Holy[2], Harald Sitte[2], Alexander Gottschalk[3] and Dirk Trauner[1]

[1] Department of Chemistry, Ludwig-Maximilians-University Munich and Center of Integrated Protein Science Munich; Butenandtstr. 13, 81377 Munich, Germany

[2] Center for Physiology and Pharmacology; Medizinische Universität Wien, Währinger Straße 13A, 1090 Wien, Austria

[3] Institute of Biochemistry and Buchmann Institute for Molecular Life Sciences, Johann Wolfgang Goethe-University, Max-von-Laue-Straße 15; 60438 Frankfurt, Germany;

Introduction:

The alkaloid temuline (1) was described as one of the bioactive constituents of *Lolium temulentum* by Franz Hofmeister in his publication "the active constituents of the Taumellolch" (transl. from German -„Die Wirksamen Bestandtheile des Taumellolchs") in 1892.[1] At the time, livestock poisoning was suspected to be caused by food contaminated with *Lolium* seeds. Several researchers reported to experience confusion, headaches, changes to vision, nausea and other impairments after consuming contaminated bread.[1] Further investigations showed that ergot alkaloids, which are also products of tall fescue, accounted for these observations.[2, 3] The contribution of loline alkaloids (Figure 1) such as loline (2), *N*-formyl loline (3), *N*-acetyl loline (4), temuline (1), *N*-formyl temuline (5), and *N*-acetyl temuline(6)[4] to this effect, however, could neither be confirmed nor ruled out. Furthermore, in the late 1980s, the occurrence of loline alkaloids in pasture and wild grasses could be linked to the infection with symbiotic endophytes (*Neotyphodium* species).[5, 6] This symbiosis endowed the plants with tolerance to pathogens like insects and nematodes.[7] Christopher L. Schard and colleagues showed that the concentration of loline alkaloids in plants correlated with levels of anti-aphid activity.[8] Recently, it was reported that *N*-formyl loline attracted nematodes (*Pratylenchus Scribneri*) at low concentrations, while at higher concentrations it acted as a repellent.[9]

The molecular biological targets of loline and its derivatives are still unknown. Extensive pharmacological studies were never carried out due to poor availability of these substances. So far, the extraction of loline from natural sources resulted in low quantities of only a small number of loline derivatives. Until recently, the chemical synthesis of these alkaloids involved a costly 20-step synthesis. Consequently, Dirk Trauner and Mesut Cakmak developed an efficient, high-yielding ten-step synthesis providing pure loline and its derivatives.[10]

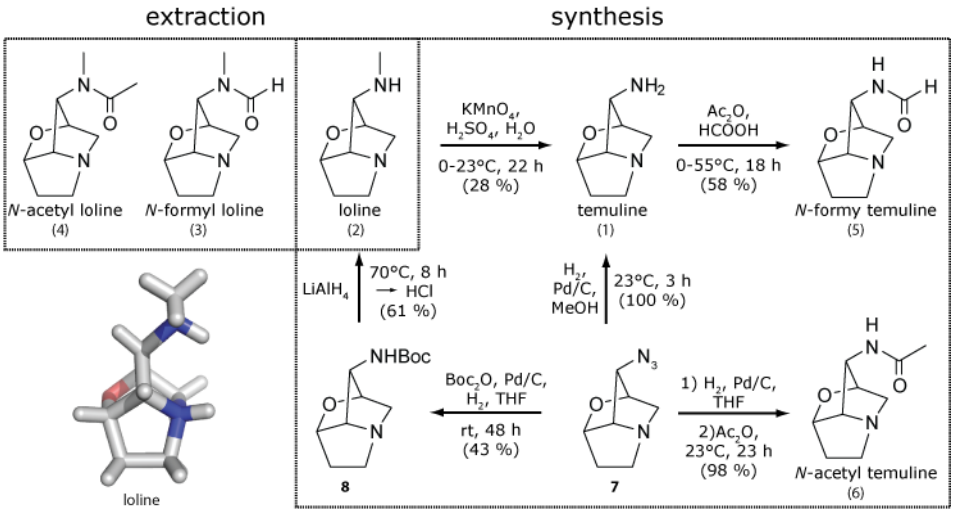

Figure 1. Extraction and synthesis of loline alkaloids. Chloroform extraction from plant seeds yields loline (2), *N*-formyl loline (3), and *N*-acetyl loline (4). Temuline (1) and its derivatives can be achieved by chemical synthesis. Crystal structure of loline (2) is taken from reference 10.

The growing resistance of pests to available crop protection substances is becoming a significant problem in modern agriculture. Plant protecting products should be specific to pathogens alone and have no effect on other plants and animals, especially vertebrates. This makes the natural pesticide loline an interesting candidate for the development of an environmentally friendly pesticide. Here, optimization of loline extractions from plant seeds (*Festulolium loliaceum*, infected with *Neotyphodium uncinatum*) and the chemical derivatization of loline to temuline and its derivatives are described (Figure 1). The effect of loline on the nematode *Caenorhabditis elegans* (*C. elegans)* and human serotonin transporter (hSERT) are further investigated.

Results and Discussion:

Extraction. To extract loline alkaloids, ground Lolium seeds (*Festulolium loliaceum*, infected with *Neotyphodium uncinatum*) were extracted with chloroform using a Soxhlet extractor. Loline (2), *N*-formyl loline (3), and *N*-acetyl loline (4) could be seperated *via* column chromatography.

Synthesis. Loline alkaloids share a common heterocyclic core and are saturated 1-aminopyrrolizidines bearing an oxygen bridge. Through chemical synthesis (Figure 1) temuline can be accessed either through demethylation of loline (2) or hydrogenation of the azide **7**. Treatment of the azide **7** with Ac_2O gave *N*-acteyl temuline (6) in excellent yield. Alternatively, reduction of **7** in the presence of di-*tert*-butyldicarbonate gives *N*-Boc protected temuline **8**, which can be further transformed into **2** using lithium aluminum hydride. Formylation of temuline (1) with a mixture of Ac_2O and formic acide gave *N*-formyl temuline (5) in good yields.

Loline promotes swimming behavior in *C. elegans.* First, we investigated the effect of loline alkaloids on the swimming behavior of the nematode *C. elegans*. In solution, the nematode is able to swim by performing dorso-ventrally alternating c-shaped body postures (Figure 2a). These so called "thrashing movements" are often used to quantify locomotion behavior and motility. To test the influence of several loline alkaloids on the swimming behavior of nematodes, thrashing assays were performed. Up to 10 animals were placed into a 96 well plate with a physiological buffer solution (M9). During the time

course of one minute the thrashes were counted (Figure 2b). The animals in M9 thrashed 107 ± 1.9 (n = 30) times per minute. In M9 supplemented with *N*-acetyl temuline (6; 100 mM) or of loline (2; 100 mM) the thrashes increased significantly to 113 ± 1.8 (n = 18) and 128 ± 2.2 (n = 14) thrashes per minute, respectively. These results suggest that *N*-acetyl temuline (6) and loline (2) evoke a flight-like-behavior in *C. elegans*. The nematode tries to escape the repelling compound by increasing the number of thrashes per minute.

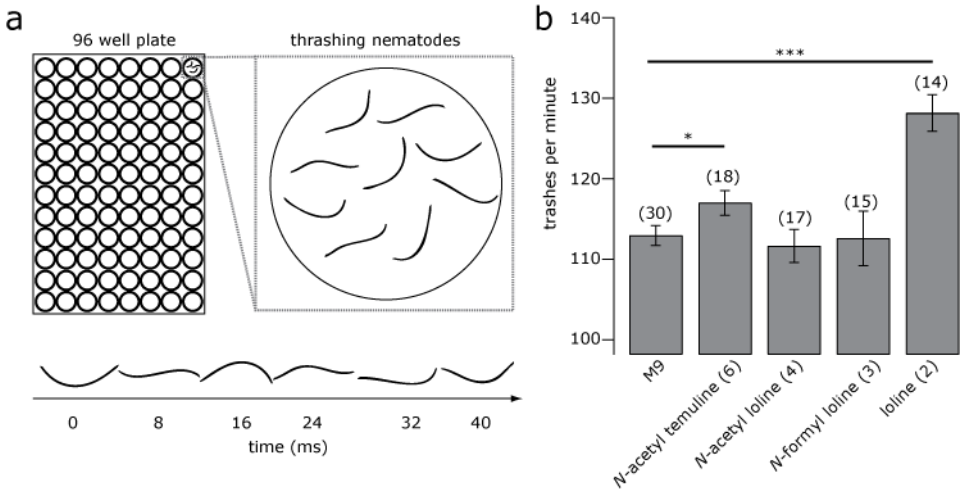

Figure 2. Thrashing assay of *C. elegans* strain N2 (wild type). a) Illustration of a 96 well plate with 9 nematodes swimming in buffer (M9) with 100 mM of the indicated molecule. The thrashing movement is depicted over time. b) Quantitative analysis of thrashes in: M9 (112.9 ± 1.2; n = 30), *N*-acetyl temuline (6, 117.0 ± 1.5; n = 18), *N*-acetyl loline (4, 111.6 ± 2.0; n = 17), *N*-formyl loline (3, 112.6 ± 3.3; n = 15), and loline (2, 128.1 ± 2.2; n = 14). Bars represent mean; error bars represent SEM; numbers of cells tested are in parentheses above bars. Significance was calculated via student t-test with *** for p<0.001, ** p = 0.01 to 0.001, and * for p = 0.05 to 0.01.

Drug screening indicates putative targets of loline alkaloids. To test, whether the loline alkaloids have an effect on human receptors, we turned to a drug screening assay. In collaboration with Brian Roth (University of North Carolina) a Psychoactive Drug Screening Program (PDSP) on the synthesized loline derivatives was carried out (Table 1). First results have shown that some derivatives bind to nicotinic acetylcholine receptors (nAChR). For instance, *N*-formyl loline (3) binds to the α4/β4 nAChR with nanomolar affinity. The molecules *N*-acetyl chloropyrrolizidine (9), *N*-formyl temuline (5), and *N*-acetyl temuline (6) show binding to the dopamine receptor 5 (D5). Furthermore, temuline (1) and *N*-acetyl loline (4), show binding to the the serotonin transporter (SERT). Nevertheless, radio ligand binding assays sometimes produce false positive results. Therefore, one should not over-interpret the findings.

Table 1. Targets of loline and derivatives identified by the PDSP radio ligand binding assays. Values represent inhibition (K_i in nM).

	nicotinic acetylcholine receptor					dopamine receptor	serotonin transporter
	α2/β2	α2/β4	α3/β4	α4/β2	α4/β4	D5	SERT
Temuline (1)*	-	-	-	-		-	310.0
Loline (2)*	-	-	-	-	-	-	>10,000
N-formyl loline (3)*	3,230.0	2,560.0	6,840.0	3,630.0	938.0	-	-
N-acetyl loline (4)*	-	-	-	>10,000	-	-	32.0
N-formyl temuline (5)*	-	-	-	>10,000	-	2,063.0	>10,000
N-acetyl temuline (6)*	-	-	-	4,065.0	-	1,171.0	>10,000
N-acetyl chloropyrrolizidine (9)*	-	-	-	-	-	1,781.0	469.0

**Note: molecule provided by Mesut Cakmak.*

Bioactivity of lolines on nicotinic acetylcholine receptors. Following the targets identified in the drug screening, we first aimed to investigate mode of binding of loline alkaloids to nicotinic acetylcholine receptors (nAChRs). Transient expression of nAChRs in HEK293T cells was not successful. Also the attempt to acquire a stable cell line[12] from Prof. Kellar (Georgetown University, Washington) was fruitless. Finally, the project was reoriented towards the expression of the α4β4 receptor in *Xenopus laevis* oocytes. For electrophysiological recordings from oocytes two electrode voltage clamp (TEVC) was established.

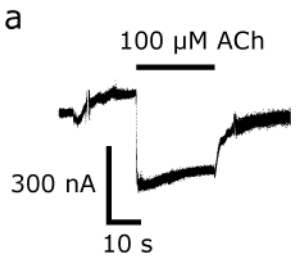

Figure 3. Activation of α4β4 nAChR expressed in *Xenopus laevis* oocytes. ACh (100 µM) was shortly applied to the oocyte.

RNA synthesis was performed using mMESSAGE mMACHINE® SP6 Transcription Kit (life technologies) according to manufacturer's instructions. Due to varying quality of delivered oocytes and unreliable expression of the receptors, lolines could not be tested yet. Nevertheless, the successful expression of the receptor could be shown by activation of the α4β4 nAChR with 100 µM acetylcholine (ACh)(Figure 3). Further experiments using the α4β4 nAChR expressed in *Xenopus* oocytes will show if the loline alkaloids can activate the receptor directly, or if they could inhibit ACh induced currents.

Bioactivity of lolines on the human serotonin transporter. The strongest binding affinity in the PDSP was observed for the interaction of *N*-acetyl loline (4) with the human serotonin transporter (hSERT). The SERT regulates the monoamine-mediated neural signaling. It terminates the synaptic transmission of serotonin by removing the

neurotransmitter from the synaptic cleft. It is the target of many psychoactive molecules, such as cocaine or MDMA (Ecstasy). In treatment of depression selective serotonin re-uptake inhibitors are often used, which act on the SERT. The molecule monensin (Mon) is used in assays to enhance the releasing capability of SERT substrates.

The SERT efflux and inhibition assays were performed in collaboration with Marion Holy (Medizinische Universität Wien, Prof. Harald Sitte) as previously described.[11]

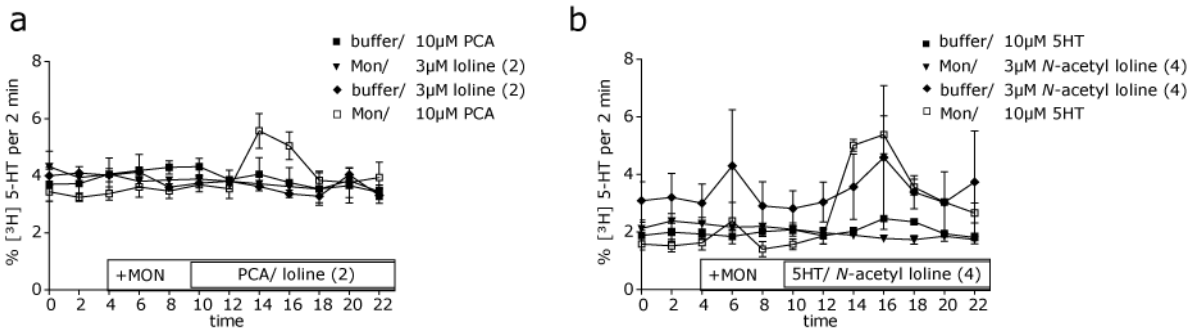

Figure 4. The SERT efflux experiment. Before the experiment, 0.3 mM of the radiolabeled substrate [^{3}H]MPP$^+$ was added to the HEK293 cells expressing hSERT and incubated for 20 min. The coverslips were transferred to small chambers (volume 0.2 ml) and superfused with Ringer buffer at to establish basal efflux. After basal efflux had stabilized, the experiment was initiated, with the collection of fractions every 2 min. After 6 min, the Na^+/H^+ ionophore monensin (25 mM) or control buffer was added to the cells. After 14 min, the ligand of interest was added. Finally, the remaining radioactivity was recovered by superfusing the cells for 6 min with 1 % SDS. a) loline (2) induced or b) *N*-acetyl loline (4) induced release of radioactivity at any time point was compared with the amount released in the absence of drugs and is expressed as percentage released.

Figure 3 demonstrates that loline (2) as well as *N*-acetyl loline (4) produce no change in efflux of [^{3}H]5HT in presence of Mon in HEK cells expressing SERT. In contrast, Mon enhances the efflux produced by the SERT substrates *p*-chloroamphetamine (PCA) (Figure 4a) or 5HT (Figure 4b).

The assay for inhibition of serotonin uptake by the SERT shows that loline (2) and its derivatives (Figure 5a-e) do not inhibit the uptake at any concentration. In contrast, cocaine inhibits the SERT effectively (Figure 5f). Taken together, these findings suggest that loline (2) and its derivatives have no effect on SERT uptake or release.

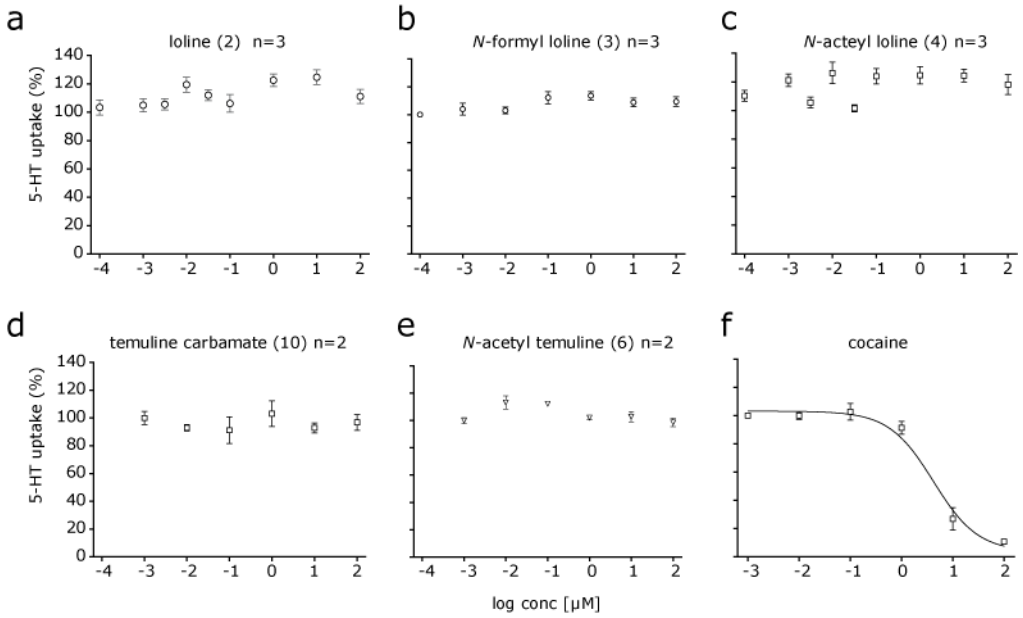

Figure 5. Effects of loline alkaloids and comparison test drug (cocaine) on inhibition of uptake at SERT in rat brain synaptosomes. Synaptosomes were incubated with different concentrations of loline alkaloids or cocaine, in the presence of 400 nM [^{3}H]serotonin. Data are percentage of [^{3}H]transmitter uptake expressed as mean ± s.e.m. for n = 2–3 experiments.

Summary

In summary, loline (2), *N*-formyl loline (3), and *N*-acetyl loline (4) can reproducibly be extracted from fescue seeds and easily derivatized to temuline (1), *N*-formyl temuline (5), and *N*-acetyl temuline (6). In swimming nematodes loline (2) and *N*-acetyl temuline (4) increase the number of thrashes per minute. Experiments on the hSERT showed no activity of lolines on the transporter. Functional expression of the α4β4 nAChR could be achieved in *Xenopus* oocytes.

Experimental section

Chemical procedures:

Flash column chromatography was carried out on silica gel 60 (0.040–0.063 mm, Merck). Reactions and chromatography fractions were monitored by thin layer chromatography (TLC) on (Merck) silica gel 60 F254 glass plates (Merck). The spots were visualized either under UV light at 254 nm or with appropriate staining method (KMnO4, Ninhydrin) followed by heating.

NMR spectra were recorded in deuterated solvents on VARIAN Mercury 200, BRUKER AXR 300, VARIAN VXR 400 S, BRUKER AMX 600 and BRUKER Avance III HD 400 (equipped with a CryoProbe™) instruments and calibrated to residual solvent peaks (1H/13C in ppm): CDCl3 (7.26/77.16), DMSO-d6 (2.50/39.52), MeCN-d3 (1.94/1.32), acetone-d6 (2.05/29.84), CD3OD (3.31/49.00). Multiplicities are abbreviated as follows: s = singlet, d = doublet, t = triplet, q = quartet, br = broad, m = multiplet. Spectra are reported based on appearance, not on theoretical multiplicities derived from structural information.

Mass spectra were measured by the analytic section of the Department of Chemistry, *Ludwig-Maximilians-Universität München*. Mass spectra were recorded on the following spectrometers (ionisation mode in brackets): MAT 95 (EI) and MAT 90 (ESI) from *Thermo Finnigan GmbH.* Mass spectra were recorded in high-resolution. The method used is reported at the relevant section of the experimental section.

Solvents for column chromatography and reactions were purchased in HPLC grade or distilled over an appropriate drying reagent prior to use. If necessary, solvents were degassed either by freeze-pump-thaw or by bubbling N_2 through the vigorously stirred solution for several minutes. Unless otherwise stated, all other reagents were used without further purification from commercial sources.

Optimized extraction procedure. Ground Lolium seeds (*Festulolium loliaceum*, infected with *Neotyphodium uncinatum*, 30 g) were suspended in chloroform (300 mL) and stirred at reflux with a Soxhlet extractor for 11 h. After cooling to rt, aqueous sodium hydroxide solution (2 mL, 1M) was added and the suspension was filtered. The combined green colored organic phases were concentrated *in vacuo* to one third of the original volume. The organic phase was extracted with hydrochloric acid (5 x 50 mL, 2M), resulting in a rose-colored aqueous suspension, which was subsequently stirred at 80 °C for 3 h. The solution was cooled to rt and solid sodium hydroxide (10.8 g) was added until basic (pH = 13), whereupon the solution changed color from pink to yellow. The aqueous phase was extracted with chloroform (5 x 50 mL). The combined organic phases were concentrated *in vacuo,* giving a crude extract, a yellow oil (98 mg). The crude product was purified via column chromatography on silica gel (30 g) using chloroform/MeOH/Ammonia (9:1:0.1) as eluent, to afford *N*-acetyl loline (4 mg) and loline (19 mg).

Loline (2):
TLC (10 % MeOH in $CHCl_3$): R_f = 0.48 (Ninhydrine)*
GC-MS t_R = 6.560 min, m/z 154 (EI (CI))
^{1}H NMR (400 MHz, $CDCl_3$) δ = 4.33 (dd, *J*=4.5, 1.9, 1H), 3.95 (s, 1H), 3.34 (d, *J*=11.6, 1H), 3.26 (s, 1H), 3.10 (s, 1H), 3.00 (ddd, *J*=12.3, 8.4, 3.5, 1H), 2.86 (ddd, *J*=12.8, 9.3, 7.3, 1H), 2.40 (s, 2H), 2.34 (d, *J*=11.6, 1H), 2.00 – 1.85 (m, 3H).
^{13}C-NMR (101 MHz, $CDCl_3$): δ = 81.6, 74.0, 69.6, 68.2, 61.1, 54.5, 35.2, 33.9.
**Note: TLC plate was saturated with NH_3 vapor before running in the solvent mixture.*

N-formyl loline (3):
TLC (10 % MeOH in $CHCl_3$): R_f = 0.80 (Ninhydrine)*
GC-MS t_R = 8.025 min, m/z 182 (EI (CI))
^{1}H NMR** (400 MHz, $CDCl_3$) δ = 8.43 (s, 1H), 8.07 (d, *J*=1.0, 1H), 4.75 (d, *J*=2.5, 1H), 4.54 (dd, *J*=4.4, 1.8, 1H), 4.45 (dd, *J*=4.5, 1.9, 1H), 4.22 (d, *J*=2.3, 1H), 4.07 – 3.99 (m, 1H), 3.88 – 3.80 (m, 1H), 3.44 (t, *J*=1.4, 2H), 3.32 – 3.22 (m, 2H), 3.13 (s, 2H), 3.12 – 2.97 (m, 1H), 2.95 (s, 3H), 2.49 (dd, *J*=15.9, 11.9, 2H), 2.09 (dt, *J*=8.7, 6.6, 2H), 2.03 – 1.96 (m, 2H).
^{13}C NMR** (101 MHz, $CDCl_3$) δ = 164.3, 163.0, 82.7, 80.9, 74.7, 73.8, 68.7, 68.2, 66.1, 63.1, 61.7, 61.2, 55.4, 55.3, 34.2, 33.7, 33.4, 30.7.
**Note: TLC plate was saturated with NH_3 vapor before running in the solvent mixture.*
***Note: Compound exists as a mixture of rotamers in solution.*

N-acetyl loline (4):
TLC (10 % MeOH in $CHCl_3$): R_f = 0.80 (Ninhydrine)*
GC-MS t_R = 8.125 min, m/z 196 (EI (CI))
^{1}H-NMR (400 MHz, MeOD) δ = 5.02 (d, *J*=1.6, 1H), 4.91 (s, 1H), 4.66 (dd, *J*=4.6, 2.2, 1H), 4.14 (s, 1H), 3.88 (d, *J*=12.5, 1H), 3.73 (t, *J*=7.8, 2H), 3.39 (d, *J*=12.5, 1H), 3.09 (s, 3H), 2.44 (dtd, *J*=14.8, 7.4, 4.9, 1H), 2.39 – 2.27 (m, 1H), 2.15 (s, 3H), .
^{13}C NMR (101 MHz, MeOD) δ = 175.8, 80.2, 74.9, 73.0, 66.5, 63.3, 54.8, 37.0, 30.9, 23.1.
**Note: TLC plate was saturated with NH_3 vapor before running in the solvent mixture.*

Reactions:

Temuline (1):
Loline (2, 15 mg, 0.097 mmol, 1.0 eq.) was dissolved in H_2SO_4 (20 %, 1 mL). $KMnO_4$ (6.3 mg, 0.040 mmol, 0.40 eq.) dissolved in H_2O (1 mL) was slowly added to the reaction mixture at 0 °C within 15 min. The mixture was stirred for 4 h at 0 °C and 18 h at ambient temperature. The reaction was cooled to 0 °C before another portion of $KMnO_4$ (6.3 mg, 0.040 mmol, 0.4 eq.) in H_2O (1 mL) was added to the reaction mixture within 15 min. The mixture was stirred for 2 h at ambient temperature. The reaction mixture was filtered through a pad of Celite and the filtrate was basified with NaOH (2 mL, 2 M). The aqueous phase was extracted with $CHCl_3$ (6 x 10 mL). The combined organic phases were concentrated *in vacuo* and purified by column chromatography on silica gel using chloroform/MeOH/Ammonia (9:1:0.1) as eluent to yield temuline (1, 3.8 mg, 0.027 mmol, 28 %) as a yellow oil.

TLC (10 % MeOH in $CHCl_3$): R_f = 0.31 (Ninhydrine)*
GC-MS t_R = 6.6130 min, m/z 140 (EI (CI))
^{1}H NMR (400 MHz, $CHCl_{3z}$) δ = 4.40 (dd, *J*=4.4, 1.8, 1H), 3.87 – 3.82 (m, 1H), 3.63 – 3.58 (m, 1H), 3.53 (dd, *J*=11.8, 1.1, 1H), 3.16 – 3.05 (m, 2H), 2.96 (ddd, *J*=12.9, 9.4, 7.3, 1H), 2.44 (d, *J*=11.8, 1H), 2.09 – 1.96 (m, 2H), 1.92 (s, 2H).
^{13}C NMR (101 MHz, $CDCl_3$): δ = 81.7, 76.3, 72.1, 61.0, 60.5, 54.6, 34.1.
**Note: TLC plate was saturated with NH_3 vapor before running in the solvent mixture.*

N-formyl temuline (5):
A mixture of formic acid (1.0 mL, 27 mmol, 124 eq.) and acetic anhydride (2.0 mL, 21 mmol, 99 eq.) was stirred for 2 h at 55 °C and then added to temuline (1, 30 mg, 0.214 mmol, 1 eq.). The reaction mixture was stirred at ambient temperature for 16 h and then treated with MeOH (5 mL) at 0 °C and stirred for 5 min. The reaction mixture was concentrated *in vacuo*. The crude product was purified by column chromatography on silica gel using chloroform/MeOH/Ammonia (9:1:0.1) as eluent to yield *N*-formyl temuline (5, 21 mg, 0.13 mmol, 58 %) as a yellow oil.

TLC (10 % MeOH in $CHCl_3$): R_f = 0.62 (Ninhydrine)*
GC-MS t_R = 7.670 min, m/z 168 (EI (CI))
HRMS: (ESI) calcd for $C_8H_{12}N_2O_2$ $[M+H]^+$: 169,0977; found: 169.09717.
^{1}H NMR (400 MHz, $CDCl_3$): δ = 8.19 (s, 1H), 6.98 (br, 1H), 4.56 – 4.42 (m, 2H), 4.26 (d, *J*=1.9, 1H), 3.36 (d, *J*=11.8, 1H), 3.15 (ddt, *J*=12.3, 8.4, 4.3, 2H), 2.99 (ddd, *J*=12.9, 9.4, 7.4, 1H), 2.50 (d, *J*=10.0, 1H), 2.17 – 2.00 (m, 2H).
^{13}C NMR (101 MHz, $CDCl_3$) δ = 161.4, 81.0, 73.9, 69.9, 61.0, 56.4, 54.7, 33.7.
**Note: TLC plate was saturated with NH_3 vapor before running in the solvent mixture.*

N-acetyl temuline acetic acid salt (6):
A solution of azide (8, 21 mg 0.13 mmol, 1.0 eq.) and 10 % Pd/C (7.0 mg, 0.065 mmol, 0.50 eq.) in THF (9 mL) was degassed with N_2 in a sonicator for 5 minutes, then flushed with H_2 and stirred for 3 h at rt under H_2 atmosphere (balloon). The atmosphere was exchanged for N_2 and Ac_2O (22 mg, 0.22 mmol, 1.2 eq.) was added. The reaction mixture was stirred for 16 h at ambient temperature, filtered through a pad of Celite and the filtrate was concentrated *in vacuo* to afford *N*-Acetyl temuline acetate (6, 30 mg, 0.18 mmol, 98 %) as a yellow oil.

TLC (10 % MeOH in $CHCl_3$): R_f = 0.62 (Ninhydrine)*
GC-MS t_R = 7.681 min, m/z 182 (EI (CI))
^{1}H NMR (400 MHz, $CHCl_3$) δ = 12.97 (s, 1H), 8.85 (d, *J*=6.2, 1H), 4.58 – 4.52 (m, 2H), 4.41 (d, *J*=2.6, 1H), 3.70 (dd, *J*=11.9, 1.1, 1H), 3.65 – 3.58 (m, 1H), 3.25 (ddd, *J*=8.8, 6.4, 2.9, 2H), 2.68 (d, *J*=11.9, 1H), 2.31 – 2.10 (m, 2H), 2.02 (s, 3H), 1.99 (s, 3H).
^{13}C NMR (101 MHz, $CDCl_3$) δ = 178.0, 171.7, 80.2, 74.0, 69.6, 61.0, 57.2, 53.7, 31.7, 22.8, 22.6.
**Note: TLC plate was saturated with NH_3 vapor before running in the solvent mixture.*

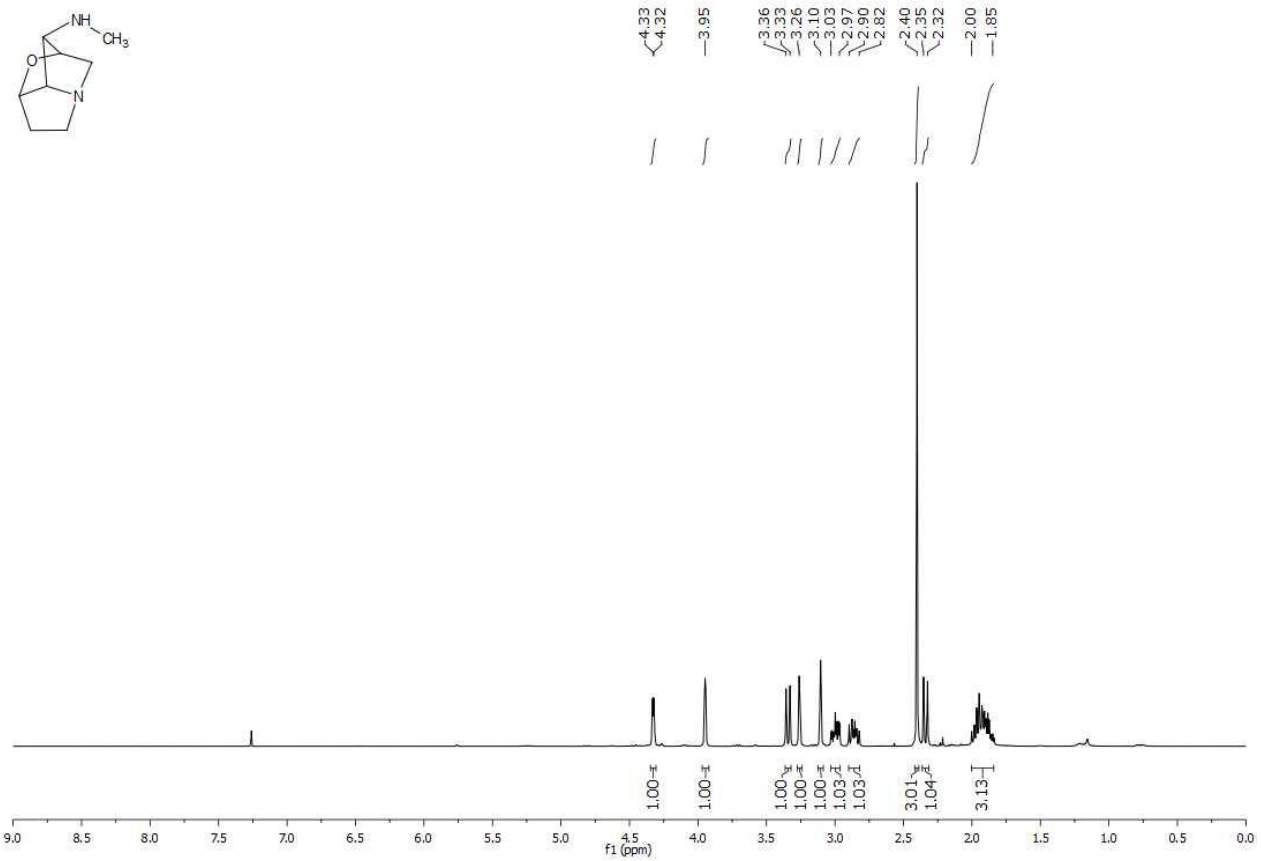
NH
CH3
O
N
4.33
4.32
3.95
3.36
3.33
3.26
3.10
3.03
2.97
2.90
2.82
2.40
2.35
2.32
2.00
1.85
1.00
1.00
1.00
1.00
1.03
1.03
3.01
1.04
3.13
f1 (ppm)

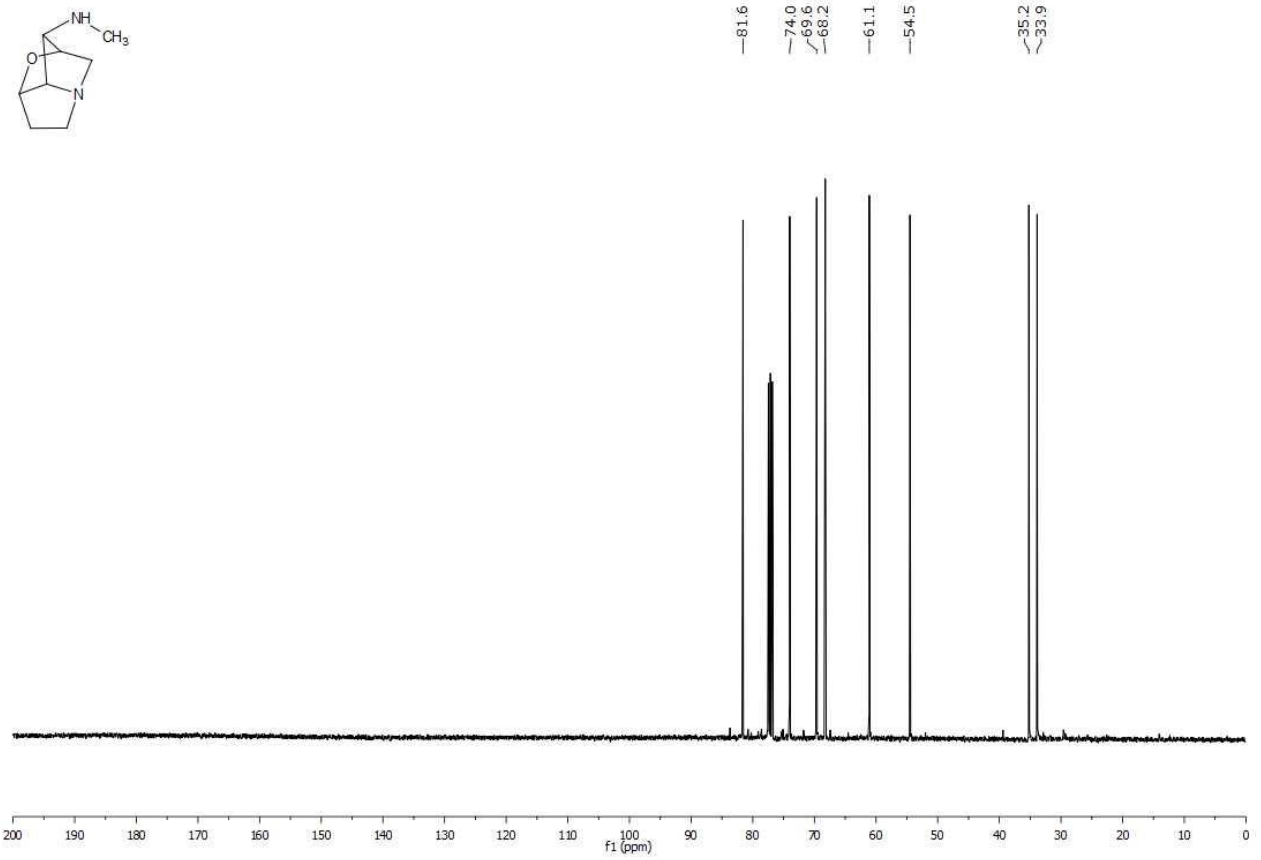
NH
CH3
O
N
81.6
74.0
69.6
68.2
61.1
54.5
35.2
33.9
f1 (ppm)

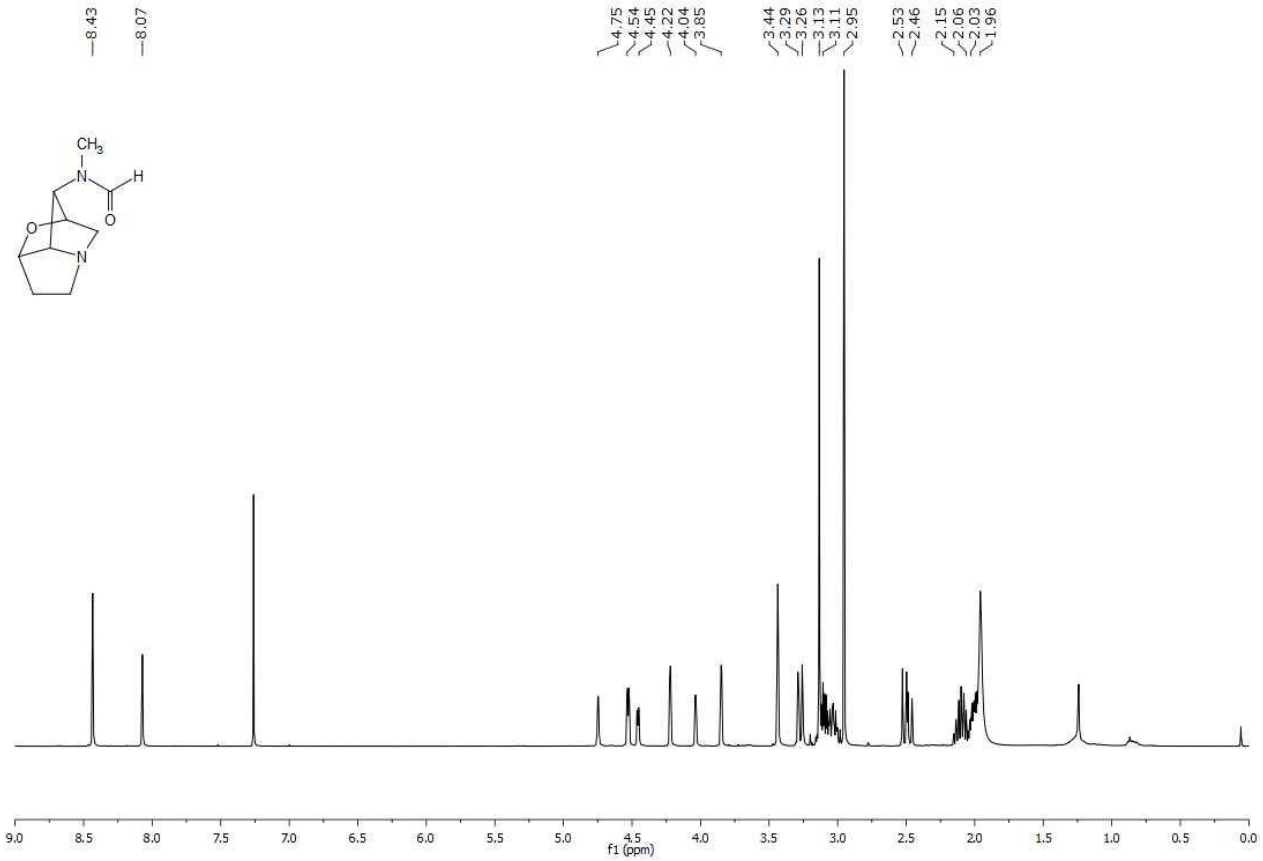
8.43
8.07
4.75
4.54
4.45
4.22
4.04
3.85
3.44
3.29
3.26
3.13
3.11
2.95
2.53
2.46
2.15
2.06
2.03
1.96
CH3
N
H
O
O
N
f1 (ppm)

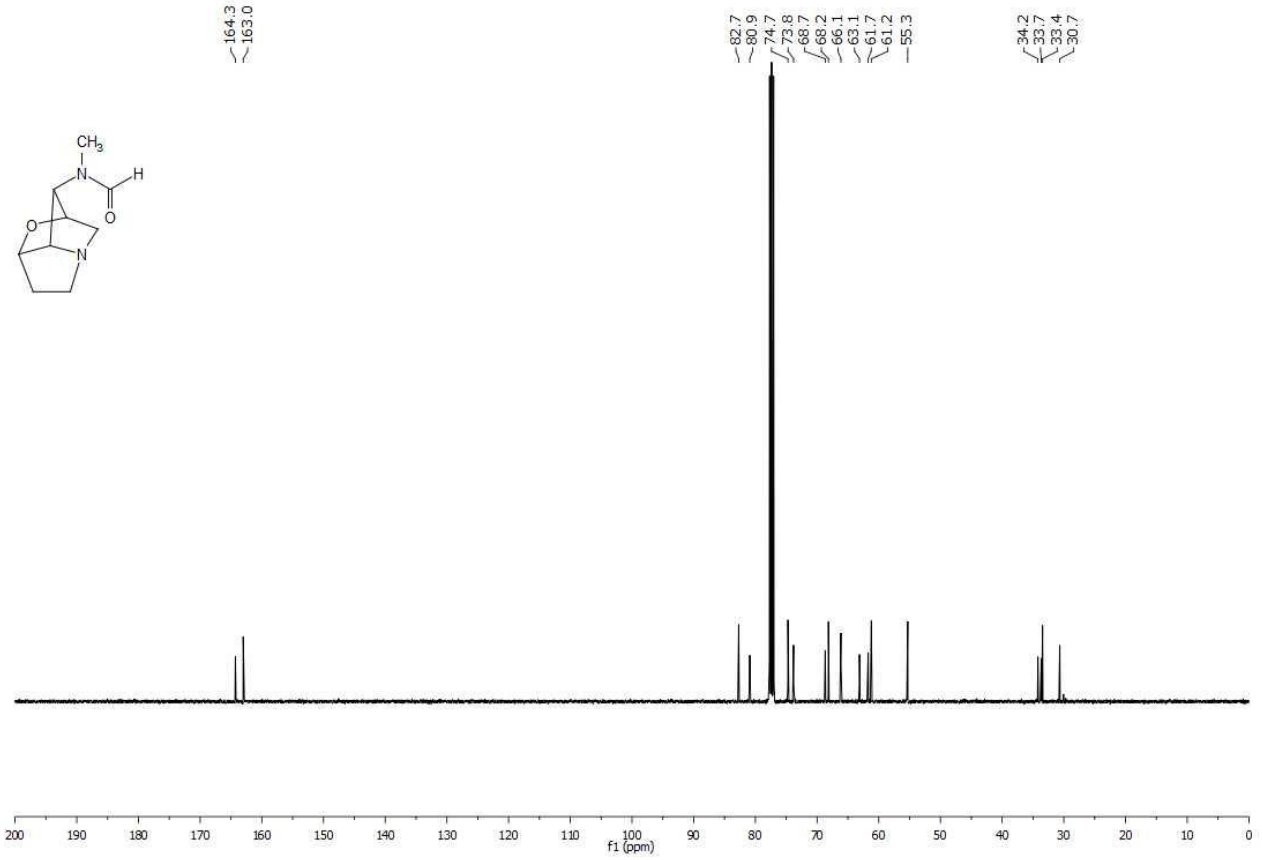
164.3
163.0
82.7
80.9
74.7
73.8
68.7
68.2
66.1
63.1
61.7
61.2
55.3
34.2
33.7
33.4
30.7
CH3
N
H
O
O
N
f1 (ppm)

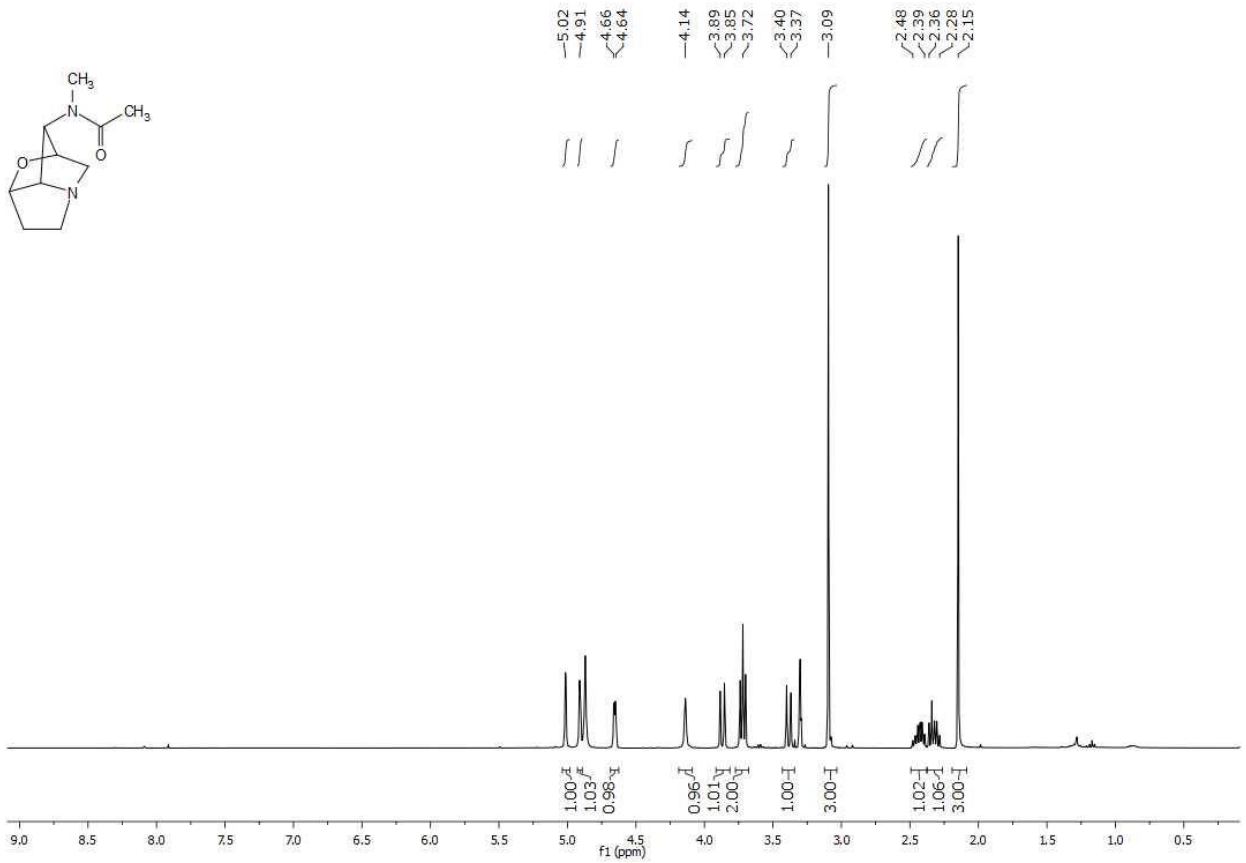
5.02
4.91
4.66
4.64
4.14
3.89
3.85
3.72
3.40
3.37
3.09
2.48
2.39
2.36
2.28
2.15
1.00
1.03
0.98
0.96
1.01
2.00
1.00
3.00
1.02
1.06
3.00
f1 (ppm)

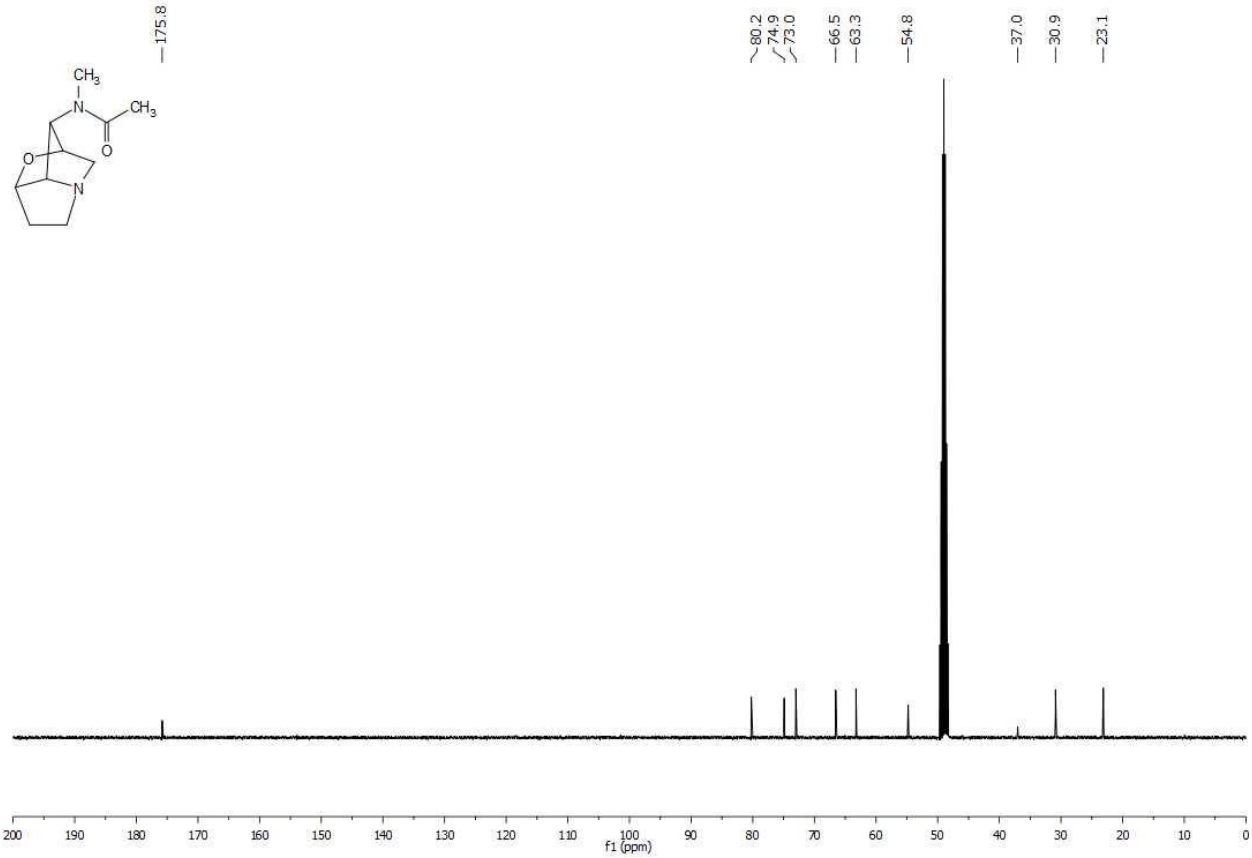
175.8
80.2
74.9
73.0
66.5
63.3
54.8
37.0
30.9
23.1
f1 (ppm)

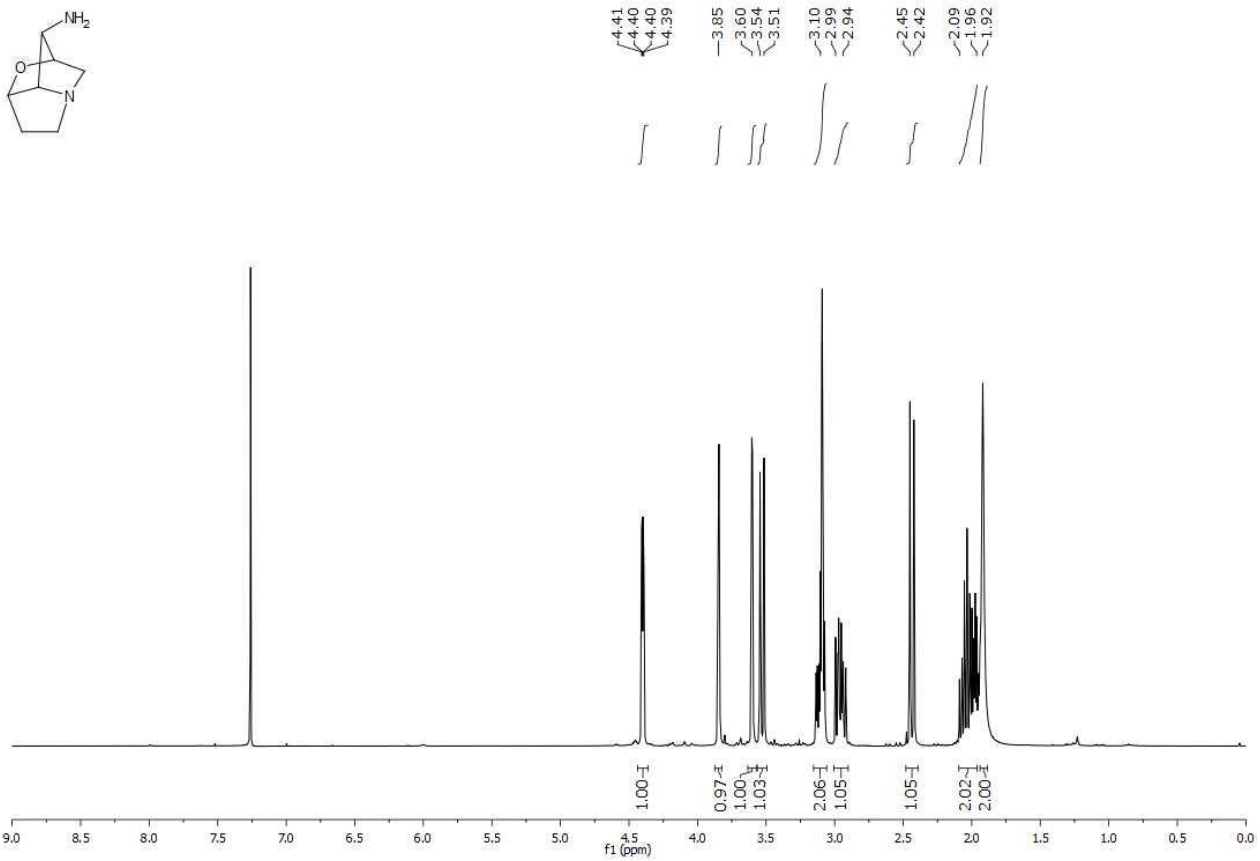
NH2
O
N
4.41
4.40
4.40
4.39
3.85
3.60
3.54
3.51
3.10
2.99
2.94
2.45
2.42
2.09
1.96
1.92
1.00
0.97
1.00
1.03
2.06
1.05
1.05
2.02
2.00
f1 (ppm)

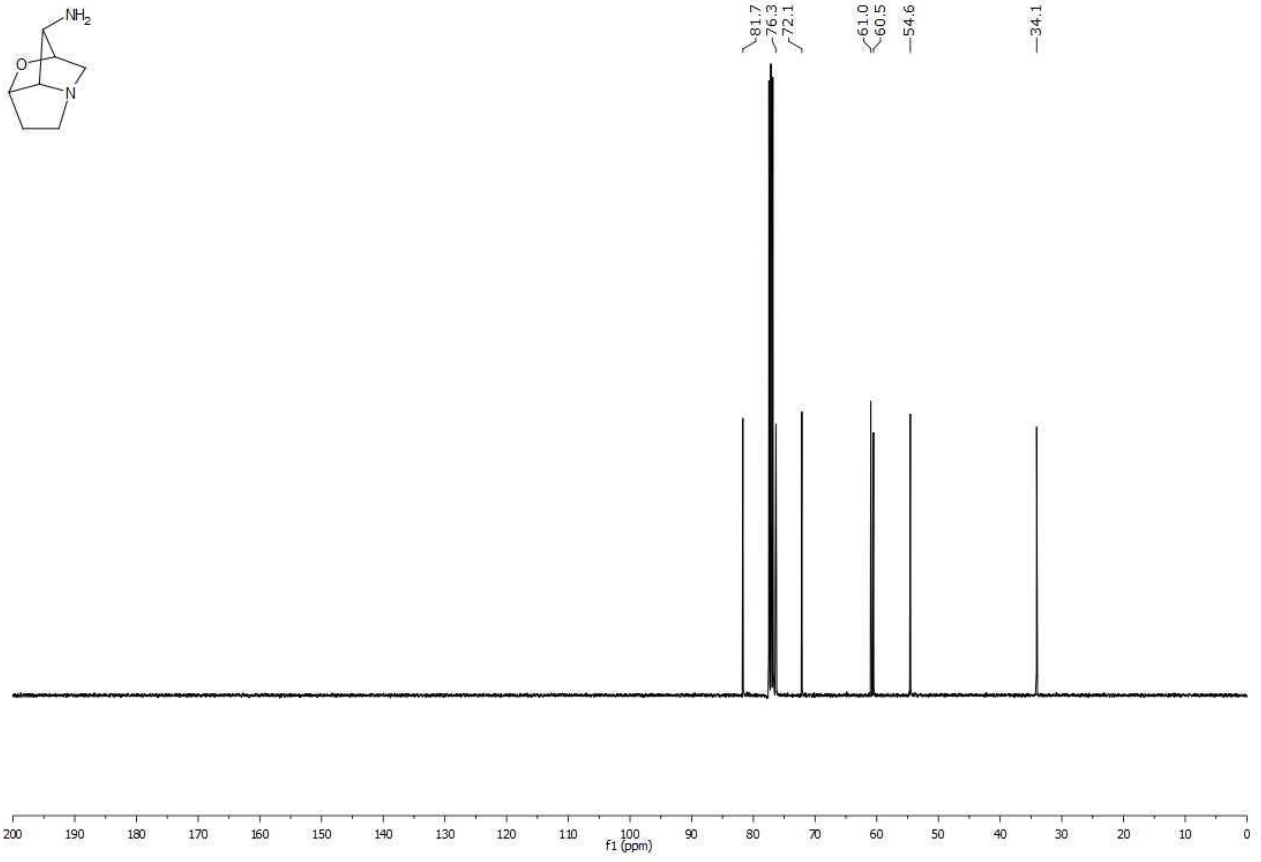
NH2
O
N
81.7
76.3
72.1
61.0
60.5
54.6
34.1
f1 (ppm)

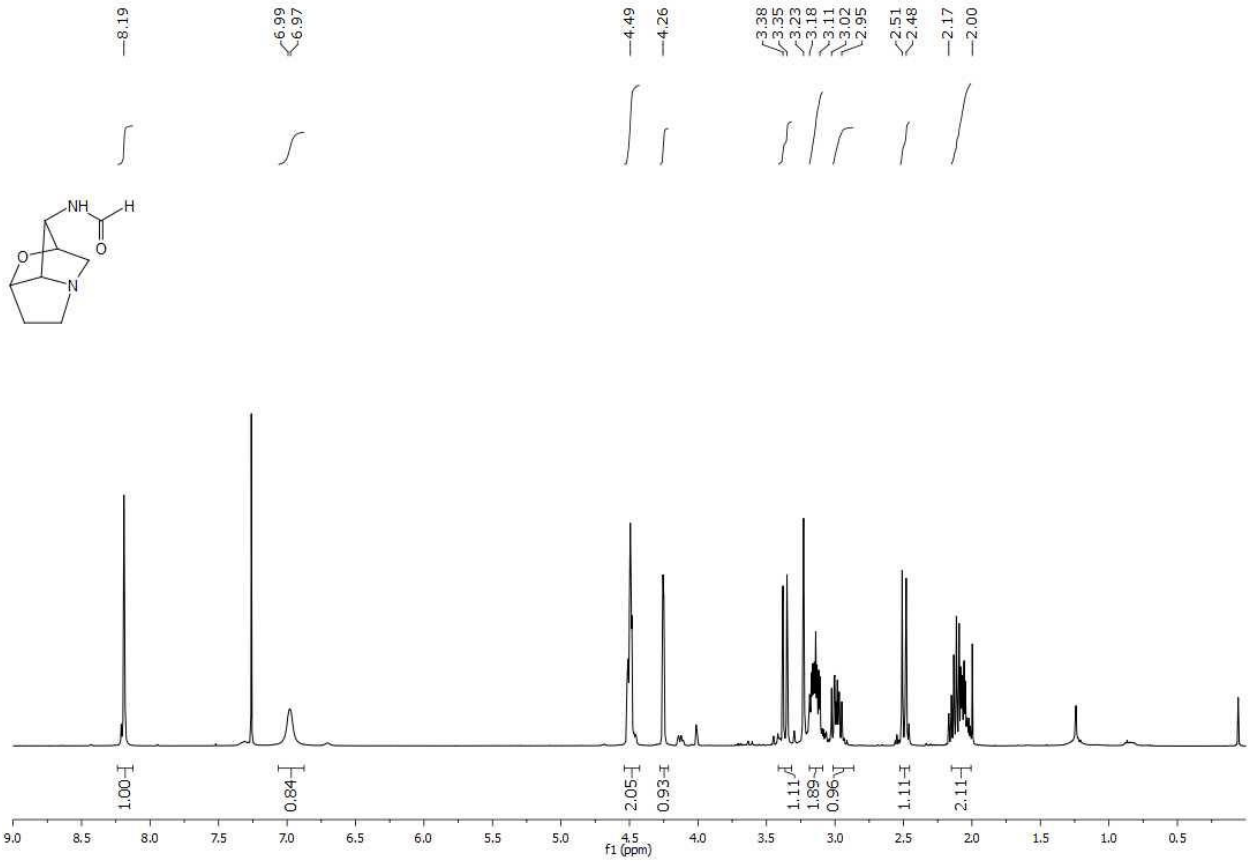
8.19
6.99
6.97
4.49
4.26
3.38
3.35
3.23
3.18
3.11
3.02
2.95
2.51
2.48
2.17
2.00
NH
H
O
O
N
1.00
0.84
2.05
0.93
1.11
1.89
0.96
1.11
2.11
f1 (ppm)

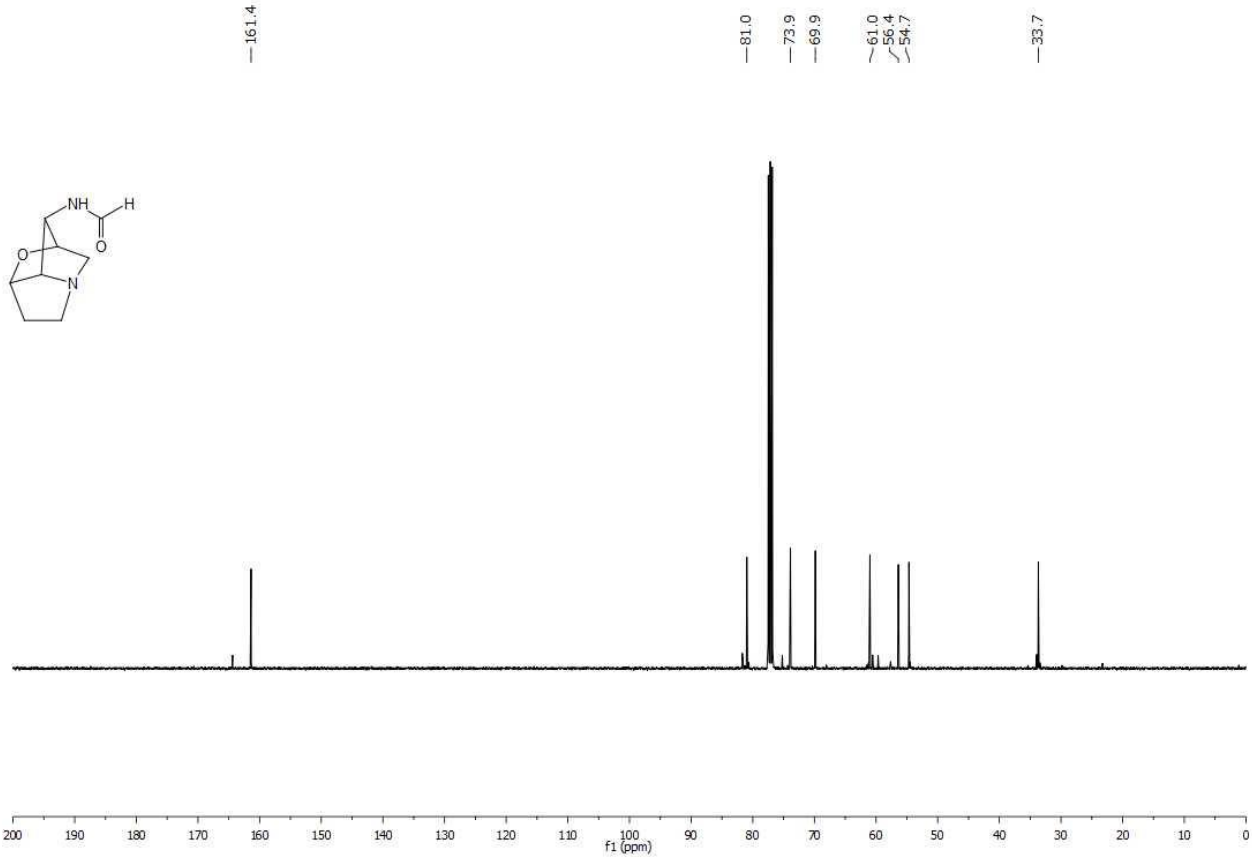
161.4
81.0
73.9
69.9
61.0
56.4
54.7
33.7
NH
H
O
O
N
f1 (ppm)

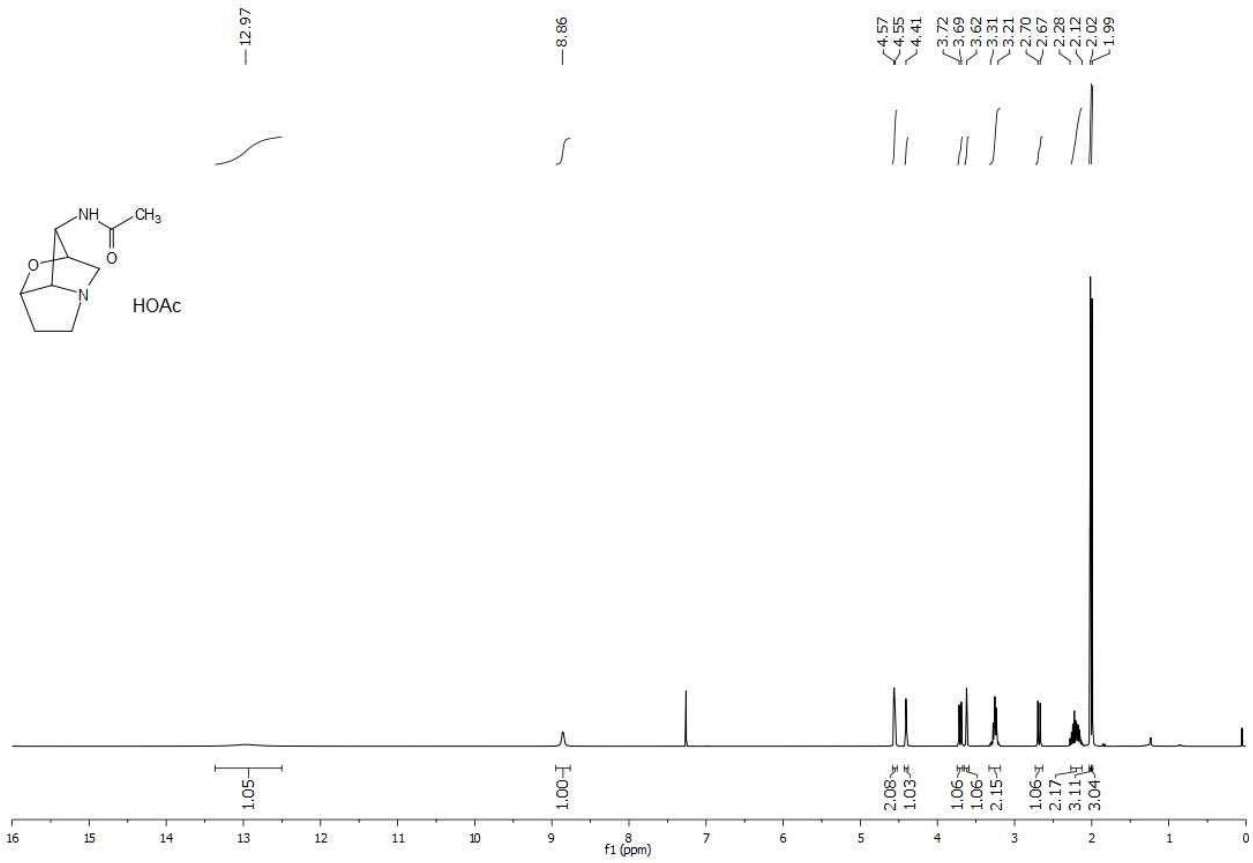
12.97
8.86
4.57
4.55
4.41
3.72
3.69
3.62
3.31
3.21
2.70
2.67
2.28
2.12
2.02
1.99
NH
CH3
O
O
N
HOAc
1.05
1.00
2.08
1.03
1.06
1.06
2.15
1.06
2.17
3.11
3.04
f1 (ppm)

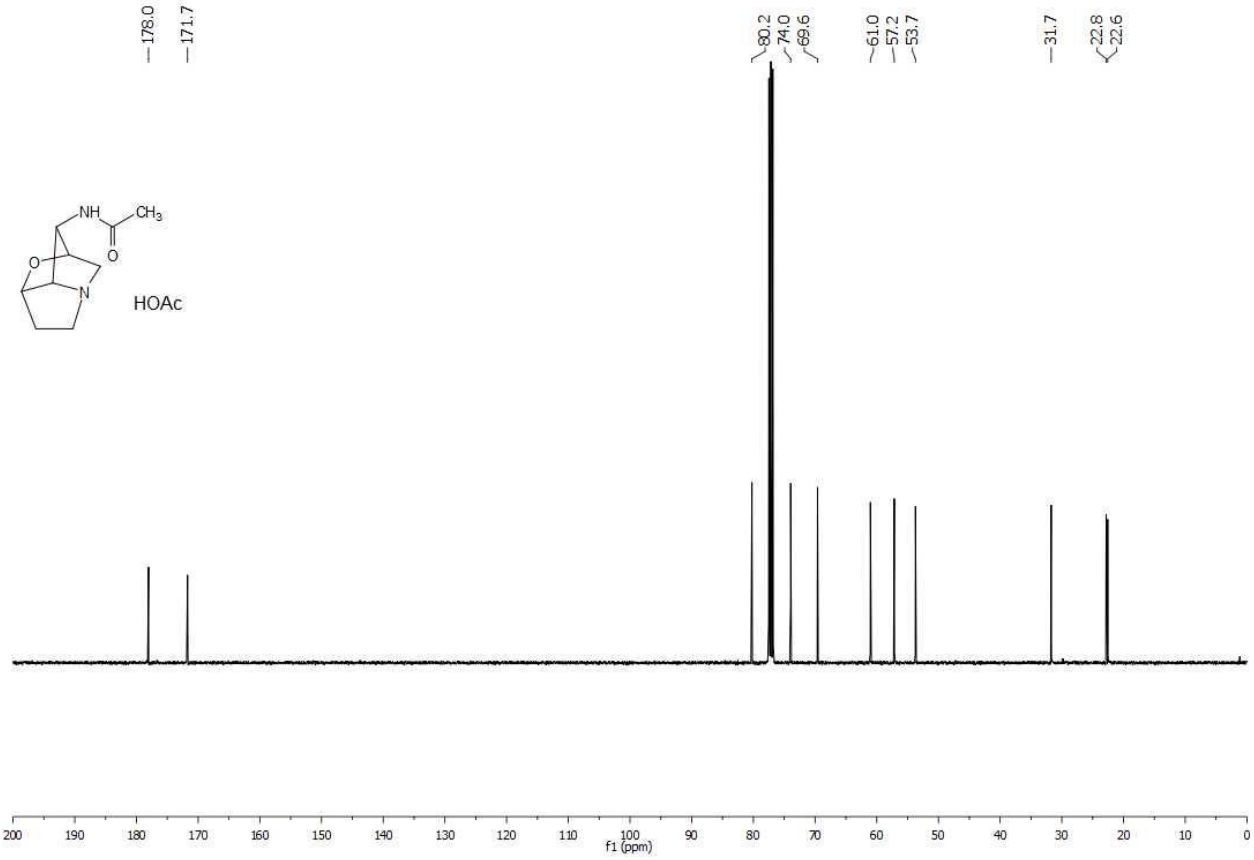
178.0
171.7
80.2
74.0
69.6
61.0
57.2
53.7
31.7
22.8
22.6
NH
CH3
O
O
N
HOAc
f1 (ppm)

References:

1. Hofmeister, F. (1892) Die wirksamen Bestandtheile des Taumellolchs. *Archiv f. experiment. Pathol. u. Pharmakol 30*, 202-230.
2. Bacon, C. W., Porter, J. K., Robbins, J. D., and Luttrell, E. S. (1977) Epichloe typhina from toxic tall fescue grasses. *Appl Environ Microbiol 34*, 576-81.
3. Lyons, P., Plattner, R., and Bacon, C. (1986) Occurrence of peptide and clavine ergot alkaloids in tall fescue grass. *Science 232*, 487-489.
4. Pan, J., Bhardwaj, M., Nagabhyru, P., Grossman, R. B., and Schardl, C. L. (2014) Enzymes from fungal and plant origin required for chemical diversification of insecticidal loline alkaloids in grass-Epichloe symbiota. *PLoS One 9*, e115590.
5. Bush, L. P., Wilkinson, H. H., and Schardl, C. L. (1997) Bioprotective Alkaloids of Grass-Fungal Endophyte Symbioses. *Plant Physiol 114*, 1-7.
6. Bush, L. P., Fannin, F. F., Siegel, M. R., Dahlman, D. L., and Burton, H. R. (1993) Chemistry, occurrence and biological effects of saturated pyrrolizidine alkaloids associated with endophyte-grass interactions. *Agriculture, Ecosystems & Environment 44*, 81-102.
7. Schardl, C. L., Grossman, R. B., Nagabhyru, P., Faulkner, J. R., and Mallik, U. P. (2007) Loline alkaloids: Currencies of mutualism. *Phytochemistry 68*, 980-996.
8. Wilkinson, H. H., Siegel, M. R., Blankenship, J. D., Mallory, A. C., Bush, L. P., and Schardl, C. L. (2000) Contribution of Fungal Loline Alkaloids to Protection from Aphids in a Grass-Endophyte Mutualism. *Molecular Plant-Microbe Interactions 13*, 1027-1033.
9. Bacetty, A. A., Snook, M. E., Glenn, A. E., Noe, J. P., Nagabhyru, P., and Bacon, C. W. (2009) Chemotaxis disruption in Pratylenchus scribneri by tall fescue root extracts and alkaloids. *J Chem Ecol 35*, 844-50.
10. Cakmak, M., Mayer, P., and Trauner, D. (2011) An efficient synthesis of loline alkaloids. *Nat. Chem. 3*, 543-5.
11. Baumann, M. H., Partilla, J. S., Lehner, K. R., Thorndike, E. B., Hoffman, A. F., Holy, M., Rothman, R. B., Goldberg, S. R., Lupica, C. R., Sitte, H. H., Brandt, S. D., Tella, S. R., Cozzi, N. V., and Schindler, C. W. (2013) Powerful cocaine-like actions of 3,4-methylenedioxypyrovalerone (MDPV), a principal constituent of psychoactive 'bath salts' products. *Neuropsychopharmacology 38*, 552-62.
12. Xiao, Y., and Kellar, K. J. (2004) The comparative pharmacology and up-regulation of rat neuronal nicotinic receptor subtype binding sites stably expressed in transfected mammalian cells. *J Pharmacol Exp Ther 310*, 98-107.

Acknowledgements

First, I want to thank my advisor and mentor Prof. Dr. Dirk Trauner for providing an exciting and challenging research environment. I am grateful to Prof. Trauner for giving me the freedom to develop my own ideas and to lead projects in diverse directions.

I want to thank Prof. Thomas Gudermann for appraising my PhD thesis and for being member of my thesis advisory committee (TAC) throughout the last 3.5 years.

I am thankful to the members of my rigorosum committee: Dr. Thomas Magauer, Prof. Karaghiosoff, Prof. Bracher and Prof. Hoffmann-Röder.

Further, I want to thank:

Prof. Alexander Gottschalk, my "Diplom-Vater", who always supported me, from my first small steps in science to the first big step (publication). I will always be thankful that you evoked my interest in molecular neuroscience.

Dr. Martin Sumser. Thank you, for teaching me one of the few left "crafts" of neuroscience – electrophysiology.

Heike and Aleks. Thank you for the support during the last years and especially in the last days!

Luis de la Osa de la Rosa and Carrie, thank you for helping me so much with all my projects and for keeping the lab running.

Matthias, I think you know what an impact you had on my scientific development and how thankful I am for this. I learned so much from you. Not only in science.

Kathi, you made the everyday life in the lab so much easier and more enjoyable (except Tuesdays). I especially appreciated the little things, like coming to the office to chat while your tea water boils up. Scientifically, you had a strong impact on my understanding of chemistry.

David B., I have to be honest about something here. I did not like writing the review with you. I loved it! Also, my favorite premier league team somehow developed to be Arsenal!

Daniel H., during my time in the green lab (back then, when I still had a hood), you supported me during difficult times and became a very close friend. Go Werder!

Anto, Guilliaume and Matthias – the gentlemen's club! Thanks for all the manly hikes in the Alps and evenings in the bars.

Kutti und Mesi, you were the guys who made my first weeks in the lab a wonderful experience. You showed me so many tricks in everyday alkaloid synthesis, that even I sometimes can help real chemists with some issues. I'm sure that this new thing – flash column chromatography – will soon be a popular way to separate molecules in laboratories all over the world.

Nina and Felix. It is soo good to have you around. Scientifically and socially you both are amazing. It is not exaggerated to say, that you are the cornerstones of the group. This is only topped by Nina's engagement regarding keeping the group running smoothly and

Felix’s beard. Thank you for your patience when I was constantly asking questions about the loline NMRs!

Ben. You are the best neighbor in the world. I understand so much more about chemistry now, because of our many discussions.

Nils. We went through some tough times with the oocytes. I hope it will somehow pan out in the end.

David K. We were a brilliant team. You are always so optimistic about everything. Never lose that! It is a pleasure to work on a project with you.

Daniel. I hope you will have a lot of fun at the Bodensee.

Thanks to all the amazing people in the Lab. Dr. Nic, Dr. Henry, Dr. JB, Giulio, Shu-An, James, Robin, Philipp and Peter. You all are great scientists!

The Magauers, especially Adriana, Tatjana, and Teresa, for an awesome Saalfelden experience. Cedric, for helpful discussions and Klaus for all the help with the loline project.

And almost last but not least. No, I did not forget you this time… Laura. You helped me a lot during our studies in Frankfurt. I don’t know how I would have done it without your help (not to mention handing in the diploma thesis in time). Thank you.

Thanks to all my friends in Munich. Steven and Laurencija: you made my life here so very much enjoyable! Gyti: thanks for being a good friend and BBall team mate. Dalia and Flo: thank you for all the nice evenings!

Maike and Ryan: You were the best IMPRS co-presidents that I could have wished for. I think we made a good team and achieved a lot. Thank you!

Hans-Joerg, Ingrid, Maxi and Katharina. You are the best graduate school coordinators one can imagine. Please, keep on doing this with the same passion and enthusiasm as always!

Jatin. Thank you for all the interesting discussions about life, science and everything. I wish you all the best in the world!

Jakob Vörkel. It is something special to be able to discuss science within the family. It’s amazing, when this turns into a shared project! Thank you!

Most, I want to thank my Family, whom I dedicate this thesis to.

My parents, Romana and Vingaudas: Thank you for being the best parents. When I was a kid you bought me a microscope and helped me analyze the water and soil from our garden. You always gave me strong support, no matter what I wanted to do.

My big brother: Darius. Thank you for always being there for me. Without you I would have gotten into a lot of fights in school!

Theo: Thank you for always being there for me!

My family in Poland: Julija, Artūras, Adomas, Anelė, Juozas, Tomas. Ačiū jums visiems už nuostabų palaikymą.

Especially I want to thank my wonderful wife Silvija. You are the most amazing person I know and the love of my life! Writing this thesis would have not been possible without you. I know, sometimes it was not so easy, but you always supported me. Whenever I was sad, you made me happy again. We went through many chapters in our lives together. I am so much looking forward to entering the next chapter together with you! Be tavęs, mano meilė, visą tai būtų buvę visiškai neįmanoma. Ačiū už begalinį palaikymą per geriausius ir per sunkiausius laikus.